

**Universidade do Algarve**

***Locust bean gum-based microparticles for  
pulmonary delivery of antibiotics***

**Ana Bernardina Cotrim Dias Alves**

**Dissertação para a obtenção do Grau de Mestre em Ciências Biomédicas**

**Trabalho efetuado sob a orientação de:**

**Professora Doutora Ana Margarida Moutinho Grenha**

**Faro 2015**

**Universidade do Algarve**

***Locust bean gum-based microparticles for  
pulmonary delivery of antibiotics***

**Ana Bernardina Cotrim Dias Alves**

**Dissertação para a obtenção do Grau de Mestre em Ciências Biomédicas**

**Trabalho efetuado sob a orientação de:**

**Professora Doutora Ana Margarida Moutinho Grenha**

**Faro 2015**

# ***Locust bean gum-based microparticles for pulmonary delivery of antibiotics***

## **Declaração de autoria de trabalho**

**Declaro ser a autora deste trabalho, que é original e inédito. Autores e trabalhos consultados estão devidamente citados no texto e constam da listagem de referências incluída.**

**Copyright © 2015**

**Ana Bernardina Cotrim Dias Alves**

---

A Universidade do Algarve tem o direito, perpétuo e sem limites geográficos, e arquivar e publicitar este trabalho através de exemplares impressos reproduzidos em papel ou de forma digital, ou por qualquer outro meio conhecido ou que venha a ser inventado, de o divulgar através de repositórios científicos e de admitir a sua cópia e distribuição com objetivos educacionais ou de investigação, não comerciais, desde que seja dado crédito ao autor e editor.

## **Agradecimentos**

A realização desta tese, quer a nível do desenvolvimento experimental quer na sua redação, só foi possível, com a colaboração e disponibilidade de todo um conjunto de pessoas, de que uma forma mais ou menos direta, me apoiaram durante este percurso.

A Professora Ana Grenha, orientadora desta Tese, Principal Investigador e líder do grupo *Drug Delivery Laboratory*, pela oportunidade que me deu, de ter apostado em mim, mesmo antes de acreditar ser possível chegar até aqui. Serei sempre grata pela sua disponibilidade em me orientar e ensinar, permitindo-me a aprendizagem de novos conhecimentos, e “saberes práticos”. Como também a sua receptividade, a compreensão, a preocupação e a cooperação durante todo este processo.

A Professora Ana Costa, pela sua ajuda preciosa na área da Química Orgânica, permitindo o desenvolvimento das formulações, ensaios de quantificação de fármacos e de reações de síntese de polímeros. Como também o seu espírito crítico e cooperativo no sentido de se poder sempre melhorar os resultados obtidos.

A Investigadora Manuela Gaspar, pela sua disponibilidade em nós receber e orientar nas determinações de densidade real, realizadas na Faculdade de Farmácia da Universidade de Lisboa. Bem como a também a sua cooperação e preocupação durante a estadia nesta faculdade.

Ao Professor Jorge Martins, pela sua cooperação em nos ajudar a interpretar os resultados de citometria de fluxo.

Ao Professor João Lourenço, pela sua ajuda e disponibilidade nas análises de XRD, assim, como as suas explicações sobre os resultados obtidos.

A Susana, a sua ajuda, cooperação e amizade, merece um especial destaque. Há tanto a agradecer, partilhamos tantos “porquês”, “conhecimentos”, “desenvolvimentos”, “impasses”, “ resultados”... Obrigado pela paciência, ensinamentos e companheirismo.

A Joana, por ter tido a disponibilidade e a vontade de apreender mais, e ao mesmo tempo, com a sua ajuda, prática e conhecimentos, ter-me ajudado a desenvolver e testar as novas abordagens nas formulações de LBG.

Aos meus restantes colegas do laboratório: Jorge, Tatiana, Filipa, Flávia e a Ludmylla. Por terem sempre proporcionado um bom ambiente de trabalho, haver disponibilidade para a troca de saberes, experiências, interajuda e motivação.

A Minha Família e Amigos pelo apoio e incentivo incondicional.

*A todos o meu sincero obrigado...*

## Resumo

A administração de fármacos por via pulmonar tem sido abordada com elevado interesse, conduzindo-se ao crescimento do desenvolvimento de sistemas de libertação específicos para esta via. A sua reduzida atividade enzimática, a prevenção do metabolismo hepático, a superfície elevada, o fino e permeável epitélio alveolar e a vasta rede vascular, tornam-na elegível para a administração sistémica. Mas também, por permitir a elevada deposição de fármaco em elevada concentração numa zona específica do pulmão, permitindo assim, aumentar a sua ação terapêutica, reduzindo a dose total, efeitos adversos sistémicos e efeito de primeira passagem. É largamente utilizada para a veiculação de fármacos para o tratamento local de doenças respiratórias como a asma e fibrose cística, e atualmente investigada para a veiculação de antibióticos para o tratamento de doenças infecciosas, como a pneumonia ou a tuberculose.

A tuberculose apresenta ainda uma elevada prevalência e incidência a nível mundial, em 2012, estimou-se o aparecimento de 8.6 milhões de novos casos e 1.3 milhões de casos de mortalidade. Sendo que uma das principais causas de morte é a baixa adesão a terapia oral atual, e consequentemente a falha terapêutica desta. A administração de sistemas que veiculem fármacos antituberculosos tem sido vista como uma abordagem terapêutica que potencialmente será eficaz e segura. Os sistemas microparticulados produzidos, por exemplo, por atomização, tem sido bastantes explorados, devido, a se poderem modular as suas características, de modo, a que exibam características aerodinâmicas adequadas (tamanho geométrico, densidade e forma) para alcançar a região alveolar.

A goma de alfarroba (LBG) é um polissacarídeo neutro, que é extraído a partir das sementes de alfarroba, e tem sido largamente utilizado, em aplicações farmacêuticas, devido, a sua baixa citotoxicidade, propriedade bioadesivas e gelificantes. Este polímero pertence a classe dos galactomananos, e é composto por unidades de mannose e galactose, num *ratio* aproximadamente de 4/1. A sua estrutura molecular consiste numa ligação linear de unidades (1-4)- $\beta$ -mannose com uma unidade de (1-6)- $\alpha$ -galactose. A obtenção de micropartículas com esta estrutura, e com capacidade de atingirem a região alveolar, permite proporcionar o direcionamento destes sistemas para os macrófagos alveolares, onde reside o agente infeccioso, *Mycobacterium tuberculosis*, e permitirem que haja a libertação intracelular dos fármacos veiculados. Este direcionamento deve-se ao facto de os macrófagos alveolares infetados expressarem o receptor da mannose, que ao reconhecer estruturas com mannose, irá conduzir a sua fagocitose, de um modo, mais específico e rápido, comparativamente com sistemas que não tenham esta estrutura.

Neste contexto, este trabalho propõe o desenvolvimento de sistemas microparticulados, utilizando a goma de alfarroba, para a produção de micropartículas através da técnica de atomização. Pretende-se que este polímero veicule dois fármacos antituberculosos de primeira linha, a isoniazida (INH) e a rifabutina (RFB). Os sistemas microparticulados obtidos serão caracterizados em termos de propriedades aerodinâmicas, de eficácia de encapsulação e capacidade de permitirem a libertação dos fármacos num ambiente alveolar e do fagolisossoma. A sua biocompatibilidade será analisada em duas linhas celulares representativas do epitélio alveolar (A549) e dos macrófagos alveolares (macrófagos diferenciados a partir de THP-1). A capacidade de as partículas com uma matriz de LBG em serem fagocitadas será avaliada na dose de 50 µg/cm<sup>2</sup> em duas linhas celulares de macrófagos, macrófagos diferenciados a partir de THP-1 e em macrófagos alveolares provenientes de ratinho (NR8383). A capacidade destas micropartículas em ativarem macrófagos será também avaliada nos macrófagos diferenciados a partir de THP-1.

A utilização da goma de alfarroba neste contexto nunca fora descrita anteriormente. Pelo que torna as quatro formulações desenvolvidas com diferentes *ratios* de fármacos, uma nova abordagem/proposta para a terapêutica de tuberculose, ou a sua potencial adaptação para outra doença infecciosa do trato inferior respiratório. Deste modo as formulações desenvolvidas foram: partículas sem fármaco: *Unloaded LBG* e partículas com fármaco (*ratio* polímero:fármaco), LBG.INH 10:1, LBG.RFB 10:0.2, 10:0.5, 10:1 e LBG.INH.RFB 10:1:0.5 e 10:1:1.

Apesar de a goma de alfarroba formar dispersões viscosas, devido a não solubilizar por completo, foi necessário a adição de ácido clorídrico (HCl) 0.1 M, para que fosse possível a sua atomização. Permitindo-se assim obter com um rendimento satisfatório (entre 58 a 71%), micropartículas com tamanho adequado para a administração alveolar (entre 1.26 a 1.50 µm). Para além do tamanho adequado, apresentam também valores de densidade real (aproximadamente 1.45 g/cm<sup>3</sup>) e de diâmetro aerodinâmico (entre 1.27 a 1.90 µm), que indicam a sua capacidade de atingirem a zona alveolar.

Apesar de a INH ser um fármaco hidrofílico e a RFB ser um fármaco hidrofóbico, foi possível a sua encapsulação na matriz hidrofílica da LBG, com valores elevados de eficácia de encapsulação (> 82%). Outra justificação para a adição de HCl na formulação, foi a necessidade, de na molécula de RFB, haver um processo de desprotonação, que permitisse a sua solubilização em meio aquoso. O perfil de libertação de INH e RFB foi analisado a partir da formulação LBG.INH.RFB 10:1:0.5, verificando-se a libertação de ambos os fármacos num perfil semelhante em meio com pH 7.4, representativo da região alveolar. O perfil de libertação de INH a partir da formulação de LBG.INH foi avaliado, em dois meios, o representativo da região alveolar, e um representativo do fagolisossoma dos macrófagos,

pH 5, estrutura formada após a fagocitose da micropartícula, e onde se irá libertar o fármaco. Em ambos os meios se obteve um perfil de libertação rápido de INH.

A biocompatibilidade dos fármacos, matéria-prima e sistemas microparticulados produzidos foi avaliada em duas linhas celulares, uma representativa do epitélio alveolar (A549) e outra representativa dos macrófagos alveolares (macrófagos diferenciados a partir de células THP-1). E é feita através da avaliação da atividade metabólica (MTT) e da libertação da enzima lactato desidrogenase (LDH). Os resultados obtidos nos dois testes foram concordantes entre si, e verificou-se que nas concentrações testadas o fármaco RFB é citotóxico, com um índice de concentração que inibe a proliferação/população celular em 50 % (IC<sub>50</sub>), nestas duas linhas celulares, idêntico aos *ratios* testados. Apenas formulações que contêm RFB, se observa uma redução da viabilidade celular para estas duas linhas celulares, abaixo, do limite aceitável para formulações farmacêuticas (70%). No polímero observa-se alguma citotoxicidade nas células A549, que não está presente nas *Unloaded* LBG. Diversas razões foram apresentadas para a explicação desta citotoxicidade da RFB, sendo que por comparação com as *Unloaded* LBG MPs, se justifica, que a presença de HCl necessário na formulação, em associação com a RFB faz com que exista um efeito sinérgico na redução da viabilidade celular. É proposto a redução do ratio de *RFB* para um inferior aos desenvolvidos, usar HCl 0.01M para a sua encapsulação, e testar um novo excipiente para a redução da viscosidade da LBG.

A biocompatibilidade foi também avaliada, quando os sistemas microparticulados são apresentados em aerossol. As micropartículas selecionadas foram as seguintes: *Unloaded* LBG, LBG.INH 10:1, LBG.RFB 10:0.5 e LBG.INH.RFB 10:1:0.5 na dose 303 µg/cm<sup>2</sup>, correspondente à concentração mais elevada em que amostras foram testadas quando apresentadas em solução. As micropartículas foram insufladas sobre uma monocamada de macrófagos alveolares. Como em todas se apresentou uma elevada redução de citotoxicidade, selecionou-se as *Unloaded* LBG e LBG.INH.RFB 10:1:0.5 e testou-se na dose 50 µg/cm<sup>2</sup>, verificando-se um aumento da viabilidade celular, em ambas, mas maior nas partículas brancas. Reforçando também, que as doses testadas são elevadas, comparativamente com a dose fármaco/sistema administrada *in vivo*, onde se esperam melhores resultados de viabilidade celular.

Através de citometria de fluxo, foi analisado a capacidade de os macrófagos fagocitarem micropartículas com a matriz de LBG nas linhas celulares referidas. Onde se verificou a existência de uma elevada percentagem de fagocitose nos macrófagos diferenciados a partir de THP-1 (99,5 %), e nas NR8383, uma preferência significativa por micropartículas de LBG (94,35 %) comparativamente com um polímero sem mannose na sua estrutura (53,16%).

Após comprovada a capacidade dos macrófagos em fagocitarem micropartículas de LBG, foi avaliada a capacidade deste galactomanano em ativar macrófagos, diferenciados a partir de THP-1, e que se encontram no estado M0 de ativação, para o estado M1, com capacidade pro-inflamatória. Após a exposição destas células, á uma solução da matriz de LBG e de micropartículas de LBG.INH.RFB 10:1:0.5 na dose de 303 µg/cm<sup>2</sup>, verificou-se que, devido a sua estrutura, a LBG tem a capacidade de induzir a libertação de citocinas, factor de necrose tumoral α e interleucina 8, num nível idêntico ao lipopolissacarídeo, presente na parede bacteriana, e com num nível superior e estatisticamente significativo comparativamente com o nível basal.

Estes resultados reforçam que as micropartículas obtidas a partir deste polímero, através de atomização, apresentam propriedades aerodinâmicas que permitem que atinjam a região alveolar, e sejam veículos de fármacos antituberculosos ou de um outro antibiótico. E devido a sua estrutura com mannose, permitem que haja um reconhecimento específico pelos macrófagos alveolares infetados, permitindo potenciar a sua fagocitose. Após este processo, estas micropartículas permitem a libertação dos fármacos em meio intracelular, e ainda, activarem os macrófagos, para um estado de ativação pro-inflamatório, que irá melhorar a resposta inflamatória, e conseqüentemente, um melhor controlo o agente infeccioso.

**Palavras-chave:** Administração pulmonar, goma de alfarroba, isoniazida, macrofagos alveolares, micropartículas, rifabutina, tuberculose.

## Abstract

Locust bean gum (LBG) is a polysaccharide composed of galactose and mannose residues, a composition that might be of interest in the ambit of pulmonary tuberculosis treatment. The polymer can be processed by spray-drying to produce microparticles that act as carriers for antitubercular drugs via inhalation. Once in the alveolar region, where alveolar macrophages hosting *Mycobacterium tuberculosis* reside, these microparticles are expected to be phagocytosed by macrophages, then releasing the drugs in the intracellular compartment where the bacteria are located. Considering that alveolar macrophages have specific surface receptors recognizing preferentially mannose residues and also with affinity for galactose units, an improved targeting of antibiotic loaded microparticles towards the bacteria hosts is expected.

In this work the production of LBG microparticles by spray-drying is reported for the first time, exhibiting adequate properties for inhalation with the aim of reaching the alveolar zone (aerodynamic diameters between 1.27 and 1.90  $\mu\text{m}$ ). Two different first line antitubercular drugs (isoniazid and rifabutin) were effectively associated to the microparticles (association efficiencies > 82%). The cytotoxicity of the drugs, raw material and carriers (unloaded and drug-loaded) was evaluated in A549 cell line and macrophage-like cell line (macrophage differentiated THP-1 cells). It was verified that RFB has a cytotoxic effect when tested as free drug and formulations containing the drug also revealed toxicity although to a lower extension. This cytotoxic effect was more pronounced at 24h and is both time- and concentration-dependent. LBG-based carriers were also exposed to macrophage-like cells in the form of aerosol, in a dose (50  $\mu\text{g}/\text{cm}^2$ ) that was optimized to be more close to that applied in *in vivo* lung administration. Although the cell viability was not as lower for RFB-containing microparticles, some cytotoxicity was still observed. Additionally, the capture of microparticles by macrophage-differentiated THP-1 cells and NR8383 cells (rat alveolar macrophages) was evaluated by flow cytometry. In both cells lines, the microparticles were insufflated over a monolayer of macrophages at dose of 50  $\mu\text{g}/\text{cm}^2$ , where was verified a high percentage of phagocytose (> 94 %). The capacity of microparticles to activate macrophages (differentiated THP-1 cells) was also evaluated. The exposure to a dose of 303  $\mu\text{g}/\text{cm}^2$  microparticles was verified to have the ability to induce the release of cytokines (interleukin-8 and Tumor necrosis factor  $\alpha$ ), indicative of activation, at a level identical to that induced by the incubation with lipopolysaccharide.

The obtained results as a whole indicate the ability of LBG to act as matrix of inhalable drug carriers produced by spray-drying. The microparticles demonstrated capacity to effectively associate model antitubercular drugs and suitable aerodynamic properties to reach the

alveolar zone. LBG microparticles further evidenced high ability to be captured by macrophages, which is very relevant regarding tuberculosis therapy.

**Key-words:** Alveolar macrophages, antibiotic delivery, locust bean gum, microparticles, spray-drying, tuberculosis.

## Contents

<b>1. Introduction</b> .....	1
<b>1.1. Infectious lung diseases and tuberculosis</b> .....	1
<b>1.1.1. The epidemiology of tuberculosis infection</b> .....	2
<b>1.1.2. Tuberculosis pathogenesis</b> .....	2
<b>1.1.3. Antitubercular drugs</b> .....	7
<b>1.2. Pulmonary drug delivery</b> .....	10
<b>1.2.1. Lung Deposition</b> .....	11
<b>1.2.2. Pulmonary administration</b> .....	13
<b>1.3. Inhalation as a strategy in tuberculosis therapy</b> .....	15
<b>1.3.1. Spray-drying to produce inhalable dry powders</b> .....	16
<b>1.3.2. Matrix materials for inhalable dry powder formulations</b> .....	18
<b>1.3.2.1. Locust bean gum</b> .....	20
<b>1.3.2.1.1. Locust bean gum as carrier for targeting of alveolar macrophages</b> .....	22
<b>2. Objectives</b> .....	24
<b>3. Materials and Methods</b> .....	25
<b>3.1. Preparation of locust bean gum microparticles by spray-drying</b> .....	25
<b>3.1.1. Preparation of polymer dispersions</b> .....	25
<b>3.1.2. Spray-drying of polymer/drug dispersion</b> .....	27
<b>3.1.3. Production of fluorescently labelled LBG microparticles</b> .....	27
<b>3.2. Characterisation of microparticles</b> .....	29
<b>3.3. Determination of drug association</b> .....	31
<b>3.4. In vitro drug release</b> .....	33
<b>3.5. Powder Crystallinity Analysis</b> .....	33
<b>3.6. Cell culture</b> .....	34
<b>3.6.1. A549 cell line: Human alveolar epithelial cells</b> .....	34
<b>3.6.2. THP-1 cell line: Human leukemic monocytes</b> .....	35
<b>3.6.2.1. Differentiation of THP-1 cells into macrophage-like cells</b> .....	35
<b>3.6.3. Cell line NR8383: Rat alveolar macrophages</b> .....	36
<b>3.7. Cytotoxic evaluation</b> .....	36

3.7.1. MTT assay.....	38
3.7.1.1. Samples presented in solution/suspension.....	38
3.7.1.2. Samples presented by aerolisation.....	39
3.7.1.3. Determination of rifabutin IC <sub>50</sub> .....	41
3.7.2. LDH assay.....	41
3.8. Evaluation of macrophage ability to uptake LBG microparticles.....	42
3.9. Evaluation of microparticle capacity to activate macrophages.....	43
3.10. Statistical analysis.....	43
<b>4. Results and Discussion.....</b>	<b>44</b>
4.1. Preparation of locust bean gum microparticles by spray-drying.....	44
4.2. Characterisation of microparticles.....	45
4.3. Association Efficiency.....	48
4.4. <i>In vitro</i> drug release.....	50
4.5. Crystallinity pattern of MP.....	52
4.6. Cell characterisation.....	57
4.7. Cytotoxic evaluation.....	58
4.7.1. Samples presented in solution/suspension.....	58
4.7.2. Samples presented by aerolisation.....	66
4.7.3. Determination of rifabutin IC <sub>50</sub> .....	68
4.7.4. LDH Release.....	69
4.8. Evaluation of macrophage ability to uptake LBG microparticles.....	72
4.9. Macrophage activation evaluation.....	76
<b>5. Conclusion.....</b>	<b>79</b>
<b>6. References.....</b>	<b>81</b>

## List of figures

Figure 1.1: Tuberculosis pathogenesis.....	4
Figure 1.2: Effects of mycobacteria on the host cell lipidome.....	5
Figure 1.3 Persistent infection with <i>M. tuberculosis</i> . ....	7
Figure 1.4: Scheme of drug targets in <i>Mycobacterium tuberculosis</i> . ....	9
Figure 1.5: Structure and chemical formula of Isoniazid and Rifabutin. ....	10
Figure 1.6: Particle deposition in the lungs according to size. ....	12
Figure 1.7: Main mechanisms of particle deposition in respiratory tract.....	12
Figure 1.8: Scheme of the Buchi B-290 Mini Spray dryer.....	17
Figure 1.9: Locust bean gum.....	21
Figure 3.1: Schematic representation of experimental steps involved in the preparation of LBG microparticles, unloaded or loaded with antitubercular drugs.....	26
Figure 3.2: Synthesis reaction of fluorescent LBG.....	28
Figure 3.3: Isoniazid and Rifabutin spectra.....	31
Figure 3.4: Cytotoxicity assays.....	38
Figure 3.5: <i>Dry powder insufflator</i> .....	41
Figure 4.1: Microphotographs of LBG-based microparticles viewed by scanning electron microscopy. ....	46
Figure 4.2: <i>In vitro</i> release of isoniazid (INH) from LBG.INH (10:1, w/w) microparticles in pH 5 (blue line) and pH 7.4 (purple line) during 1440 minutes (24 hours).....	51
Figure 4.3: <i>In vitro</i> isoniazid (blue) and rifabutin (red) release from LBG.INH.RFB (10:1:0.5, w/w) microparticles in pH 7.4.....	53
Figure 4.4: PXRD spectra of Isoniazid before (BSD) and after spray drying (ASD).....	53
Figure 4.5: PXRD spectra of Rifabutin before (BSD) and after spray drying (ASD).....	53
Figure 4.6: PXRD spectra of locust bean gum (LBG) raw material and spray dried formulations.....	54

Figure 4.7: Interaction between aerosol particle and alveolar epithelium.....	55
Figure 4.8: Macrophage differentiation from THP-1 cells.....	56
Figure 4.9: Immunocytochemical characterization of THP-1 cells and macrophage-differentiated THP-1 cells.....	57
Figure 4.10: A549 cell viability after 3 and 24 hours of exposure to Drugs.....	59
Figure 4.11: Macrophage-differentiated THP-1 cell viability after 3 and 24 hours of exposure to Drugs.....	59
Figure 4.12: Cell viability after 3 and 24 hours of exposure to Raw material (LBG). ....	60
Figure 4.13: A549 cell viability after 3 hours of exposure to formulations. ....	61
Figure 4.14: A549 cell viability after 24 hours of exposure to formulations.....	62
Figure 4.15: Macrophage-like THP-1 cell viability after 3 hours of exposure to formulations. ....	63
Figure 4.16: Macrophage-like THP-1 cell viability after 24 hours of exposure to formulations.....	64
Figure 4.17: Powder delivered from the dry powder insufflator. ....	66
Figure 4.18: Macrophage-like THP-1 cell viability after 24 hours of exposure to exposure to unloaded LBG MPs and LBG.INH.RFB formulations at two doses.....	68
Figure 4.19: LDH released from A549 cells (A) and macrophage-like THP-1 cells (B) after 24 hours exposure to the drugs.....	70
Figure 4.20: LDH release from A549 cells after 24 hours exposure to LBG polymer, microparticles and lysis buffer.....	70
Figure 4.21: LDH release from Macrophage-like THP-1 cells after 24 hours exposure to LBG polymer, microparticles and lysis buffer. ....	71
Figure 4.22: Fluorescent signal of macrophage-differentiated THP-1 cells upon 2 hours exposure to 50 µg/cm <sup>2</sup> of unlabelled LBG microparticles (blue line) and fluorescently-labelled LBG microparticles (orange line).....	73
Figure 4.23: Fluorescent signal of NR8383 cells upon 2 hours exposure to to 50 µg/cm <sup>2</sup> of unlabelled LBG microparticles (blue line) and fluorescently-labelled LBG microparticles (orange line).. ....	73
Figure 4.24: Uptake of fluorescently-labelled PVA and LBG MPs by macrophage-differentiated THP-1 cells and NR8383 cells upon exposure to 50 µg/cm <sup>2</sup> for a period of two hours .....	74
Figure 4.25: TNF-α released from macrophage-like THP-1 cells after exposure to LBG the form of solution or dispersion of microparticles .....	77
Figure 4.26: IL-8 released from macrophage-like THP-1 after exposure to LBG the form of solution or dispersion of microparticles.....	77

## List of tables

Table 3.1. Assay conditions for determination of association efficiency and loading capacity.....	32
Table 4.1: Spray-drying production yields and microparticle Feret's and aerodynamic diameters.....	47
Table 4.2: Microparticle real, bulk and tap densities and Carr's index.....	47
Table 4.3: Drug association efficiency and loading capacity.....	49

## List of Annex

Annex I.....	90
--------------	----

## List of Abbreviations

<b>A549</b>	Human alveolar epithelial cells	<b>MPs</b>	Microparticles
<b>ANOVA</b>	One-way analysis of variance	<b>MTT</b>	3-[4, 5-dimethylthiazol-2-yl]-3,5 biphenyl tetrazolium bromide
<b>ATCC</b>	American Type Culture Collection	<b>MR</b>	Mannose receptor
<b>CCM</b>	Cell culture medium	<b>NAD</b>	Nicotinamide adenine dinucleotide
<b>CF</b>	Cystic fibrosis	<b>NR8383 cells</b>	Alveolar macrophages rat NR8383 cells
<b>CR</b>	Complement receptors	<b>NPs</b>	Nanoparticles
<b>D<sub>aer</sub></b>	Aerodynamic diameter	<b>PBS</b>	Phosphate buffer saline
<b>DMEM</b>	Dulbecco's Modified Eagle Medium	<b>PLA</b>	Polylactic acid
<b>DMSO</b>	Dimethyl sulfoxide	<b>PLGA</b>	Polylactic-co-glycolic acid
<b>DNA</b>	Deoxyribonucleic acid	<b>PMA</b>	Phorbol 12-myristate 13-acetate
<b>DOTS</b>	Directly observed treatment	<b>PVA</b>	Polyvinyl alcohol
<b>DPI</b>	Dry powders inhalers	<b>PXRD</b>	Powder X-ray diffraction
<b>EDAC</b>	N-(3-dimethylaminopropyl)-N'-ethylcarbodiimide hydrochloride	<b>PZA</b>	Pyrazinamide
<b>e. g.</b>	For example	<b>RFB</b>	Rifabutin
<b>ELISA</b>	Enzyme-linked immunosorbent assay	<b>RIF</b>	Rifampicin
<b>FBS</b>	Foetal bovine serum	<b>RNA</b>	Ribonucleic acid
<b>HIV</b>	Human immunodeficiency virus	<b>SD</b>	standard deviation
<b>IC<sub>50</sub></b>	Inhibitory concentration 50% (50% survival)	<b>SDS</b>	sodium dodecyl sulphate
<b>IL</b>	Interleukin	<b>SEM</b>	standard error of the mean
<b>INH</b>	Isoniazid	<b>SPD</b>	Spray drying
<b>InhA</b>	Inhibin $\alpha$	<b>TB</b>	Tuberculosis
<b>LBG</b>	Locust bean gum	<b>THP-1</b>	Human leukemic monocytes
<b>LDH</b>	Lactate dehydrogenase	<b>TGF - <math>\beta</math></b>	Transforming growth factor - $\beta$
<b>M/G</b>	Mannose/Galactose	<b>TNF<math>\alpha</math></b>	Tumor necrosis factor- $\alpha$
<b>MDI</b>	Metered dose inhalers	<b>XRD</b>	Drug resistant
<b>MDR-TB</b>	Multidrug-resistant tuberculosis	<b>WHO</b>	World Health Organization

## 1. Introduction

### 1.1. Infectious lung diseases and tuberculosis

Lungs are a site for gas exchange, and their direct contact with the external environment facilitate the entrance of pathogens.<sup>1</sup> This is the premise for infectious lung diseases, which can be caused by bacteria, viruses and/or fungi.<sup>2</sup> Respiratory bacterial infections are considered the major cause of death worldwide,<sup>1</sup> a scenario that is getting worse because of increased antibiotic resistance.<sup>2</sup> Some of the most popular air-borne diseases are tuberculosis, pneumonia and pertussis.<sup>3</sup> The administered drugs have to reach the pathogens, which can be in different habitats, such as the mucus, biofilms or inside host cells.<sup>2</sup> For instance, in pneumonia pathogens are in the mucus of bronchiolar or alveolar zone,<sup>2,4</sup> for example, *Streptococcus pneumoniae* presenting virulence factor that favors the adherence to alveolar epithelia.<sup>4</sup> In turn, in tuberculosis the pathogen lives inside macrophages, which are located in alveolar zone.<sup>5</sup> Furthermore, different infections might occur simultaneously.<sup>6</sup> As in many cases the therapeutic approach is made via oral antibiotherapy, the used doses are high and treatment periods are long, resulting in severe side effects with consequences at the level of patient compliance. Usually, a combination of antibiotics is needed to treat resistant pathogens. This is described, for instance, in multidrug-resistant tuberculosis (MDR-TB).<sup>2,7</sup>

Cystic fibrosis (CF) is another relevant example. Although it is a genetic disease itself, it is associated with chronic lung infection.<sup>2</sup> CF therapy thus implies the administration of antibiotics. The administration of antibiotics by inhalation is clinically implemented in this disease<sup>8</sup> and this modality has been described to increase the therapeutic efficacy, while minimising the risks of bacterial resistance and preventing patient re-infection.<sup>9</sup> This inhalation strategy, however, is not clinically implemented in tuberculosis therapy. However, there are possibly lessons to be learnt from the experience of the CF community.

Tuberculosis (TB) is an infectious disease caused by the bacillus *Mycobacterium tuberculosis* (*M. tuberculosis*). This pathology is highly contagious, as the bacillus spreads out in the air when people having pulmonary TB expel it by coughing. It is, thus, disseminated via inhalation of bacteria-containing droplets. It affects primarily the lungs and pulmonary TB represents 80% of cases.<sup>7</sup> However, TB does not affect this organ exclusively, as extrapulmonary TB affects other organs, mainly the central nervous and the circulatory systems.<sup>1,10,11</sup>

The current therapy of pulmonary TB consists in a six-month regimen of four first-line oral drugs, having a success rate of around 85%.<sup>10</sup> Treatment failure is frequently associated with lack of patient adherence to the drug regimen and to MDR-TB. This failure leads to rapid growing of MDR-TB and extensively drug resistant (XRD) strains,<sup>1</sup> which are considered a world-wide threat because of high risk of transmission.<sup>7,12</sup> The MDR-TB treatment requires

second line drugs, which are less effective and poorly tolerated.<sup>2</sup> Prevention of resistant tuberculosis needs adequate treatment of each case of TB and improvement in the compliance.<sup>10</sup> New anti-tubercular drugs and new administration systems are needed to address MDR-TB strains and to increase antibiotic efficacy.<sup>2</sup> MDR-TB is defined as resistance to at least rifampicin (RIF) and isoniazid (INH), the two most powerful antitubercular drugs, while XRD corresponds to MDR-TB plus resistance to at least one fluoroquinolone and a second-line injectable antibiotic.<sup>13</sup>

### 1.1.1. The epidemiology of tuberculosis infection

In 1993 TB was declared a global public health emergency by the World Health Organization (WHO), a distinction never granted to any other disease.<sup>1</sup> This disease remains a major global health problem, and it ranks as the second leading cause of death from an infectious disease worldwide, after the human immunodeficiency virus (HIV).<sup>2</sup> In 2012, the WHO estimated 8.6 million new TB cases, mainly in Asia (58% of the new cases) and Africa (27%), and 1.3 million of people died of TB.<sup>10</sup> Patients with HIV, due to a compromised immune system, have a higher risk to develop active TB. About 0.47 of the 1.3 million deaths were of patients with HIV associated to TB.<sup>1</sup>

Without treatment or its failure, TB mortality rates are high, with 70% of infected people dying within 10 years.<sup>10</sup> In the 1.3 million of deaths registered in 2012, about 170,000 arose from MDR-TB, a relatively high number compared with 450,000 incident cases of MDR-TB in this year.<sup>10</sup>

A worrying number is that of asymptomatic people infected with *M. tuberculosis*. These people, staying in a latent state of the disease, are estimated to make up to one-third of the global population,<sup>2,14</sup> representing an enormous reservoir of potential disease. It is estimated that about 5 -10% of people with latent TB will develop active disease.<sup>14</sup>

### 1.1.2. Tuberculosis pathogenesis

Humans are the primary host of *M. tuberculosis*, which is disseminated via inhalation of bacteria-containing droplets. People suffering from pulmonary or laryngeal TB can disseminate the disease by emission of droplets containing the tubercle bacilli from cough, sneeze, shout or sing. These airborne particles have 1 to 5  $\mu\text{m}$ , depending on the environment, and may keep suspending in the air for several hours. Upon inhalation and given their size, the infectious droplets can reach the alveolar zone, where they are phagocytosed and accumulate

inside alveolar macrophages to form granulomas in a later stage.<sup>10,15</sup> The pathogen *M. tuberculosis* might exist as actively dividing bacilli (active disease state) or in the so-called “dormant” state. In the latter case, people are infected but clinically asymptomatic, and are referred to have latent tuberculosis.<sup>14</sup> The dissemination of the disease through the infected droplets occurs only from individuals with active disease.<sup>22</sup> Both states can occur within the same infected individual, depending on the stage of TB. Although the human immune system can control the infection, this control does not lead to complete elimination of bacteria, they just stay in the referred dormant state.<sup>7</sup> In these cases, mycobacteria survive in a structure called granuloma, with no adverse effect on the health of the host, even up to the life time.<sup>15</sup>

*M. tuberculosis* is an intracellular bacterium and alveolar macrophages (AM) are its “favorite” host, although it can affect other cell types,<sup>14</sup> resulting in extrapulmonary tuberculosis. The granuloma structure probably represents a balance between active and latent TB.<sup>15</sup> If a deterioration of host immunity occurs in a person with latent TB, there is increased probability of developing the disease.<sup>16</sup> Only about 10% of infected people develop TB, because in most healthy individuals, the immune defense system is sufficient to eliminate mycobacterium at the initial stage, which has a duration of 4 to 6 weeks.<sup>14</sup> Figure 1.1 resumes the whole process of TB pathogenesis, since infection, initial stage and progress for adaptive immune response with granuloma formation, and propagation of the disease.

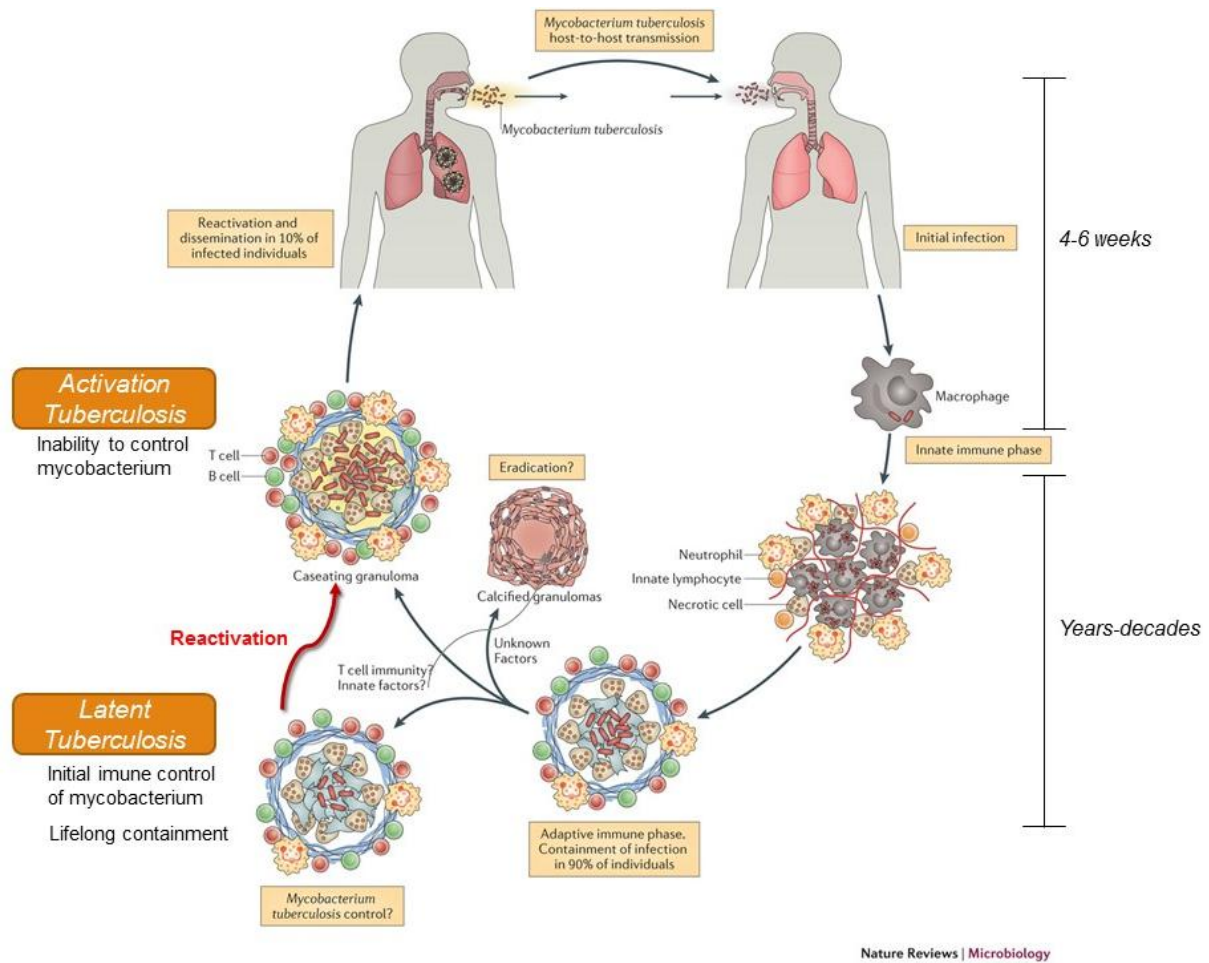


**Figure 1.1: Tuberculosis pathogenesis.** Infection is initiated by the inhalation of droplets that contain bacteria. The first immune response is innate and involves the recruitment of inflammatory cells. In lymphoid node, dendritic cell presentation of bacterial antigens leads to T cell activation, and these cells recruit more cells. These cell agglomerates lead to the establishment of granulomas. Some individuals can control the infection, remaining in a “latent” state. A small percentage of these people will eventually progress and develop active disease, which can lead to the release of *M. tuberculosis* from granulomas that have eroded into the airways. Adapted from Nunes-Alves *et al.*<sup>14</sup>

*M. tuberculosis* and seven very close species of Mycobacterium genus (*M. bovis*, *M. pinnipedii*, *M. canetti*, *M. africanum* and *M. mungi*, *M. microti* and *M. caprae*) belong to the so-called *M. tuberculosis* complex. Some of them may cause the disease in humans.<sup>10</sup> When *M. tuberculosis* is phagocytosed by macrophages, a series of phenomena occur, including membrane invagination, budding, and fusion events, that finally result in the formation of a phagosome. Bacilli are distributed further within the cell through a series of vesicle trafficking events delivering the material to the antigen processing and presentation pathway. When endosomes gain endolitic capacity they are designated as lysosomes. These vesicles then fuse with the phagosomes, forming the phagolysosomes, where extensive degradation occurs resulting in clearance of potentially harmful material and subsequent destruction of pathogens.<sup>7,14</sup> Infected macrophages can remain in the lung or disseminate to other organs in the body.<sup>7</sup>

The binding of *M. tuberculosis* with the phagocytes is mediated by complement receptors (CR1, CR2, CR3 and CR4), mannose receptors (MR), dendritic cell-specific intercellular adhesion molecule (ICAM)-3-grabbing nonintegrin (DC-SIGN), and Fc receptors. The complex structure of the macrophage cell surface is accountable for the capacity of multiple receptor molecules to internalize mycobacterium.<sup>7</sup> In the initial stages of the infection, after phagocytosis by alveolar macrophages, an innate immune response is developed. If the appropriate stimuli are activated, transference of the phagocytosed bacilli to the destructive phagolysosome occurs. However, some bacilli are able to escape lysosomal delivery and survive within the macrophage.<sup>7</sup> After phagocytosis the fate of *M. tuberculosis* can assume three distinct possibilities: a) escape from phagosome, b) prevent phagosome-lysosome fusion or c) survive inside of phagolysosomes.<sup>17</sup> When inside the phagosome or phagolysosome, *M. tuberculosis* has the ability to encode a number of enzymes involved in lipogenesis and lipolysis. These enzymes will interfere with lipidome of host cell causing modifications, which involve cell signalling traffic membrane, lipid storage in lipid droplets and fusion organelles. Allowing inhibition of activity phagolysosome in the host cell and apoptosis, also, there is a lipid delivery resource for mycobacterium. These mechanisms will also permit maintenance, survival and replication (Figure 1.2).<sup>18</sup>

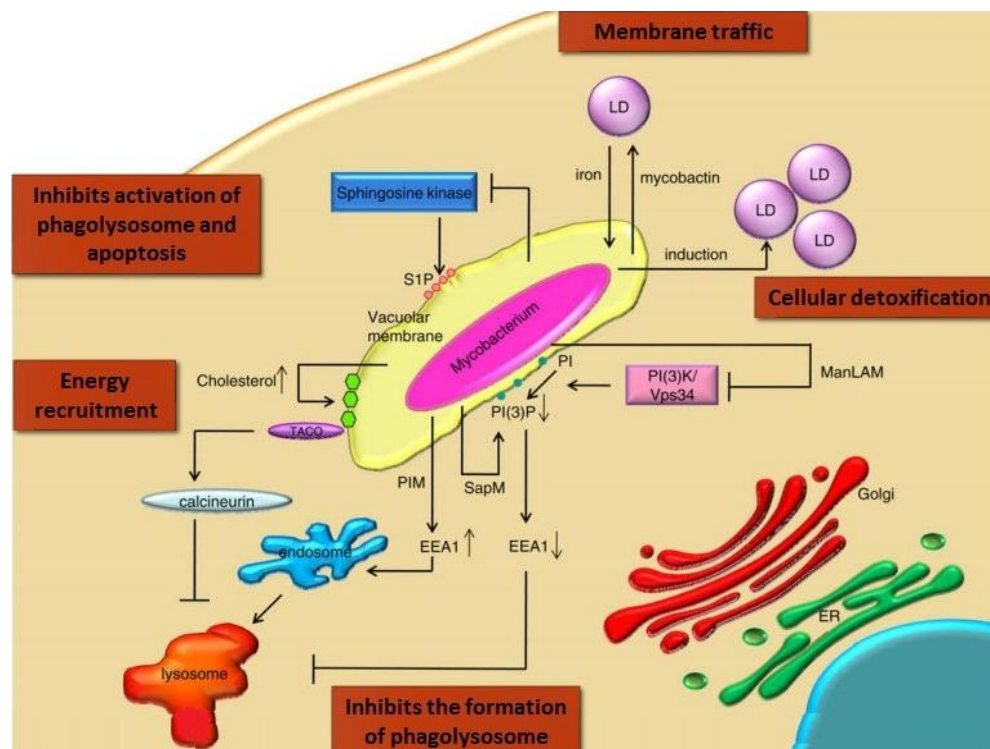


**Figure 1.2: Effects of mycobacteria on the host cell lipidome.** LD: lipid droplet; S1P: sphingosine-1-phosphate; SapM: *M. tuberculosis* effector molecule; PI(3)P: phosphatidylinositol-3-phosphate; EEA1: Early endosomal antigen 1; PI(3)K/Vps34: phosphoinositide 3-kinase; PIM: phosphatidylinositol mannoside; ManLAM: mannose-capped form of Lam (lipoarabinomannan); ER: endoplasmic reticulum; TACO: tryptophan aspartate containing coat protein. Adapted from van der Meer-Janssen *et al.*<sup>18</sup>

Before the infection by *M. tuberculosis*, alveolar macrophages are said to be in steady-state conditions, as they have not yet been activated (assumed as M0 activation state). Based on their function, activated macrophages are divided broadly into two categories: classical M1 and alternative M2 macrophages. When a *M. tuberculosis* infection occurs, macrophages generally activate towards a M1 phenotype in the early stage of the infection.<sup>19</sup> When macrophage receptors recognise the mycobacteria, the activation leads to the production of a high amount of pro-inflammatory mediators (interleukin(IL)-1, tumour necrosis factor (TNF)- $\alpha$ ), which eliminate the invading organisms and activate the adaptive immunity.<sup>17</sup> To counteract this excessive inflammatory response, macrophages undergo apoptosis or activate to an M2 phenotype to protect the host from excessive injury and facilitate wound healing.<sup>17,19</sup>

The induction of adaptive immune response occurs later, when *M. tuberculosis* disseminates to lymph nodes. The presentation of bacterial antigens by dendritic cells leads to priming and expansion of antigen-specific T cells, which differentiate from naïve T cells into effector T cells (T CD4<sup>+</sup> cells). In parallel, the pro-inflammatory mediators (transforming growth factor (TGF)- $\beta$  and Interleukin-12) stimulate the migration of T<sub>Helper</sub> cells.<sup>20</sup> These cells migrate to the infected lung, and, in association with other leukocytes, induce the formation of granulomas.<sup>14</sup> The activation of macrophages is also mediated by secreted by CD4<sup>+</sup> T cells. These T cells secrete cytokines and chemokines, thus keeping the macrophages in an activated state and ensuring the recruitment of other immune cells to the site of infection.<sup>7</sup> As an example, dendritic cells are also recruited to the lungs in order to complement the bactericidal effect of macrophages.<sup>14</sup> Additionally, the activation of macrophages is expected to restrict the dispersion and replication of *M. tuberculosis*. In the granuloma, macrophages can coexist in M0, M1 and M2 state of activation.<sup>7</sup> Figure 1.3 exposed the interaction between these cells in formation of granuloma.

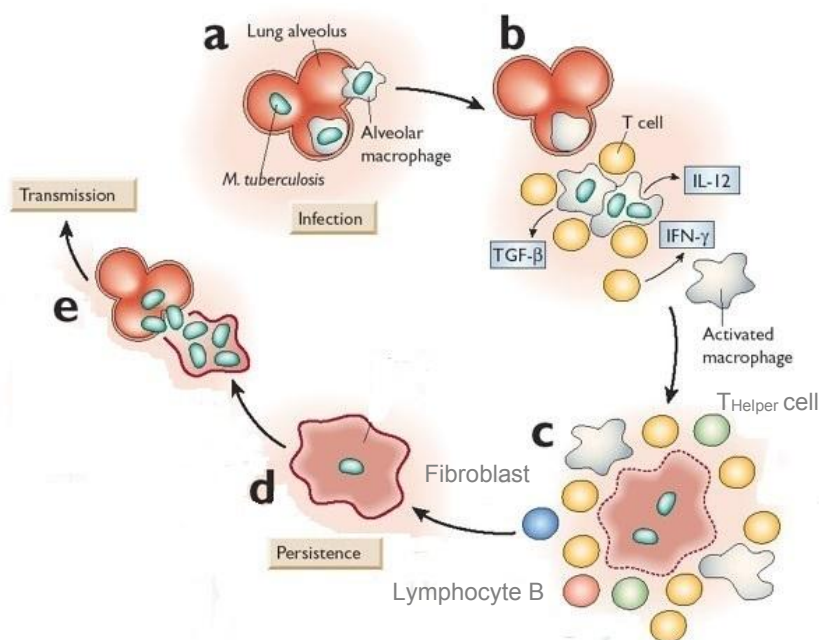


**Figure 1.3 Persistent infection with *M. tuberculosis*.** (a) Infecting mycobacteria taken up by alveolar macrophages in the lung resist killing by subverting phagosome maturation. (b) Inflammatory signaling in response to mycobacterial components results in the recruitment of T cells. T cell-mediated activation of macrophages enhances their ability to control mycobacteria. (c) Remaining viable mycobacteria are sequestered within a granuloma made up of macrophages and a variety of T cell subsets. (d) *M. tuberculosis* is able to persist in an asymptomatic form within the host. (e) Reduced immunity is associated with reactivation disease. Adapter from Young *et al.*<sup>20</sup>

Granulomas are important structures in the pathogenesis of tuberculosis.<sup>7</sup> These are very organized structures where *M. tuberculosis* resides within macrophages for a long time in a dynamic process.<sup>16</sup> Where infected macrophages begin the apoptosis process, can occur their elimination through phagocytosis by newly macrophages that were attracted to the granuloma.<sup>15,16</sup> They organize in clusters, containing infected macrophages in the centre, surrounded by macrophages, epithelioid macrophages, giant cells, dendritic cells, lymphocytes, neutrophils and fibroblasts.<sup>2,5,7,15</sup>

### 1.1.3. Antitubercular drugs

The goals of chemotherapy include cure without subsequent relapse, impediment of mycobacterium transmission, to minimize risk of death and disability, and prevention of drug resistance.<sup>10</sup> To achieve these goals, a long-term treatment is required, with a combination of drugs. The antitubercular drugs have different mechanisms of action and targets, which allow complementarity and an increase in the rate of efficiency. The antibiotics used in TB treatment are from different classes of antibiotics and have been classified as follows:

- a) **First-line antitubercular agents:** RIF, rifabutin (RFB), INH, pyrazinamide (PZA), ethambutol and streptomycin;
- b) **Second-line antitubercular agents:** ethionamide; fluoroquinolones (e. g. levofloxacin), aminoglycosides (e. g. capreomycin), para-aminosalicylic acid, and cycloserine;

The current recommended TB chemotherapy is a six-month regimen of four co-administered drugs in a directly observed treatment, ((DOTS) short-course)). For TB the following multi-drug therapy has been applied:

- a) An initial intensive phase of INH, RIF, PZA, and ethambutol daily for 2 months. A subsequent phase of RIF and INH for further 4 months, either daily or three times per week.<sup>7,10</sup>

The initial intensive phase aims at reducing the rapidly dividing bacilli load. In the second phase, a combination of two or three drugs for at least 4 months, is necessary to sterilize lesions containing fewer and slow—growing bacilli.<sup>10</sup>

Figure 1.4 indicates on the left current antitubercular drugs and their respective targets in *M. tuberculosis*. On the right side, new targets for potential drugs are indicated.<sup>7</sup> New targets and new drugs are necessary due to the emergence of MDR and XDR strains, the associations of drugs, with different mechanism of action, has the objective of raising the efficiency of treatment.

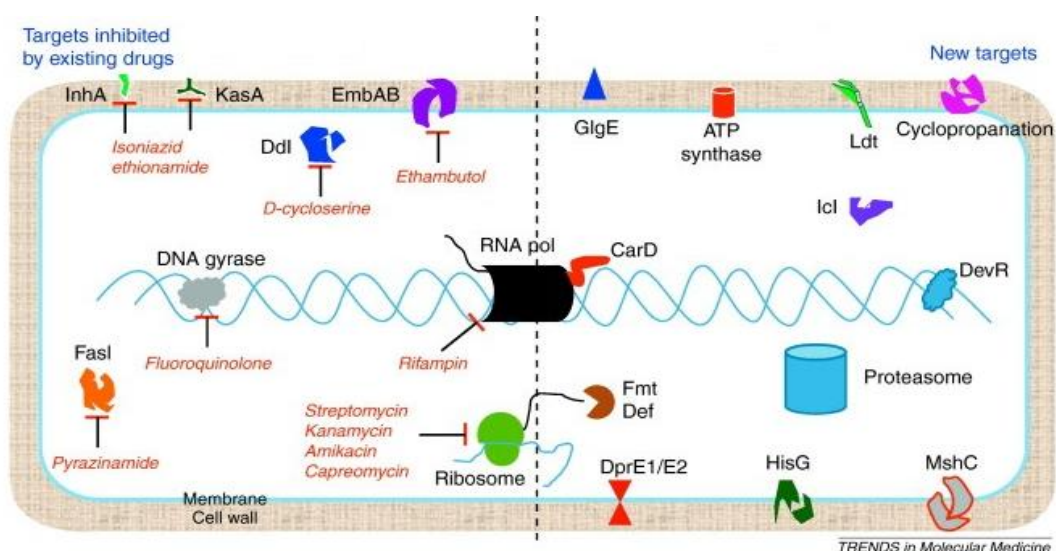


**Figure 1.4: Scheme of drug targets in *Mycobacterium tuberculosis*.** The targets that can be inhibited by existing drugs in the left and new targets in right side. Fatty acid synthase (Fasl), enoyl-acyl-carrier protein-reductase (InhA), b-ketoacyl ACP synthase (KasA), arabinosyltransferase (EmbAB), D-alanyl-D-alanine ligase (Ddl), DNA dependent RNA polymerase (RNA pol), DNA gyrase and ribosome are shown as targets inhibited by existing drugs used to treat TB. Recently identified targets include maltosyltransferase (GlgE), ATP synthase, L,D-transpeptidase (Ldt), decaprenylphosphoryl-b-D-ribose 20-epimerase (DprE1/E2), ATP phosphoribosyl transferase (HisG), mycothiol ligase (MshC), mycolic acid cyclopropanation, DosR(DevR), CarD, methionine aminopeptidase (Fmt), deformylase (Def), the proteasome complex and isocitrate lyase (Icl). Reprinted from Reference 25.

INH is a prodrug and must be activated by bacterial catalase. Specifically, the activation of this enzyme is associated with the reduction of the mycobacterial ferric KatG catalase-peroxidase by hydrazine and reaction with oxygen to form an oxyferrous enzyme complex.<sup>7,10</sup> Inhibin  $\alpha$  (InhA), a NADH-dependent enoyl-acyl-carrier protein-reductase, present in *M. tuberculosis*, and was initially identified as the target of isoniazid.<sup>21</sup> Once activated, INH forms a covalent adduct with the NAD cofactor. It is the INH-NAD adduct that acts as a slow, tight-binding competitive inhibitor of InhA. This inhibition blocks reductase of fatty acid synthase II (InhA) in mycolic acid biosynthesis, essential components of the bacterial cell wall.<sup>22</sup> At therapeutic levels, INH is bactericidal against actively growing intracellular and extracellular *Mycobacterium tuberculosis* organisms.<sup>23</sup>

RFB belongs to the group of rifamycins, sharing the same mechanism of action.<sup>7</sup> It inhibits bacterial ribonucleic acid (RNA) synthesis by binding to the  $\beta$ -subunit of bacterial deoxyribonucleic acid (DNA)-dependent RNA-polymerase, leading to blocking of the initiation chain formation in message RNA synthesis,<sup>7,10,21</sup> and, consequently, leading to death of *M. tuberculosis*.<sup>24</sup>

Although RFB is preferable to RIF because of the superior *in vitro* activity and the decreased risk of drug interactions,<sup>25</sup> RIF is mostly used due its lower cost comparatively with RFB.<sup>26</sup> RFB has been indicated by WHO, in the Guidelines for MDR-TB treatment, which include RFB as

first-line oral agent due to its potency and efficacy. This drug is strongly recommended for the treatment of HIV patients having TB.<sup>13</sup>

For the work presented in this thesis, INH and RFB were chosen as model antitubercular drugs. INH is a hydrophilic drug and its chemical structure is depicted in Figure 1.5 A. It has a molecular mass of 137.14 g/mol and the solubility is  $1.4 \times 10^5$  mg/L (25 °C).<sup>23</sup> In turn, RFB is a lipophilic drug (Figure 1.5 B), with molecular mass of 847.01 g/mol and minimal solubility in water ( $1.9 \times 10^{-4}$  mg/mL). Annex I presents a complementary characterisation of these drugs.

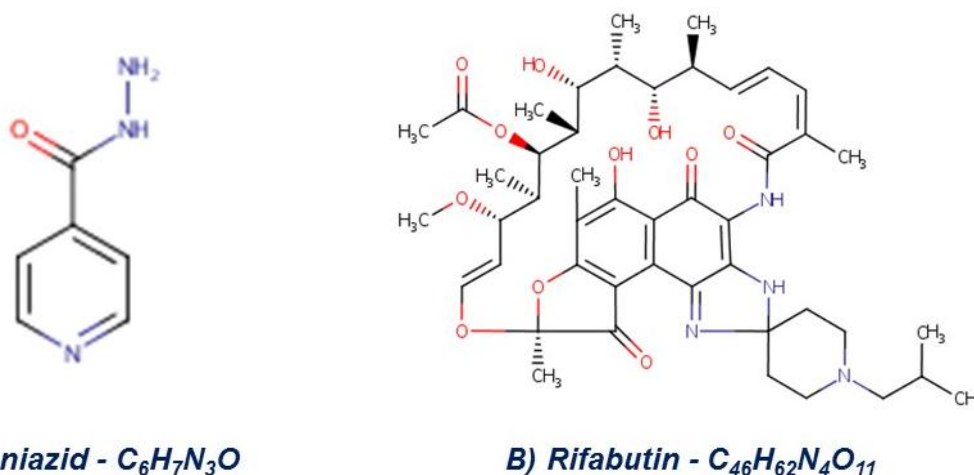


Figure 1.5: Structure and chemical formula of Isoniazid and Rifabutin. Adapted from DrugBank.<sup>23,24</sup>

## 1.2. Pulmonary drug delivery

Pulmonary drug delivery is a relevant approach in the treatment of respiratory diseases, as it allows direct targeting of the therapeutic agents to the site of action. As compared with a systemic delivery mediated by the oral or parenteral routes, pulmonary delivery permits site-specific drug deposition at high concentrations. In many cases, this local drug delivery is reported to reduce systemic exposure to the drug and, consequently, the occurrence of systemic side effects. Additionally, it provides the possibility of obtaining drug therapeutic effect with lower dose comparing with oral delivery, further permitting a more rapid response.<sup>27,28</sup> Inhalable therapy for the treatment of asthma and chronic obstructive pulmonary disease has been established and routinely used for decades.<sup>29</sup>

Systemic delivery of therapeutics via the lungs has been also investigated, mainly due to the identification of several advantageous characteristics of the lung for this effect. These characteristics include a high surface area (80 – 100 m<sup>2</sup>) available for absorption in the alveolar region, strong irrigation and a highly permeable epithelium for the absorption of drugs into systemic circulation.<sup>28</sup> Drug molecules are absorbed more efficiently from the lung than from any other non-invasive routes of drug administration. Pulmonary route offers multiple

advantages over oral route for large protein molecules, for instance, allowing to eliminate the degradation associated to the gastrointestinal tract and the first-pass effect.<sup>28</sup> For example, insulin and antigens have been tested in different carriers for pulmonary administration,<sup>12</sup> and insulin is currently available as inhalable product.

Inhaled drugs are becoming increasingly available on the market to treat various diseases, reflecting the advantage of the non-invasiveness of the route and the acceptance by the patient.<sup>27</sup>

### 1.2.1. Lung deposition

The effectiveness of an inhaled therapy is dependent of the aerosol characteristics, lung morphometry and pulmonary physiology. The site of deposition of an aerosol depends on its ability to reach a determined zone, which is strongly related with its aerodynamic properties, but also depends on the breathing pattern of the patient.<sup>27</sup> The aerodynamic properties are mainly defined by the aerodynamic diameter ( $D_{aer}$ ), a parameter commonly referred in the ambit of dry powder formulation, which congregates the contribution of both the geometric size of a particle and its density. The theoretical definition indicates that the  $D_{aer}$  of a particle is the diameter of a spherical particle of unit density ( $\rho_0$ ) which settles at the same terminal velocity as the particle in question.<sup>30</sup> There are several slightly different formulas enabling a theoretical calculation of this parameter. One of the most used in recent years is the following, which considers not only particle geometric size and density, but also its shape:<sup>27</sup>

$$D_{aer} = d \sqrt{\frac{\rho_{real}}{\rho_0 \lambda}}$$

Where  $d$  is the geometric diameter of the particle,  $\rho_{real}$  is the real density,  $\rho_0$  is unit density, and  $\lambda$  is the dynamic shape factor denoting deviation of shape from sphericity.<sup>30</sup>

Particle size is a parameter of major influence in lung deposition (Figure 1.6). Large particles ( $> 10 \mu\text{m}$ ) are reported to deposit in the upper airways (mouth, oropharyngeal and pharynx) by inertial impaction. When the size is between 5 and 10  $\mu\text{m}$ , the deposition mainly occurs in the trachea and bronchi. Particles with a size within 0.5 and 5  $\mu\text{m}$  deposit by gravitational mechanism (see below) and reach deeper areas. Sizes between 2 and 5  $\mu\text{m}$  are mainly deposited in bronchioles, while fine particles ( $< 2 \mu\text{m}$ ) mostly reach the alveolar zone, where they can be phagocytosed by macrophages (0.5 – 2  $\mu\text{m}$ ).<sup>31</sup> Smaller particles are mostly exhaled,<sup>27</sup> although some of them might deposit by Brownian diffusion in the alveolar region.

The latter results from the random movements of colloidal particles caused by collision with gas molecules.<sup>32</sup>

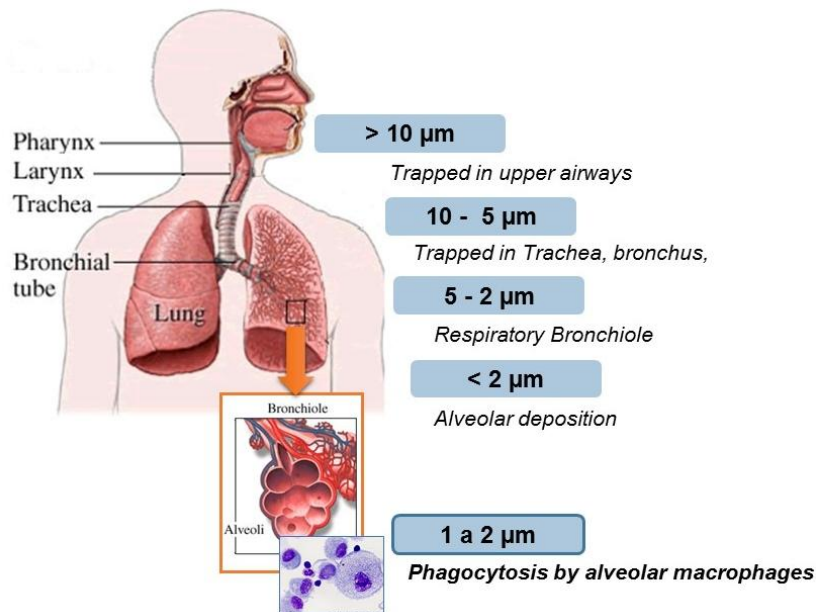


**Figure 1.6: Particle deposition in the lungs according to size.** Adapted from Nahar *et al.*<sup>33</sup>

The mechanisms of deposition are variable and depend on the lung region and particle physical parameters. Depending on their aerodynamic diameter, three mechanisms of deposition have been described: (1) inertial impaction, (2) sedimentation, (3) diffusion.<sup>1</sup> Figure 1.7 illustrated the three main mechanisms (from 1 to 3).

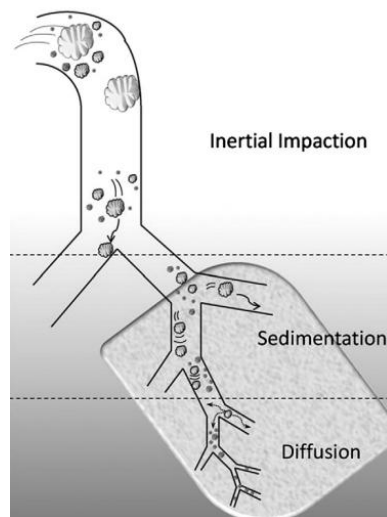


**Figure 1.7: Main mechanisms of particle deposition in respiratory tract.** Reprinted from reference 1.

Large particles are unable to maintain the movement on air stream due to their large size. Therefore, they tend to preferentially deposit in upper airways and tracheobronchial airways,

by inertial impaction. Smaller particles deposit by gravitational sedimentation in the tracheobronchial tract. Particles with  $D_{aer}$  of 0.5 to 1  $\mu\text{m}$  are subject to Brownian diffusive deposition. Some of these, as well of those having less than 0.5  $\mu\text{m}$  will possibly be exhaled.

Finally, it is important to mention that the mechanism(s) of deposition affecting a single particle might be influenced by the patient breathing pattern and, more specifically, its rate. Slow inhalation benefits the deposition of large particles, which normally deposit by impaction, allowing their increased penetration into lungs. In turn, smaller particles are much less sensitive to fast/slow inhalation variations. Additionally, a breath hold favours the capacity of particles to penetrate deep into the lungs and to sediment on airway surfaces.<sup>27</sup>

### **1.2.2. Pulmonary administration**

Pulmonary administration of drugs must be done using an inhalation system and, in recent years, it has been considered advantageous to use suitable vehicles to carry the drugs. The ideal device must generate an aerosol with suitable size for the intended objective of the administration, allowing reproducibility of drug dosing. Regarding the carrier, this is required to protect the drug formulation from the point of view of physical and chemical stability, evidencing a good aerosolisation pattern and reaching the desired site of action or absorption, features that are dependent on the aerodynamic properties. Moreover, the ideal inhalation system (device) must be simple to use, convenient, portable and inexpensive.<sup>34</sup>

The inhalation device might work with formulations under solid state (Dry Powders Inhalers – DPIs) or under liquid state. In the latter, Metered Dose Inhalers (MDIs) or nebulisers are the available systems.<sup>35</sup> Nebulisation is reported as the easiest administration mode to deliver aqueous solutions or suspensions of drugs of interest, namely antibiotics.<sup>36</sup> In this regard, tobramycin and aztreonam solutions have been approved in Europe for nebulisation in the ambit of CF.<sup>37</sup>

Nebulisers were the first inhalation devices available in the pharmaceutical market,<sup>34</sup> and the delivery is considered to occur under a controlled rate.<sup>35</sup> During nebulisation, liquid aerosols are generated by mechanical or electrical mechanisms. These devices have advantages, as they are easily used in all ages, from new-borns to the adulthood, including when patients are breathing tidally.<sup>9</sup> Moreover, they generate the aerosol with great efficiency, allow drug administration in high doses and independently of the breathing pattern of the patient.<sup>34</sup> However, some important disadvantages apply, as the administration by nebulisation is a time-consuming process (average of approximately 30 minutes) with simultaneous drug administration and clearance possibly occurring in this period, and presents poor

reproducibility. Moreover, medication preparation and time dedicated to equipment maintenance are long, associated to uncomfortable transport of the device.

Metered Dose Inhalers are devices using an aerosol propellant and a dose-metering valve to regulate the exit of defined doses by inhalation. These devices are extremely portable, a great advantage comparing with nebulisers, but require patient training to coordinate inspiration and actuation of the device. A long period between emission of the aerosol from the device and the beginning of inhalation leads to wastage of a proportion of the emitted dose.<sup>38</sup> Thus, poor coordination of actuation and inhalation, associated to high particle exit velocity, are parameters leading to major dose losses. The deposition of an aerosol in the upper airways can vary considerably according to the application technique. In MDI devices, losses of aerosol are routinely great than 70% and can exceed 90% and, consequently, the effectiveness of current aerosol therapy protocols are compromised.<sup>34</sup>

Dry Powders Inhalers (DPIs) were developed as an alternative to the previously described devices, presenting the great difference (and also advantage) of providing the drugs in solid state, in the form of dry powders.<sup>38</sup> As MDIs, DPIs are portable, but do not use propellants, instead combining powder technology with device design to disperse dry particles as an aerosol in patient's inspiratory airflow.<sup>34</sup> Studies have revealed improvement of treatment efficiencies and patient adherence as compared with nebulisers.<sup>36</sup> Again in the ambit of antibiotic delivery, tobramycin DPI has shown better results comparing with the nebulized formulation.<sup>9</sup>

The advantages of DPIs over other devices are noticeable. Apart from the referred portability and quick administration, DPIs are easy to use and maintain. The formulations, in dry powder, are more stable as compared with liquid counterparts,<sup>12</sup> do not require refrigeration and the maintenance of formulation sterility is ensured during the life-time of the device content, which is an important consideration for patients frequently highly susceptible to lung infection.<sup>9</sup> These advantages contribute to increased treatment efficiency and patient adherence, which was demonstrated for instance with the tobramycin DPI.<sup>36</sup> Naturally, DPIs also present disadvantages, the most important being a consequence of the proper actuation mechanism. As the inhaled dose is removed from the device by the inspiration of the patient, the aerosol characteristics and the lung deposition are highly dependent on the inhalation profile generated by the patient through the DPI. In this regard, forceful inhalation generates high inspiratory flows and possibly results in high deposition in upper airways, which can induce cough. Contrarily, slow and deep inhalation has been reported to improve the deposition into small airways, reducing upper airway deposition.<sup>9</sup> As a relevant feature, dry powders have a tendency to undergo particle agglomeration, increasing the aerodynamic diameters and, thus, lowering the respirable fractions. As a consequence, a lower number of particles reaches the

alveolar zone, which might affect the therapeutic effect of any formulation requiring reaching that zone, such as formulations aiming at a systemic effect or a local effect in the alveolar zone.<sup>31</sup> Another disadvantage of DPI concerns the amorphous or partly amorphous pattern of powders produced by spray-drying, a technique frequently used for their formulation. In that case, physical and chemical instability might arise, principally under conditions of high humidity.<sup>36</sup>

### 1.3. Inhalation as a strategy in tuberculosis therapy

The use of inhalable dry powders has been proposed in the context of tuberculosis therapy. The main interest is the formulation of INH, RIF, RFB and PZA dry powders, for their applications against MDR-TB and XDR, as it is expected that higher local concentrations of these drugs can be reached via the pulmonary route.<sup>13</sup> This approach might make resistant mycobacterium strains more susceptible to these drugs.<sup>5</sup> New drugs like TMC207, PA-824 and BTZ043 are in development for TB therapy and could also be interesting for pulmonary administration,<sup>12,38</sup> but so far no studies on their delivery through the lung route are available.<sup>12,39</sup> The use of new drugs, new formulations and the exploration of alternative routes of administration, other than the oral route, are necessary and urgent in order to revert the increasing bacterial resistance of *M. tuberculosis* against a growing number of currently used antitubercular drugs.

Different formulations and carriers are reported in the literature to provide good *in vivo* results regarding bacteria elimination upon inhalation. As an example, RIF, INH and PZA were loaded in alginate-chitosan nanoparticles by Zahoor *et al.*<sup>40</sup>, formulation presenting a high encapsulation efficiency (> 70%). About 80% of the nebulised formulation presented a suitable aerodynamic diameter for inhalation ( $1.1 \pm 0.4 \mu\text{m}$ ). Biodistribution studies performed in guinea pigs evidenced plasma bioavailability for a period exceeding 10 days, and concentrations higher than the minimum inhibitory concentration for up to 15 days in the main affected organs (lungs, liver and spleen). The formulation allowed increased drug residence time in the infection site comparing to free drugs. Chemotherapeutic studies in infected animals during 15 days (three nebulised doses) revealed a comparable result with 45 daily doses of free oral drugs, resulting in undetectable mycobacterial colony forming units in lung and spleen homogenates. Nanoparticles were also found to not elicit signs of hepatotoxicity, supporting their safety.<sup>40</sup>

Another relevant example concerns the use of liposomes. For example, INH-entrapped liposomes of dipalmitoylphosphatidylcholine presented about 750 nm in diameter and associated INH with efficiency of around 37%. *In vitro* alveolar deposition using the twin

impinger exhibited about 25-27% of INH deposition in the alveolar chamber upon one minute of nebulisation. Results further showed the biocompatibility and antimicrobial activity of the formulation.<sup>41</sup>

Notwithstanding the interest of the above formulations, dry powder formulations are frequently referred as the most adequate, particularly when lung delivery is at play. Several arguments can be used in favour, which include higher stability, low price, and disposable devices enabling the use in developing countries, where MDR and XDR-TB prevalence is higher.<sup>10, 36, 42</sup> Again, the literature displays many examples of dry powders proposed for tuberculosis therapy. Most of them are based on synthetic polymers. A relevant example is comprised of polylactic-co-glycolic acid (PLGA) microparticles encapsulating RIF. Spherical RIF-PLGA microspheres had  $D_{aer}$  of 1.9  $\mu\text{m}$  and were taken up efficiently by NR8383 cells (rat alveolar macrophages). Fluorescent microscopic analysis has shown that RIF-PLGA microparticles were localized in phagolysosomes, and then degraded.<sup>43</sup>

There are many methods to produce dry powders, which include spray-drying, freeze-drying and emulsification-based techniques, among others. Depending on the used technique, either hydrophilic or hydrophobic drug molecules might be integrated in the formulations.<sup>12</sup> In occasions, both types simultaneously.<sup>44</sup> Drug physicochemical properties should be taken in account and, ideally, drugs inhaled as dry powders should be crystalline for maximal stability.<sup>42</sup> Spray dried, spray-freeze dried and freeze dried powders are obtained from solution and, due to the rapid drying, they are mostly amorphous.<sup>36,42</sup> These are more susceptible to water uptake, which may lead to re-crystallisation and solid bridge formation between the particles, which does not benefit powder dispersion.<sup>12</sup> The chemical nature of a drug can also influence the resulting dry powder properties,<sup>42</sup> such as cohesiveness, flowability and compatibility, which interfere in the dispersion efficiency and retention in the inhaler, as well as on the size, surface properties and shape distribution.<sup>12</sup>

### **1.3.1. Spray-drying to produce inhalable dry powders**

Spray drying (SPD) has been frequently used to produce dry powders with suitable properties for lung inhalation and presents the great advantage of permitting scaling-up.<sup>36</sup> A spray-dryer can be operated in different modes: open cycle, closed-cycle and semi-closed cycle with or without aseptic conditions.<sup>45</sup> The open cycle consist in intakes of drying gas from atmosphere and the expulsion of air into atmosphere after separation of microparticles by a cyclone. The closed-cycle operates with formulations containing flammable solvents. Semi-closed cycle is an intermediate between open and closed cycle dryers. In this system the drying gas is

recycled and it has a very low oxygen content, making it suitable for materials that cannot be exposed to oxygen, either because of risk of explosion or product degradation.<sup>46</sup>

SPD process consists of four steps, as described in figure 1.8: (a) atomization of a feed solution or suspension into a spray; (b) warm spray-air interpenetrating into flow; (c) drying of sprayed droplets at elevated temperatures; and (d) separation of dried product from the air in cyclone.<sup>45</sup> Obtained powders are collected in the product vessels.<sup>47</sup> In figure 1.8 is schematized the operating mode of Spray dryer mini B290.<sup>48</sup>

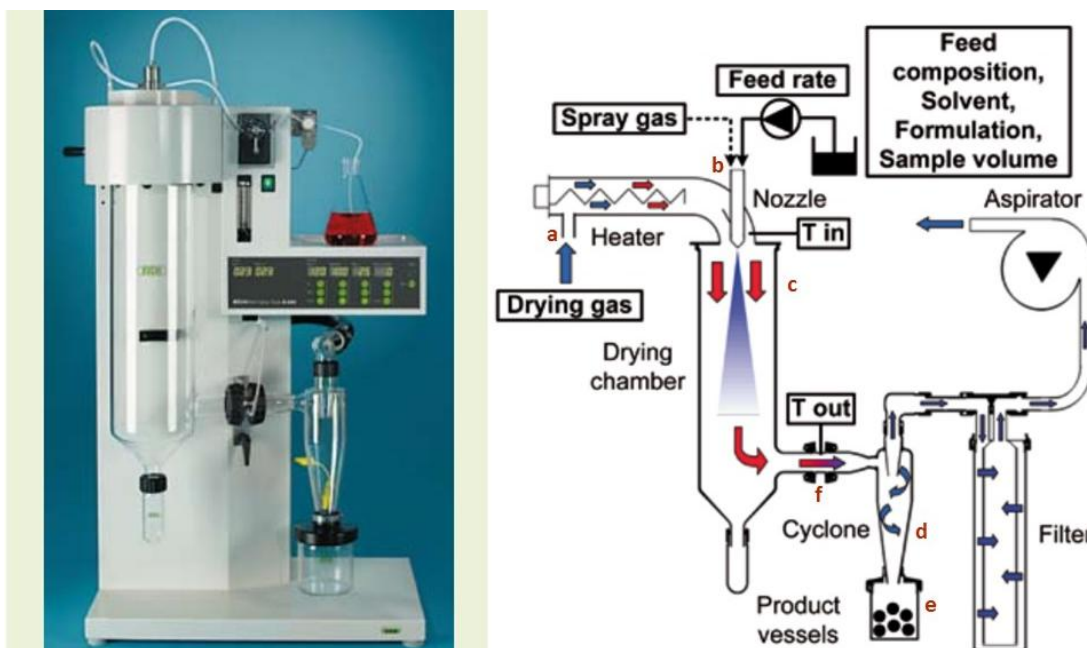


**Figure 1.8: Scheme of the Buchi B-290 Mini Spray dryer.** The figure shows an open-mode. Solution or suspension with drugs/proteins and carriers get in nozzle where a spray is formed. (a) The drying gas is heated at a defined temperature (Inlet T) and interpenetrates into flow (b), (c) the droplets are dried in a drying chamber, (d) and enter the cyclone, where they are separated by helical motion of the air flow. (e) The obtained powder is collected in product vessels. (f) Outlet temperature is recorded after evaporation of the solvent. Reprinted from reference 48.<sup>48</sup>

Spray-drying is a cost-effective particle engineering technique that permits the modulation of MPs characteristics, namely geometric size, density, and shape. An adequate combination of these parameters enables the production of MPs with suitable aerodynamic properties for pulmonary delivery.<sup>45</sup> To the optimization of the final microparticles product should be tested different combinations between the operating parameters, such as drying temperature (inlet) and flow rate of drying gas, feed properties, feed rate, pressure and amount of atomizing air into drying chamber.<sup>45</sup> The combination of these parameters, which might be adjusted by the operator, will influence the following parameters: droplet size, outlet temperature of air, drying efficiency and physical properties of final product, as particle size, moisture content and hydrosocopicity.<sup>49</sup>

Some parameters are more important than others and have a major impact in the process. The difference in the inlet and outlet temperature, and the percentage of liquid in the formulation are the driving force for the drying process.<sup>48</sup> These two parameters are interdependent. Spray dryer dimension and the drying airflow rate are determinant on the residence time of the droplets in drying chamber, which influences the drying time. The volume of atomized droplet has a control over particle size, and the solution or suspension concentration control the average density.<sup>47</sup>

Particle shape/morphology can be controlled by varying the feed solvent, where a mixture of alcohol and water can be included, or adjusting the outlet drying temperature.<sup>47</sup> Atomization rate and feed concentration can be concomitantly wrought to generate particles with different degrees of surface corrugation. The production of particles with a rough surface might be achieved by the inclusion of common excipients, such as polysorbate 20 and lactose.<sup>45</sup> The addition of some excipients such as leucine or mannitol can improve dispersibility. Adding leucine to the feed solution leads to weaker particulate interactions, due to the low surface-energy leucine that forms a rough shell or coating on the outer surface of spray-dried particles.<sup>36</sup>

SPD can be further adjusted for better product recovery and larger production scale, particularly for thermolabile materials such as proteins and peptides. Design of high-efficiency cyclone separation is crucial for this engineering to be economically acceptable on an industrial scale.<sup>45</sup> This technique can be rendered more versatile by suitable modification to select specific needs.<sup>48</sup> For example, the dryer can be adapted to aseptic processing of heat sensitive materials by ultrasonic atomization of feed solution into an atmosphere under reduced pressure to aid removal of the solvent at a much lower temperature.<sup>45</sup> This technique has been employed for the manufacturing of inhaled proteins, for example, insulin (Exubera<sup>®</sup>, Pfizer), or antibiotics (Tobramycin TOBI<sup>®</sup> Podhaler<sup>®</sup>, Novartis), or for the development of microparticles, such as PulmoSphere<sup>™</sup> technology.<sup>36</sup>

SPD is a particle engineering technique that allows microencapsulation of proteins, thermolabile and/or hygroscopic drugs,<sup>36</sup> and the amount of solvent in the final product is residual comparing with other techniques.<sup>34</sup>

### **1.3.2. Matrix materials for inhalable dry powder formulations**

Biopolymers have been widely explored as matrix materials of drug carriers, owing to structural flexibility, biocompatibility and biodegradability.<sup>50</sup> The non-immunogenicity and non-cytotoxic properties of many polymers are preferential for applications in biomedical

sciences.<sup>51</sup> Furthermore, the possibility of undergoing enzymatic or hydrolytic degradation becomes an eligible mechanism for controlled drug release. It is also necessary that the degradation products are biocompatible.<sup>52</sup> Natural polymers have great advantages over synthetic polymers, not only because they are in principle more prone to biodegradability and biocompatibility, but also because they exhibit structural flexibility and are readily available at relatively low prices.<sup>53</sup> Moreover, they are easily modified by simple chemical reactions<sup>52</sup> and their processing for drug carrier production usually does not involve organic solvents, as happens with synthetic polymers, because of the hydrophilic nature. Therefore, there is no need to eliminate solvent residues and associated production costs are decreased. Natural polymers, however, present some disadvantages, which include the inter-batch variability, as well as complex and varied composition and low mechanic properties.<sup>11</sup>

Polysaccharides have been marking a strong position in the biomedical field, due to their favourable physical properties and the chemical structure that allows applications in different areas, such as drug delivery, tissue engineering and diagnostic. They can be used as emulsifying, gelling, hydrating, thickening and suspending agents in diverse applications in the above cited areas.<sup>51</sup>

Regarding the formulation of new carriers with application in inhalable tuberculosis therapy, synthetic polymers belonging to the group of polyesters take the leadership of proposals.<sup>12</sup> Particularly, polylactic acid (PLA) and PLGA are the most envisaged.<sup>10,52</sup> However, because of the properties that were mentioned above for natural and synthetic polymers, using the former could be advantageous. Natural polymeric carriers might be produced involving in their matrixes polysaccharides, polynucleotides and proteins. Polysaccharides are cheaper materials having a very flexible structure and have been used very frequently in drug delivery in general, and also in the particular application of tuberculosis inhaled therapy.<sup>11</sup>

Polysaccharides are saccharide polymers that are composed of saccharide units linked together by glycosidic unions.<sup>54</sup> The basic units composing these polymers are mainly D-glucose, D-fructose, D-galactose, L-galactose, D-Mannose, L-arbinose and D-xylose, although D-glucose is the most frequently found. Some polysaccharides further present monosaccharide derivatives in their structure, such as simple sugar acids (gluronic acid and iduronic acid) and the amino sugars D-glucosamine and D-galactosamine and their derivatives, such as N-acetylneuraminic acid.<sup>51</sup> The specific monosaccharides and their derivatives, the degree and steric configuration of the substitutions, the linkages and the final molar mass, are some of the features of polysaccharides dictating their specific physicochemical properties, such as solubility and viscosity, as well as the bioactive properties.<sup>53</sup>

Polysaccharides are many times divided in groups according to their composition, for example, celluloses, hemicelluloses and pectins.<sup>54</sup> Hemicelluloses, for instance, are a type of heterogeneous polysaccharides composed of glucose, xylose, mannose, and galactose.<sup>53,54</sup> Xylans present a backbone of  $\beta$ -(1-4)-linked xylopyranosyl units.<sup>53</sup> Mannans include galactomannans, which have a  $\beta$ -(1-4)-linked D-mannose backbone to which is attached a single  $\alpha$ -D-galactose at the C<sub>6</sub> position of D-mannose; glucomannans, which have a random distribution of  $\beta$ -(1-4)-linked D-glucose and  $\beta$ -(1-4)-linked D-mannose in the main chain;<sup>54</sup> and galactoglucomannans with additional side chains of  $\alpha$ -D-galactose linked to the mannose backbone. Xyloglucans are also reported, which have a common structure of  $\beta$ -(1-4)-linked D-glucan, and three out of four glucose residues are substituted with  $\alpha$ -D-(1-6) xylose.<sup>53</sup> Some dry powder formulations with these polymers have been proposed for tuberculosis therapy. Microparticles of gelatin/ sodium carboxymethyl cellulose,<sup>55</sup> chitosan,<sup>56</sup> alginate/chitosan,<sup>57</sup> hyaluronic acid,<sup>58</sup> chitosan/hydroxypropylmethylcellulose and hydroxypropylcellulose,<sup>59</sup> have all been proposed to encapsulate antitubercular drugs and claimed an application in inhaled tuberculosis therapy. In some cases, spray-drying was the technique used for powder production (reference 58 and 59).

### 1.3.2.1. Locust bean gum

Locust bean gum (LBG) is a neutral polysaccharide composed of mannose and galactose monomers, thus belonging to the category of galactomannans. It is extracted from the crush of the endosperm of the seeds of *Ceratonia siliqua* (carob tree), depicted in Figure 1.9.<sup>51</sup> This tree is very abundant in the Algarve and Mediterranean regions, North Africa, South America and Asia.<sup>50</sup>

Carob seeds represent 10% of the weight of the fruit of carob tree. The endosperm of seeds is composed of about 80% galactomannan and 20% of proteins (albumin, globulin and glutelin) and impurities.<sup>60</sup> Crude galactomannan can be purified in order to eliminate these contaminants, for instance by precipitation with ethanol, methanol or isopropanol, by enzymatic and alkaline hydrolysis or by formation of copper or barium complexes. In general, whatever the option, the obtained product has a higher mannose/galactose ratio and a residual amount of proteins and impurities.<sup>50</sup>

LBG structure consists of a linear chain of a (1-4)-linked  $\beta$ -D- mannopyranosyl units with (1-6)-linked side chains of  $\alpha$ -D-galactose, as represent in figure 1.9.<sup>50,51,61</sup>

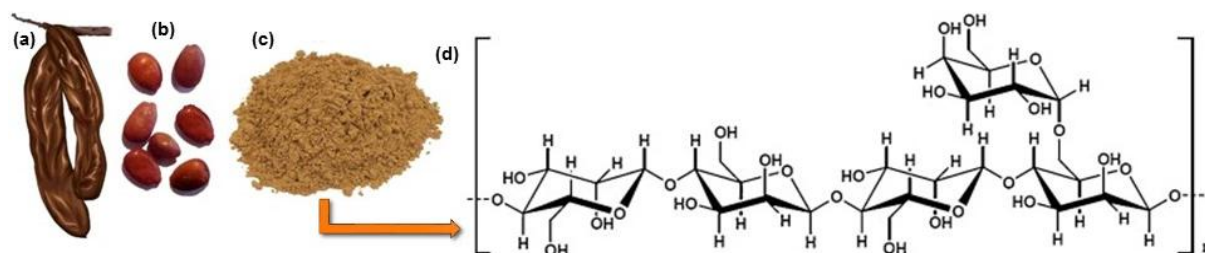


**Figure 1.9: Locust bean gum:** Pod (a), seeds (b), crude powder (c) and chemical structure (d). The structure is a linear backbone of (1-4)- $\beta$ -linked mannose units with single (1-6)- $\alpha$ -D-galactose units attached. Adapted from reference 50 and 51.<sup>50,51</sup>

The ratio of D-galactose to D-mannose differs in the various galactomannans, reflecting different substitution pattern of side-chain units. The molecular weight is also different, being influenced by the origin and growth conditions of the plant during production, harvesting and manufacturing practices, amongst other factors.<sup>51</sup> For these reasons, the Mannose and galactose (M/G) ratios of galactomannans are always referred as approximate (3/1 for tara gum and 2/1 for guar gum).<sup>50</sup> In the literature, specific data indicates for LBG a variation from 3.1/1 to 4/1. As such, LBG molecular weight is generally described to be approximately 310 kDa, but different sources refer values ranging from 0.3 to 2.0 million Da.<sup>61</sup>

The polymer is reported to have an acceptable shelf-life.<sup>51</sup> The physicochemical properties of galactomannans are also influenced by the distribution and number of galactose units along the mannose backbone. The solubility is strongly influenced by the M/G ratio, due to the fact that mannose chains are relatively hydrophobic and galactose units are more hydrophilic. For this reason, LBG solubility is limited, forming aggregates in cold water, as the long segments of unsubstituted mannose are likely to undergo aggregation.<sup>50</sup> Although it is a neutral polymer, solubility and viscosity are described to be slightly affected by pH changes within the range of 3-11.<sup>51</sup>

For biopharmaceutical and tissue engineering applications, an important issue to assess is the *in vivo* biodegradability and biocompatibility of polymer-based materials. Dey *et al.* classified LBG as biocompatible, bioabsorbable and biodegradable, showing ready excretion of degradation products.<sup>62</sup> It is non-teratogenic and non-mutagenic according to the Joint Food American Organization/WHO Expert Committee on Food Additives held in Geneva, in April'75.<sup>51</sup>

LBG has been explored in some applications of the pharmaceutical and biomedical sciences. In pharmaceutical technology, it has been included in drug delivery systems for different applications: mucoadhesive formulations and matrix tablet preparations. Furthermore, different administration routes have also been addressed, including the oral, buccal, colonic, ocular and topical.<sup>51</sup> For example, a commercially available tablet system (TIMERx<sup>®</sup>) developed by

Penwest Pharmaceuticals Company consisting of locust bean gum and xanthan gum displays both *in vitro* and *in vivo* controlled release potential. Nevertheless, to the best of our knowledge, the application of LBG in the context of pulmonary delivery was not proposed before, neither was its processing using spray-drying. With its composition based on mannose and galactose, LBG is a strong candidate for the formulation of carriers aimed at macrophage targeting.

#### **1.3.2.1.1. Locust bean gum as carrier for targeting of alveolar macrophages**

Tuberculosis infection occurs principally in respiratory tract due to the propagation of *M. tuberculosis* via inhalation. For this reason, the airways are the main target area for antitubercular drugs. Currently, investigators and clinicians argue the replacement of oral and intravenous therapies with inhaled antibiotics therapy, due to the fact that this therapy would allow higher local drug concentrations and less systemic side effects with the same dose. Different approaches are discussed and three strategies can be distinguished: (a) inhaled antibiotics can be used for replacement or added-onto oral and intravenous therapy; (b) specific targeting of alveolar macrophages; (c) searching for synergistic drug combinations. These strategies can be developed and applied in association.<sup>12</sup>

Targeted drug delivery of the alveolar macrophages has been considered an attractive strategy for the treatment of infectious diseases related with intracellular pathogens, such as *Mycobacterium tuberculosis*, *Mycobacterium leprae* and *Salmonella enterica*.<sup>6</sup> Specifically, *M. tuberculosis* survives for a long time and can replicate in the phagosomes of the alveolar macrophages, and dendritic cells. Therefore, it is important to consider for TB therapy a high antibiotic concentration on the alveolar area where infected macrophages reside, along with a strategy to specifically target alveolar macrophages.<sup>12</sup>

Aerosolizing antitubercular drugs without any carrier may not be adequate to target *M. tuberculosis* residing inside macrophages. Their formulation in delivery systems that can simultaneously have an adequate aerodynamic diameter and be phagocytosed by macrophages would be the most adequate. Particles with  $D_{\text{aer}}$  between 0.5 to 2  $\mu\text{m}$  are suitable to reach the alveolar zone and those of 1-2  $\mu\text{m}$  have an ideal size for macrophage uptake.<sup>63</sup> Another advantage is that, after phagocytosis, macrophages may migrate to the periphery of lung granulomas leading to increased drug penetration.<sup>5</sup> As described above, different delivery systems have been engineered to incorporate antibiotics to target macrophages. Although targeting macrophages is a promising approach, there are several uncertainties and risks that need to be considered, particularly regarding long term

toxicological effects of the used excipients.<sup>12</sup> Synthetic microparticles, such as those composed by PLGA and PLA, have been tested as carriers of antitubercular drugs. As they are insoluble in water, dissolution and systemic absorption will not occur and, therefore, macrophage uptake is favoured.<sup>63</sup> However, natural polymers might be preferred over synthetic ones regarding the matrix composition because of higher propensity for biocompatibility and biodegradability, which are expected to provide better long-term toxicological profile.

Several drug carriers, microparticles and nanoparticles, have been produced with modified surfaces to exhibit ligands with specific affinity for macrophage surface receptors.<sup>64</sup> For example, Brandhonneur *et al.* demonstrated that surface modification by grafting cell-specific ligands (agglutinin, RGD and mannose-PEG3-NH<sub>2</sub>) on PLGA microparticles increased their uptake by macrophages.<sup>65</sup>

As mentioned before (section 1.1.2), macrophages have unique surface receptors that might recognise preferentially several polysaccharide moieties present on the surface of infecting organisms, including in the bacterial cell wall.<sup>57,64</sup> Phagocytosis-related receptors present on macrophage surface are ideal structures for macrophage-targeted therapy.<sup>17</sup> One of the receptors involved in macrophage surface recognition of materials is the mannose receptor, known to recognise not only mannose units, but also fucose, N-acetylglucosamine units and sulphated sugars.<sup>17,66</sup> For this reason mannose has been described as a functional group that can mediate the direct targeting of carriers to macrophages,<sup>67</sup> and its use has been approached in several works describing the mannosylation of antitubercular drug carriers.<sup>6,63</sup>

Benefiting from a similar composition regarding the referred moieties, polysaccharides might be good candidates to compose the matrix of drug carriers aimed at macrophage targeting, as they can use the same recognition pathways of the infecting organisms.<sup>17</sup> Additionally, polysaccharides present the advantage of being natural polymers, with the consequent propensity for biocompatibility and biodegradability described before. In particular, galactomannans having a composition based on mannose and galactose units, are promising regarding the described approach, as mannose and galactose units are expected to be favourably recognised, respectively, by mannose receptors and galactose lectin receptors, potentiating macrophage uptake.<sup>6,17,68</sup>

## 2. Objectives

This proposal is aimed at developing and testing the ability of locust bean gum (LBG) to be used as matrix material of microparticles produced by spray-drying, and proposing these as carriers for the pulmonary administration of antibiotics. The antibiotics isoniazid and rifabutin were selected as model drugs, thus directing the developed formulations to the treatment of tuberculosis.

To accomplish the referred general objective, several partial objectives were considered, which are disclosed below:

- 1) To optimize the conditions to produce LBG-based microparticles with the particular focus of enabling deep lung delivery;
- 2) To associate to the microparticles the model antibiotics isoniazid and rifabutin, either individually or in association;
- 3) To characterize the microparticles regarding their morphology and aerodynamic properties;
- 4) To investigate the drug release profile in media relevant for the objective of lung delivery and tuberculosis therapy;
- 5) To evaluate the cytotoxicity of microparticles in human cell lines that are relevant for the application;
- 6) To evaluate *in vitro* the microparticle capacity to induce macrophage activation and capture, in two lines of macrophages (human and rat).

### **3. Materials and Methods**

#### **3.1. Preparation of locust bean gum microparticles by spray-drying**

##### **3.1.1. Preparation of polymer dispersions**

Microparticles were designed to have a polysaccharide matrix based on locust bean gum (LBG,  $C_{30}H_{50}O_{26}$ , molecular weight approx. 310 kDa, Sigma-Aldrich, Germany). To enable the formation of a LBG dispersion with adequate viscosity to permit spray-drying, the addition of hydrochloric acid (HCl) was required.

As depicted in figure 3.1 route A, to prepare the dispersions for spray-drying LBG was triturated in a glass mortar for 10 minutes, after which 5 mL HCl 0.1 M were slowly added and grinding continued. This was followed by the addition of purified water previously heated to 85 °C, up to a final volume of 50 mL. The concentration of LBG in the final dispersion was 2% (w/v). The dispersion was maintained under magnetic stirring for 30 minutes, and subsequently placed on a water bath at 85 °C under slow stirring for additional 30 minutes. At the end, the dispersion was kept under stirring overnight, until the moment of spray-drying.

Two antitubercular drugs were associated to the microparticles, INH and RFB. These were incorporated in the dispersion at different phases, depending on their solubility in water. INH ( $C_6H_7N_3O$ , molar mass 137.14 g/mol, Sigma-Aldrich, Germany)<sup>23,69</sup> is a hydrophilic drug. It was first triturated in a porcelain mortar, then weighed in a test tube and solubilised with purified water for 10 minutes. Afterwards, the dissolution was slowly added to the LBG polymeric dispersion (2%, w/v), formed as indicated above. The LBG.INH dispersion was kept under stirring another 90 minutes until spray-drying (Figure 3.1, route A and B). The amount of drug incorporated in the formulation corresponded to an LBG.INH mass ratio of 10:1.

RFB ( $C_{46}H_{62}N_4O_{11}$ , molar mass 847.00 g/mol, Chemos, Germany)<sup>70</sup> is a lipophilic drug and was mixed with LBG powder prior to any dissolution. The mixture of the two solid materials was performed by geometric dilution, and trituration took place in a glass mortar. After grinding, the same procedure used to prepare the LBG dispersion (without drugs) was followed (Figure 3.1, route C). RFB was associated to LBG in amounts leading to LBG.RFB mass ratios of 10:1, 10:0.5 and 10:0.2.

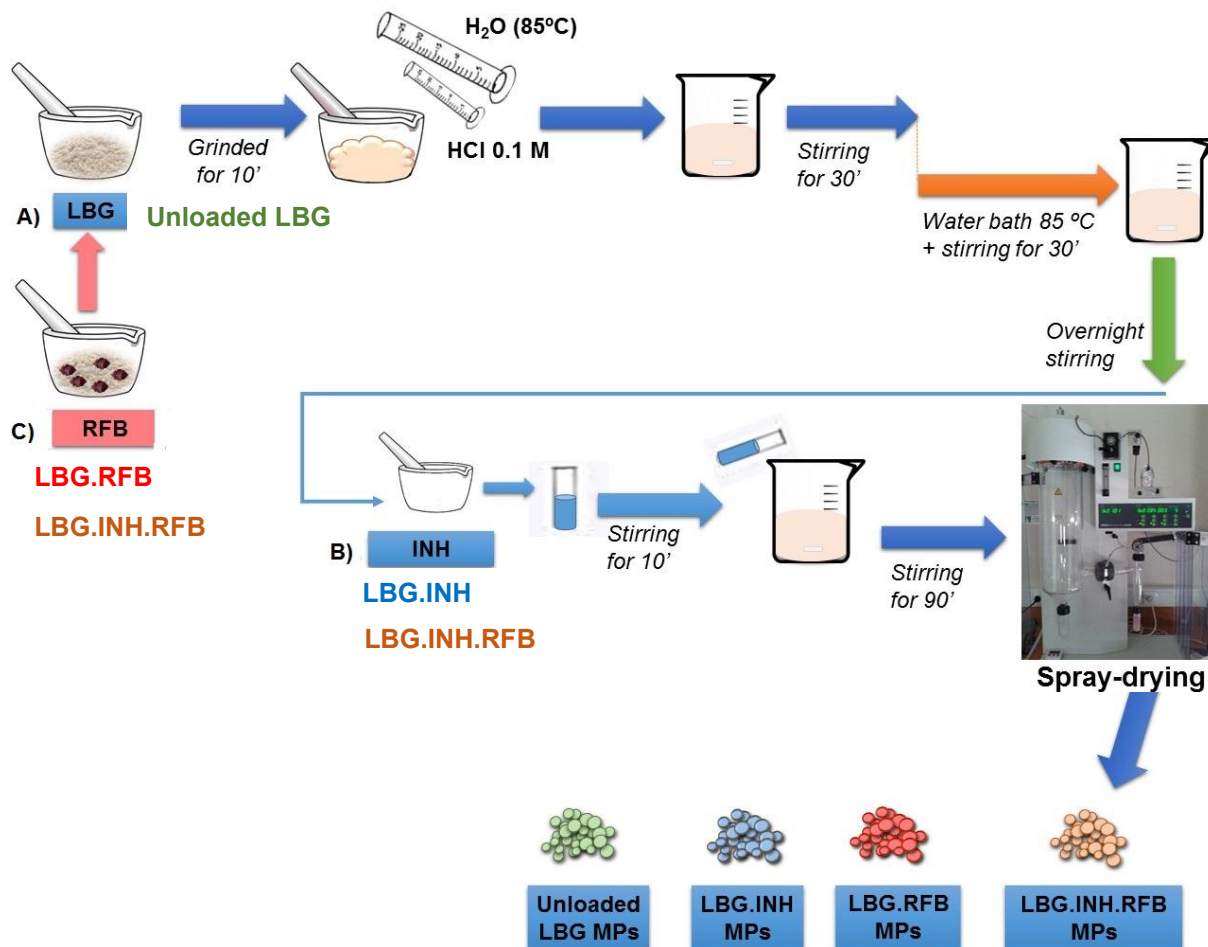


**Figure 3.1: Schematic representation of experimental steps involved in the preparation of LBG microparticles, unloaded or loaded with antitubercular drugs.** A) Method of preparation of LBG dispersion is the basis of the process. B) INH was previously triturated and dissolved in water, being subsequently added to the LBG or LBG.RFB dispersion for the preparation of formulations LBG.INH and LBG.INH.RFB, respectively. C) Rifabutin was added to the LBG powder, and both were triturated. Rest of protocol was the same applied for LBG only. INH: Isoniazid, LBG: Locust bean gum; RFB: Rifabutin.

When a concomitant association of both drugs was performed, the procedures used for the isolated drugs were applied. In summary, RFB was always added at the beginning, undergoing grinding with LBG, and INH was first dissolved separately and then added to the previously formed dispersion of LBG.RFB (Figure 3.1, route B and C). The formulations of drug association reflected the drug amounts of individual formulations: INH was always associated at a LBG.INH mass ratio of 10:1, while RFB was associated at both 10:1 and 10:0.5. Therefore, two formulations of drug association were produced: LBG.INH.RFB = 10:1:1 and 10:1:0.5.

### **3.1.2. Spray-drying of polymer/drug dispersions**

Polymeric dispersions (LBG) with or without drugs were spray dried using a Büchi B-290 laboratory mini spray dryer (Büchi Labortechnik AG, Switzerland) equipped with a high performance cyclone. In order to obtain microparticles with adequate aerodynamic and flowing properties regarding the objective of lung delivery to reach the alveolar zone, the operating parameters were optimized as follows: inlet temperature:  $160 \pm 2$  °C; aspirator setting: 85%; feeding speed:  $0.8 \pm 0.1$  mL/min; and spray flow rate: 473 L/h. These conditions resulted in outlet temperature of  $102 \pm 1$  °C. After spray-drying, the microparticles were collected, placed in a dark flask and stored inside a desiccator until further use.

Mannitol ( $C_6H_{14}O_6$ , mass molecular 182.17 g/mol, Sigma-Aldrich, Germany)<sup>71</sup> microparticles were also produced to be used as control in certain assays. A solution of 2% (w/v) was prepared and spray-dried at inlet temperature: 160 °C, aspirator setting: 80%; feeding speed:  $1.6 \pm 0.1$  mL/min; and spray flow rate: 473 L/h. These conditions resulted in outlet temperature of  $88 \pm 1$  °C. After spray-drying, the microparticles were collected, placed in a flask and stored inside a desiccator until further use.

The spray-drying yield was calculated by gravimetry, comparing the total amount of solids initially added for the preparation of the spraying dispersions with the final amount of microspheres that was collected ( $n = 3$ ).

### **3.1.3. Production of fluorescently labelled microparticles**

Certain assays required the use of fluorescent microparticles, such as the determination of microparticle uptake. Unloaded fluorescent LBG microparticles were obtained by spray-drying in the same conditions described above for unlabelled LBG (the only modification was a slight adjustment of acid volume, in this case 1.5 mL for the 50 mL of final volume). The attribution of a fluorescent label was provided by fluorescein, which was chemically associated to LBG polymeric structure. The setup of the chemical reaction was performed taking into account the number of primary nucleophilic groups ("OH") in each LBG monomer, and it was decided to label 10% of this structural unit. Figure 3.2 describes the synthesis reaction. At pH 4, fluorescein reacted with N-(3-dimethylaminopropyl)-N'-ethylcarbodiimide hydrochloride (EDAC), which donates one "OH" group to fluorescein, resulting in the formation of reactive groups in this molecule. These groups will then react with the nucleophilic groups present in the structure of LBG, thus allowing the synthesis of a fluorescent polymer.

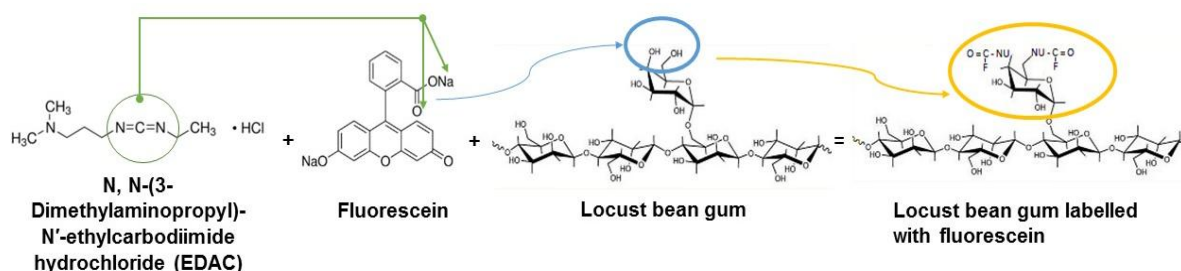


**Figure 3.2: Synthesis reaction of fluorescent LBG:** N, N-(3-Dimethylaminopropyl)-N'-ethylcarbodiimide hydrochloride (EDAC) reacts with fluorescein (green arrows), forming a reactive group that will attack the nucleophilic group of LBG structure (indicated in blue). LBG labelled with fluorescein is obtained, which is represented by F, this group being surround in yellow.

To initiate the reaction, LBG (1.0 g) was solubilized in HCl at the concentration of  $1 \times 10^{-4}$  M (pH 4) in order to obtain a final LBG concentration of 1% (w/v). The dispersion was maintained under magnetic stirring for 30 minutes, and subsequently placed on a water bath at 85 °C, under slow stirring, for additional 30 minutes. At the end, the dispersion was kept under stirring overnight, until the addition of fluorescein and EDAC.

Fluorescein (45.5 mg) was solubilised in ethanol 96% (v/v) and added to the previously formed LBG dispersion. The added amount of fluorescein was calculated to represent approximately 2% of number of moles of LBG. EDAC (34.79 mg) was dissolved in milli-Q water, and added to the dispersion. This was kept under stirring for 72 hours, protected from light.

After this time, the dispersion was inserted on a dialysis membrane (Sigma Aldrich, Germany; molecular-weight cut off of 2000 Da) in order to eliminate unreacted fluorescein and other reaction sub products. In dialysis, a low stirring rate was maintained, and water was changed twice a day during one week. When the water became clear, the dialysis was assumed to be finished, the suspension was placed in glass petri dishes and placed at -20 °C. After initial freezing, samples were placed at -80 °C for 3 days and finally lyophilized for 48 hours (FreeZone Benchtop Freeze Dry System, LABCONCO, USA). The labelled polymer was weighed and stored in a desiccator until further use, under light protection.

Poly (vinyl alcohol) (PVA) was also labelled for the same purpose, following the same protocol described above for LBG. As PVA ( $[-\text{CH}_2\text{CHOH}-]_n$ ,  $M_w$  89 - 98 kDa, Sigma-Aldrich, Germany)<sup>72</sup> has higher amount of nucleophilic groups as compared with LBG, in order to maintain the percentage of labelling, a comparison of the number of carbon atoms per monomer in PVA and LBG was established. PVA has  $\frac{1}{4}$  of LBG carbons and it was decided to label only 0.5% of moles of this polymer. PVA (1 g) was dissolved in HCl  $10^{-5}$  M at 1% (w/v). This solution was maintained at 80 °C under stirring overnight, until two hours before adding fluorescein and EDAC. Fluorescein (43 mg) was pre-dissolved in ethanol 96% (v/v), EDAC (33 mg) was pre-dissolved in water and both were then added to the solution. This was kept under

stirring for 72 hours under light protection. After this time, the solution was transferred to a dialysis membrane, and was kept in dialysis for one week. As in LBG, the solution was frozen at -20 °C, then placed under -80 °C, and lyophilised for 48 hours. After this procedure, the recovered polymer was weighed and stored in a desiccator until further use, ensuring light protection.

PVA was grinded in a mortar and then dissolved in water, being kept under stirring at 80 °C until complete dissolution (2 hours). Before spray drying fluorescently labelled PVA (2%, w/v), spray-drying parameters were optimised. The selected parameters were: inlet temperature:  $155 \pm 2$  °C; aspirator setting: 80%; feeding speed: 1.07 mL/min; and spray flow rate: 473 L/h. These conditions resulted in outlet temperature of  $96 \pm 2$  °C. The fluorescent PVA microparticles were collected and stored in desiccator, protected from light, until further use.

### **3.2. Characterisation of microparticles**

The surface morphology of produced microparticles was characterised by field emission scanning electron microscopy (FESEM; FESEM Ultra Plus, Zeiss, Germany). Dry powders were placed onto metal plates and 5 nm thick iridium film was sputter-coated (model Q150T S/E/ES, Quorum Technologies, UK) on the samples before viewing.

Microparticle size was estimated as the Feret's diameter (distance between two tangents on opposite sides of a microparticle) and was directly determined by optical microscopy (Microscope TR 500, VWR international, Belgium) from the manual measurement of 300 microparticles ( $n = 3$ ).

Real density was determined using a Helium Pycnometer (Micromeritics AccuPyc 1330, Germany). Briefly, the sample was previously weighed in a sample holder of known volume that was then placed in the equipment chamber, which was sealed for measurements. Helium was then inserted in the chamber under vacuum, in order to occupy its entire volume. It has the capacity to fill pores and spaces between microparticles. The sample volume was then determined by the difference between the chamber volume and the volume of helium.<sup>73</sup> Real density ( $\text{g}/\text{cm}^3$ ) was obtained by dividing the sample weight by its volume.

Bulk and tap densities ( $\text{g}/\text{cm}^3$ ) were determined using a tap density tester (Densipro 250410, Deyman, Spain), and consisted on the volume measurement of a known weight of powder before and after tapping, respectively ( $n = 3$ ). The determination of tap density involved tapping the sample until no further reduction of powder volume was observed (which corresponded to an average of 180 taps). The Carr Index (%) was estimated as a theoretical parameter to evaluate the flow properties of microparticles<sup>30,59</sup> and was calculated, as follows:

$$\text{Carr's Index} = \frac{(\rho_{\text{Tap}} - \rho_{\text{Bulk}})}{\rho_{\text{Tap}}} \times 100 \quad (30)$$

Where  $\rho_{\text{Tap}}$  is tap density ( $\text{g/cm}^3$ ) and  $\rho_{\text{Bulk}}$  is bulk density ( $\text{g/cm}^3$ ).

The aerodynamic diameter ( $D_{\text{aer}}$ ) was determined theoretically and is defined as the diameter of a sphere of unit density that has the same terminal settling velocity as the particle under consideration. It was calculated based on the following equation:

$$D_{\text{aer}} = d \sqrt{\frac{\rho_{\text{real}}}{\rho_0 \lambda}} \quad (30)$$

Where  $\rho_s = 1 \text{ g/cm}^3$ ,  $D_g$  corresponds to geometric diameter (determined as the Feret's diameter ( $\mu\text{m}$ )),  $\rho_{\text{Real}}$  is the real density of microparticles in the same unit as  $\rho_s$  ( $\text{g/cm}^3$ ), and  $\lambda$  is the dynamic shape factor of the particle.<sup>30,74</sup> Regarding the latter, considering that the shape of microparticles is identical to the pollen-shaped described by Hassan *et al.*,  $\lambda$  was assumed to be 1.2.<sup>30,75</sup>

### 3.3. Determination of drug association

Determination of drug content in microspheres was performed by UV-Vis spectrophotometry. This technique permits relating absorbance of radiation at a specific wavelength with the concentration of the dissolved drug. The Lambert-Beer law expresses that absorbance of a solution is proportional to the solute's concentration:

$$A_\lambda = \varepsilon_\lambda \cdot l \cdot C \quad (31)$$

Where  $A_\lambda$  is absorbance at specific wavelength,  $\varepsilon_\lambda$  is the wavelength-dependent molar absorptivity coefficient ( $\text{M}^{-1} \text{cm}^{-1}$ ),  $c$  is solute concentration (M) and  $l$  is the path length (cm).<sup>76</sup>

The specific wavelength ( $\lambda$ ) to determine each drug was defined by doing a screening. For INH, the absorbance maximum was obtained at 265.5 nm, while for RFB the maximum was registered at 240 and 500 nm. The absorbance maximum of two drugs in solution is 268.5 nm. This value corresponds to the intersection between the spectrums of two drugs, as described in figure 3.3. The wavelength used for determination of INH in formulation LBG.INH was 265.5 nm, and RFB in formulation LBG.RFB was 500 nm. A screening of the matrix material (LBG) revealed no interference at the selected wavelengths.

Different conditions were, however, required for drug quantification in formulations having drug association, because RFB has absorbance at two regions, near the region of INH

quantification and also in the visible region. For formulation with both encapsulated drugs, LBG.INH.RFB, a quantification at the wavelength of 268.5 nm was performed.

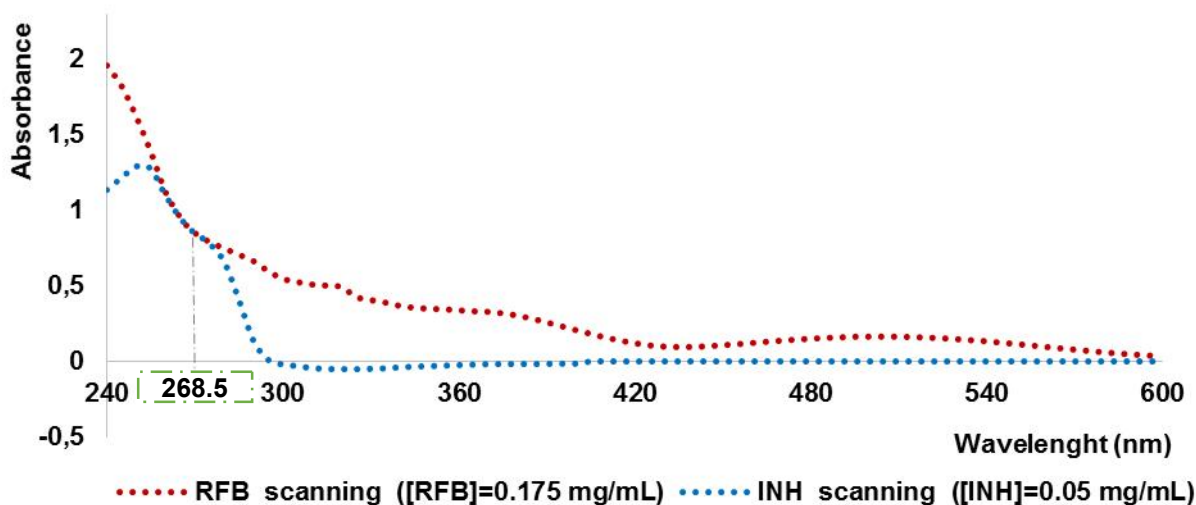


**Figure 3.3: Isoniazid and Rifabutin Spectra.** INH drug at 50 µg/mL and RFB at 175 µg/mL solubilised in HCl 0.1 M. 268.5 nm was determined experimentally as a point of intersection of the spectrum of both drugs.

At this particular wavelength, the measured absorbance is equal to the sum of INH and RFB absorbances, as described in the next equation:

For  $\lambda = 268.5$  nm,

$$A_{Total} = A_{INH} + A_{RFB} \quad (\text{Equation 1})$$

To enable the determination of the concentration of each drug in MPs, it was established that  $A_{RFB}$  was measured at 500 nm, and determination of real content of RFB in the sample was performed by linear regression from equation 2. At that wavelength, INH does not have significant absorbance, as shown in figure 3.3.

For  $\lambda = 500$  nm,

$$A_{RFB} = \epsilon \cdot l \cdot C_{RFB} \quad (\text{Equation 2})$$

After this determination, the absorbance of the sample could be measured at 268.5 nm. In this case it was necessary to dilute the sample until appropriate concentration. Then equation 1 becomes:

For  $\lambda = 268.5$  nm,

$$A_{Total} = \epsilon \cdot l \cdot C_{INH} + \epsilon \cdot l \cdot C_{RFB} \quad (\text{Equation 3})$$

With the value of RFB concentration quantified at 500 nm, it was possible to determine the value of its absorbance at 268.5 nm. The quantification of INH was also performed at 268.5 nm. To determine the final and real amount of INH, the contribution of RFB at that wavelength had to be subtracted.

$$A_{INH} = A_{Total} - A_{RFB} \text{ (Equation 4)}$$

$$\Leftrightarrow A_{INH} = \epsilon \cdot l \cdot C_{INH} \text{ (Equation 5)}$$

In order to determine microparticle drug content, a determined amount of drug-loaded microparticles was incubated with HCl 0.1 M, under magnetic stirring for 60 min. The specific conditions of the assay are described in table 3.1. Samples were then centrifuged (8000 rpm, 30 min; 5810 R, Eppendorf, Germany) and filtered (0.45 µm), before quantification by UV-Vis spectrophotometry (Pharmaspec UV-1700, Shimadazu, Japan).

For all formulations (LBG.INH, LBG.RFB and LBG.INH.RFB), a calibration curve of the corresponding drug was performed in a solution obtained from the solubilisation of LBG unloaded microparticles in HCl 0.1 M.

**Table 3.1. Assay conditions for determination of drug association efficiency and loading capacity.**

Formulations	Drugs	Wavelength (nm) used for determination	The wavelength-dependent molar absorptivity coefficient (M <sup>-1</sup> cm <sup>-1</sup> )	R-squared	MPs Weight (mg)	Volume of HCl 0.1 M (mL)
LBG.INH	Isoniazid	265.5	0.036	0.998	1.5	10
LBG.RFB	Rifabutin	500	0.003	0.999	15	10
LBG.INH.RFB	Isoniazid	268.5	0.036	0.997	15	10
	Rifabutin	500 and 268.5	0.003 and 0.030	0.998		

INH: Isoniazid; LBG: Locust Bean Gum; RFB: Rifabutin.

The estimation of drug association efficiency (AE) and microparticle loading capacity (LC) was performed as follows (n = 3):

$$AE (\%) = \frac{\text{Real amount of drug on MP}}{\text{Theoretical amount of drug on MP}} \times 100$$

$$LC (\%) = \frac{\text{Real amount of drug on MP}}{\text{Weight of MP}} \times 100$$

### 3.4. *In vitro* drug release

The determination of drug release was performed for the formulations LBG.INH = 10:1, and LBG.INH.RFB = 10:1:0.5 (w/w). The assays were conducted in a medium simulating the pH of the alveolar zone, PBS pH 7.4 (PBS tablets, Sigma-Aldrich, Germany), and also in a medium resembling the pH of macrophage phagolysosome, citrate buffer pH 5 (Sigma-Aldrich, Germany). For microparticles containing RFB, the medium was added of 1% (v/v) Tween 80® (Sigma-Aldrich, Germany) to facilitate drug dissolution and subsequent quantification. In order to establish the experimental setup, it was necessary to determine the solubility of RFB in the specific media. One of the requirements of this *in vitro* assay is maintaining sink conditions.<sup>77</sup> In experimental conditions, the RFB concentration in release medium was always less than 30% of its maximum solubility (0.496 mg/mL, determined experimentally). This is in accordance with the advised by the European Medicines Agency<sup>77</sup> and, therefore, it is considered that the assay was performed under sink conditions.

A determined amount of microparticles (of each formulation) were incubated with the respective media, under mild shaking (100 rpm, orbital shaker OS 20, Biosan, Latvia) at 37 °C. The released drug was quantified at predetermined times by collecting a sample (1 mL) and performing a quantification by UV-Vis spectrophotometry, using the calculations explained above for drug association. Sample dilutions were applied whenever needed. For each formulation a different calibration curve was used, consisting of a solution obtained from the incubation of unloaded LBG microparticles with the corresponding medium and assay conditions (microparticle concentration and duration of assay), followed by centrifugation (8000 rpm, 60 min) and filtration (0.45 µm). Specifically, for LBG.INH, 10 mg of microparticles were incubated in 12 mL of each release media in test tubes. At specific time intervals (5, 10, 15, 20, 30, 60, 90, 120, 240, 360 and 1440 minutes), samples were collected individually, filtered (0.45 µm), appropriately diluted (1:3) and the absorbance determined (n = 3).

For LBG.INH.RFB, 20 mg of microparticles were suspended in 10 mL of release medium (PBS plus 1% Tween 80®) and incubated. At specific time intervals (10, 20, 30, 60, 90, 120, 180 and 240 minutes), the samples were collected, centrifuged (16 000 x g, 15 minutes, Heraeus Fresco 17 Centrifuge, Thermoscientific, United States of America), filtered (0.45 µm), and the absorbance of RFB quantified at 500 nm. Following, the samples were diluted 1:10 and the total absorbance quantified at 268.5 nm (n = 3).

### 3.5. Powder crystallinity

The crystal structure of raw material (LBG), drugs and formulations was evaluated by Powder X-ray diffraction (PXRD). The samples were analysed in a PANalytical X'Pert Pro

diffractometer, using nickel filtered CuK $\alpha$  radiation with a wavelength of 0.154 nm. An X'Celerator detector was used and the operating conditions were 45 kV and 35 mA. The diffractograms were obtained in reflection mode from 5 to 70 ° 2theta with a step size of 0.05 ° and 1500 s per point.

### **3.6. Cell culture**

#### **3.6.1. A549 cell line: Human alveolar epithelial cells**

The A549 cell line was obtained from the American Type Culture Collection (ATCC, catalog number 185™, Rockville, USA). It derives from human lung adenocarcinoma and the cells form confluent monolayers characteristic of type II alveolar epithelium.<sup>78</sup>

Cell cultures were grown in 75 cm<sup>2</sup> tissue culture flasks (Orange Scientific, Belgium) inside an incubator having humidified 5% CO<sub>2</sub>/95% atmospheric air at 37 °C (HerAcell 150, Heraeus, Germany). Cell culture medium (CCM) was Dulbecco's Modified Eagle Medium (DMEM, Sigma-Aldrich, Germany), supplemented with 10% (v/v) Foetal Bovine Serum (FBS, Gibco, Life Technologies, USA), 1% (v/v) L-glutamine solution (Sigma-Aldrich, Germany), 1% (v/v) non-essential amino acids solution (Sigma-Aldrich, Germany) and 1% (v/v) penicillin/streptomycin (Sigma-Aldrich, Germany). The medium was exchanged twice a week and cells were sub-cultured weekly. Subculturing was initiated by rinsing the cell layer with PBS followed to 4-5 minutes exposure to trypsin-EDTA (Sigma-Aldrich, Germany). The cells were then re-suspended in new medium before and after centrifugation (1500 × g, 1 minute, room temperature, Centrifuge MPW – 223e, MedInstruments, Poland), and sub-cultivated at 1/8 ratio. Cells were used from passage 27 to 65.

#### **3.6.2. THP-1 cell line: Human leukemic monocytes**

THP-1 cell line is an acute monocytic leukemic cell line and was obtained from the Leibniz-Institut DSMZ. THP-1 cells were grown in suspension in 25 cm<sup>2</sup> or 75 cm<sup>2</sup> tissue culture flasks (Greiner Bio-one, Germany) in RPMI 1640 medium (Lonza Group AG, Switzerland) supplemented with 10% (v/v) FBS, 1% (v/v) L-glutamine and 1% (v/v) penicillin/streptomycin. Cells were maintained at 37 °C in a 5% CO<sub>2</sub>/95% air humidified atmosphere. The cell culture was maintained between 0.2 × 10<sup>6</sup> and 0.8 × 10<sup>6</sup> cells/mL. When reaching this concentration, cells were centrifuged (1500 × g, 2 minutes, room temperature, centrifuge MPW – 223e, MedInstruments, Poland), re-suspended in fresh medium and, after determination of the accurate cellular density, re-suspended in new passage at the concentration of 0.2 × 10<sup>6</sup>

cells/mL. Sub cultivation was performed two/three times a week and cells were used from passage 10 to 20 after thawing.

### 3.6.2.1. Differentiation of THP-1 cells into macrophage-like cells

Differentiation of THP-1 monocytes to provide the macrophage phenotype was performed using phorbol 12-myristate 13-acetate (PMA,  $C_{36}H_{56}O_8$ , Sigma-Aldrich, Germany).<sup>79</sup> An optimisation of conditions (PMA concentration, time of exposure) was performed to determine those permitting the adequate adhering phenotype, typical of macrophage populations *in vitro*.<sup>35,80</sup> THP-1 cells at density of  $0.2 \times 10^6$  cells/mL were suspended in 5 mL of RPMI medium supplemented with 50 nM PMA and seeded ( $1.0 \times 10^6$  cells per well), in 6-well plates (9.60 cm<sup>2</sup>, Greiner Bio-one, Germany). Cells were exposed to PMA for 48 hours, after which the medium was replaced by fresh medium without PMA for another 24 hours before the experiments. All experiments were performed in macrophage-like THP-1 cells. Different assays required the use of different plates, thus requiring an optimisation of differentiation procedures.

For assays in 6-well plates, THP-1 cells at density of  $0.2 \times 10^6$  cells/mL were re-suspended in medium supplemented with 50 nM PMA, and seeded in 5 mL final volume of cell suspension. After 48 hours, medium was replaced by 2.5 mL of fresh medium. In 12-well plates (3.85 cm<sup>2</sup>, Orange Scientific, Belgium) a final volume of 2 mL cell suspension at  $0.2 \times 10^6$  cells/mL (with PMA) was used. After 48 hours, 1 mL of fresh medium was used to replace the medium. In 96-well plates (0.33 cm<sup>2</sup>, Orange Scientific, Belgium), seeding density was  $0.035 \times 10^6$  cells per well with 100  $\mu$ L of RPMI previously supplemented with 50 nM of PMA. The cells were incubated for 48 hours in incubator. After, the medium was replaced by 100  $\mu$ L fresh medium and incubated for 24 hours before experiments. Optimal cell seeding density for these plates was confirmed in preliminary experiments through cell growth curves.

An efficient differentiation was demonstrated by an immunocytochemistry assay. After the application of the differentiation protocol, macrophages were washed twice with 5 mL of a solution consisting of a cold mixture of 3% (v/v) FBS in PBS pH 7.4. This solution will be denominated in rest of text by PBS.3%FBS. Cells were harvested by scraping, suspended in PBS.3%FBS and centrifuged ( $1500 \times g$ , 2 minutes, room temperature, centrifuge MPW – 223e, MedInstruments, Poland) twice. After that, macrophages were placed in a 6-well plate ( $1.0 \times 10^6$  cells/well) and incubated with a solution of PBS.3%FBS containing the monoclonal antibody anti-CD11b (BioLegend Inc, USA) for 1 hour at 4 °C, in a dark box. After that period, cells were washed twice with PBS.3%FBS, centrifuged and re-suspended with this solution prior to the analysis by flow cytometry (FacScalibur Cell Analyzer, BD Biosciences, Belgium).

### 3.6.3. Cell line NR8383: Rat alveolar macrophages

The cell line NR8383 was purchased from ATCC (catalog number CRL-2192™), corresponding to rat alveolar macrophages collected by lung lavage of *Rattus norvegicus*.<sup>81</sup>

NR8383 cells grow in mixed culture, half the population keeps adherent and half suspended. The used CCM consisted of Ham's F12 (Lonza, Group AG, Switzerland) supplemented with 15% (v/v) FBS, 1% (v/v) L-Glutamine and 1% (v/v) penicillin/streptomycin. Cells were maintained at 37 °C in a 5% CO<sub>2</sub>/95% air humidified atmosphere on 75 cm<sup>2</sup> flasks (Orange Scientific, Belgium). The culture was maintained by transferring suspending cells to a new flask, where about one half of the cells will re-adhere. To do so, suspending cells were placed in a falcon, centrifuged, and re-suspended in fresh medium. The medium was exchanged three times/week and the suspending cells were eliminated together with medium. Adherent cells were those used to perform the assays described below and their harvesting was made by scraping.

### 3.7. Cytotoxic evaluation

The cytotoxic evaluation of the diverse microparticle formulations developed in this work was performed *in vitro* by means of two different assays. The 3-[4, 5-dimethylthiazol-2-yl]-3,5 biphenyl tetrazolium bromide (MTT, Sigma-Aldrich, Germany) test, which will be simply referred to as MTT assay, is a metabolic assay that provides information on the effect of contact with formulations on the mitochondrial activity of cells. In this assay, yellow tetrazolium salts of MTT are reduced by the action of dehydrogenase enzymes present in mitochondria of viable cells, resulting in the formation of purple formazan that accumulates intracellularly, as described in figure 3.4. Formazan crystals are then dissolved with appropriate organic solvents and quantified by spectrophotometric analysis. The absorbance of purple formazan is directly proportional to the quantity of viable cells.

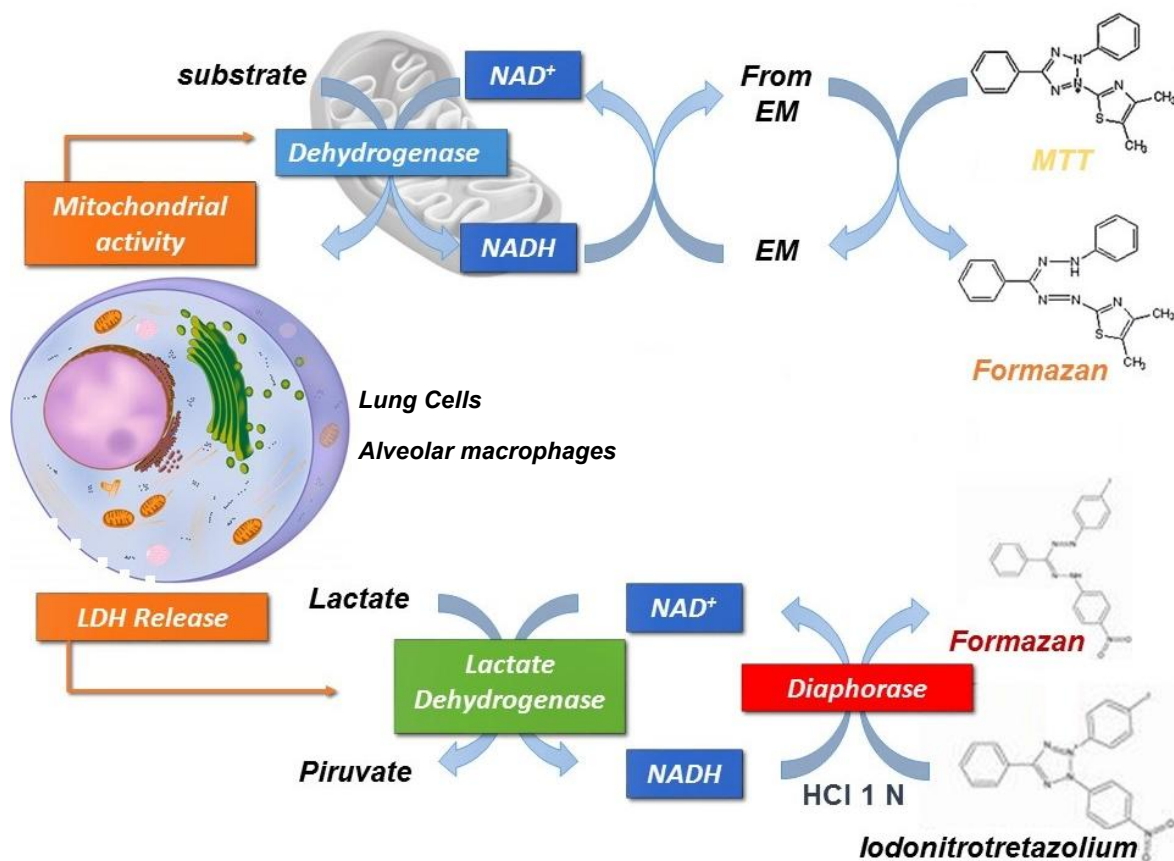


**Figure 3.4: Cytotoxicity assays:** After exposure of microparticles, metabolic activity of viable cells can be determined using 3-[4, 5-dimethylthiazol-2-yl]-3,5 biphenyl tetrazolium bromide (MTT) test, which consists in the reduction of the tetrazolium salt to formazan by cellular dehydrogenases. The presence of lactate dehydrogenase (LDH) enzyme in cell culture medium is indicator of damaged cells. Released LDH is measured with a coupled enzymatic reaction that results in the conversion of a tetrazolium salt (iodonitroretazolium) into a red color formazan by diaphorase. EM: Electron mediator; HCl: hydrochloric acid NAD/NADH: cofactor nicotinamide adenine dinucleotide.

The second assay consisted in the quantification of lactate dehydrogenase (LDH) released by cells upon contact with formulations. As LDH is a cytosolic enzyme, its release implies the disruption of the cell membrane and, thus, this assay provides data on cytotoxicity based on the evaluation of cell membrane integrity. Using an appropriate toxicity assay kit (commercial kit, Sigma-Aldrich, Germany), LDH released from cells to the culture medium will convert lactate to pyruvate via reduction of the co-factor nicotinamide adenine dinucleotide (NAD<sup>+</sup> to NADH). The enzymatic reaction is then stopped with HCl 1 M, and diaphorase also present in the reagent uses NADH to reduce a tetrazolium salt (dye solution) to red formazan product, as described in figure 3.4. The amount of formazan is quantified spectrophotometrically and is directly proportional to the amount of released LDH present in the medium.

### 3.7.1. MTT assay

The MTT assay was performed on A549 and macrophage-derived THP-1 cells. Optimal cell seeding density was confirmed in preliminary experiments for two cell lines. A549 cells were seeded at a density of  $1 \times 10^5$  cells/well on 96-well plates (Orange Scientific, Belgium), in 100  $\mu$ L of complete DMEM. Cells were incubated for 24 hours at 37 °C in 5% CO<sub>2</sub> atmosphere before use. A549 cells were exposed to the microparticles in suspension in cell culture medium without FBS. THP-1 cells were differentiated into macrophages before the experiments, according to previously described procedures. With these cells, the assay was performed either exposing the microparticles as a suspension in cell culture medium (RPMI without FBS) or as a dry powder. When the formulations were exposed as suspension, the assay was performed in 96-well plates (cell density of  $0.035 \times 10^6$  cells per well), while 12-well plates (cell density of  $0.40 \times 10^6$  cells per well) and six-well plate ( $1 \times 10^6$  cells per well) were used when aerosolisation of dry powder was performed.

#### 3.7.1.1. Samples presented in solution/suspension

The *in vitro* cytotoxicity of individual drugs, raw material (polymer) and microparticle formulations was tested in A549 and macrophage-derived THP-1 cells in the form of a solution/suspension prepared in cell culture medium. Assuming that drugs represent a maximum of 10% of the amount of polymer in each formulation, INH and RFB were tested individually at the concentrations of 0.01, 0.05 and 0.1 mg/mL. In turn, the matrix polymer as obtained commercially (LBG), unloaded LBG MPs and drug-loaded MPs (LBG.INH 10:1; LBG.RFB 10:1, 10:0.5, 10:0.2 and LBG.INH.RFB 1:1:1 and 1:1:0.5) were evaluated at the concentrations of 0.1, 0.5 and 1.0 mg/mL. Cell culture medium and sodium dodecyl sulphate (SDS, Sigma-Aldrich, Germany) at 2% (w/v) were used as negative and positive control of cell death, respectively. All test substances were solubilised/dispersed in pre-warmed CCM without FBS, and exposed to both cell lines for 3 and 24 hours.

Due to the hydrophobic character of RFB, it does not dissolve directly in CCM and, therefore, it was solubilised in dimethyl sulfoxide (DMSO, Sigma-Aldrich) at a drug concentration of 20 mg/mL, being subsequently diluted to the desired concentrations with CCM. Consequently, DMSO was at a concentration of 0.5% (v/v) in RFB solutions tested in cells. The effect of DMSO on cell viability (diluted in CCM) was determined as control, in concentrations varying between 0.0313% and 2% (v/v).

When A549 cells were used, solutions/suspensions were removed after the exposure time and MTT solution (0.5 mg/mL in PBS pH 7.4) was added. After 2 hours, any formazan crystals

generated were solubilised with DMSO and the absorbance measured by spectrophotometry (Infinite M200, Tecan, Austria) at 540 nm (background correction at 640 nm). For macrophage-like THP-1 cells, the MTT solution was added directly without removing test substances. After 2 hours in 96-well plates, for this assay, or 3 hours in 12-well plates and 6-well plates, when this assay was performed with microparticles aerosolised (next section), a surfactant solution comprising 10% of SDS in a 1:1 mixture of dimethylformamide (DMF, Sigma-Aldrich, Germany): water was used to solubilise the formed formazan crystals. Plates were incubated at 37 °C for 60 minutes (30 minutes in orbital shaker (150 rpm) and other 30 minutes at rest to maximize crystal solubilisation). Afterwards, absorbance was read by spectrophotometry (Infinite M200, Tecan, Austria) at 570 nm (background correction at 650 nm).

Relative cell viability (%) was calculated by the formula:

$$\text{Cell viability (\%)} = \frac{(A - S)}{(CM - S)} \times 100$$

where A represents absorbance of test substances, S that obtained for 2% SDS and CM that of culture medium. The viability of untreated cells (CM) was assumed to correspond to 100% of the cell viability, and viability of treated cells was compared to this control. The assay was replicated at least three times, each with six replicates.

### **3.7.1.2. Samples presented by aerolisation**

From the total set of formulations that were developed, four were selected to undergo a preliminary assessment of cell viability upon exposure to differentiated THP-1 cells in the form of a dry powder. These formulations were unloaded LBG MPs, LBG.INH 10:1, LBG.RFB 10:0.5 and LBG.RFB.INH 10:1:0.5.

The formulations were exposed to cells seeded in 12-well plates at a dose of 303 µg/cm<sup>2</sup>, which reflects the conversion of 1 mg/mL (used 96-well plates) to the area of the 12-well plate used in the assay. Samples were aerosolized using a Dry Powder Insufflator™ (Model DP-4, Penn-Century, USA), which is shown in figure 3.5, and their effect evaluated upon 24 hours exposure. Cells were in contact with the samples for two hours without CCM in order to simulate the alveolar environment. After this time, 500 µL of CCM were applied in each well, to not compromise cell viability due to dryness. A control was performed leaving cells without medium for 2 hours, after which the same volume of CCM was added to the wells. The assay was also performed at a dose of 50 µg/cm<sup>2</sup>, which is the minimum dose of formulation that can be weighed. This dose was only tested for unloaded LBG MPs and LBG.INH.RFB 10:1:0.5.

For this specific approach, cells were seeded in 6-well plates (9.60 cm<sup>2</sup>) and exposed to the microparticles for 2 hours in absence of CCM. After, 1350 µL CCM were added to each well until 24 hours of microparticle exposure. A control in the same conditions was performed, in absence of microparticles.

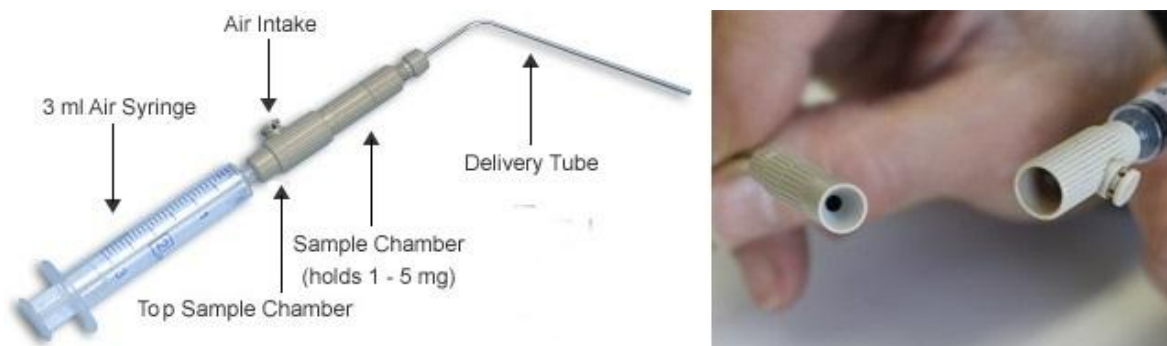


**Figure 3.5: Dry powder insufflator:** Scheme of sample chamber and air handler (top of sample chamber). Adapted from reference 79.<sup>82</sup>

The insufflator is a device designed for powder administration to animals and allows the loading of 1-5 mg of powder.<sup>82</sup> The appropriate volume of insufflated air had to be optimised for each tested dose and each formulation, as it influences the amount of microparticles released from the device. An average of 24 replicates was performed for each formulation during the optimisation phase. For the formulation of unloaded LBG MPs and LBG.INH 10:1 (303 µg/cm<sup>2</sup>), the average of released dose from device was 52.26 ± 5.2%, while for LBG.RFB 10:0.5 and LBG.INH.RFB 10:1:0.5 was 60.71 ± 3.2%. Regarding the lower dose (50 µg/cm<sup>2</sup>) is concerned, unloaded LBG MPs released 43.13 ± 4.73%, while LBG.INH.RFB 10:1:0.5 released 48.44 ± 4.30%.

Cell viability (%) was calculated with the formula mentioned above, with slight modifications, as no positive control of cell death was used:

$$\text{Cell viability (\%)} = \frac{A}{CM} \times 100$$

Where A represents absorbance of test substance and CM that of culture medium. The viability of unexposed cells (CM) was assumed to correspond to 100% of the cell viability, and viability of treated cells was compared to this control. The assay was replicated at least three times.

### **3.7.1.3. Determination of Rifabutin IC<sub>50</sub>**

As formulations containing RFB registered strong cell viability decreases, the concentration that inhibits cell proliferation/population on 50% (IC<sub>50</sub>) of this drug was determined. Serial dilutions of RFB in DMSO (0.5% v/v) were prepared (0.00156 to 0.4 mg/mL) and applied on differentiated THP-1 cells and A549 cells. After 24 hours exposure, cell viability was determined using the same positive and negative controls referred above for the assessment of drug solutions.

For determination the IC<sub>50</sub> was used the Standard curve analysis based on a four-parameter logistic in SigmaPlot software (version 13.0).

### **3.7.2. LDH assay**

The determination of LDH release was performed in both A549 and differentiated THP-1 cells upon 24 hour exposure to drugs, polymer (LBG) and microparticle formulations. Specifically, tested formulations corresponded to unloaded LBG MPs, LBG.INH 10:1, LBG.RFB 10:1, 10:0.5 and 10:0.2, and LBG.INH.RFB 10:1:1 and 1:1:0.5.

All formulations/test samples were applied over the cells in the form of solutions/suspensions, at the concentration of 1 mg/mL, the maximum concentration used in the MTT assay. However, the concentration of 0.5 mg/mL was also tested for RFB as free drug and formulations containing this drug. Cells were cultured in 96-well plates in the conditions described before for the MTT assay (the assays were in fact performed simultaneously). Upon exposure, cell culture supernatants were collected (MTT uses the proper cells, while this assay uses the supernatants), centrifuged (16 000 x g, 5 minutes, 4 °C) and processed using a commercial LDH assay kit (Sigma-Aldrich, Germany). Briefly, supernatants were incubated with the reaction mixture for 20 minutes and after this time the enzymatic reaction was stopped with HCl 1 M (Sigma-Aldrich, Germany). Absorbance was measured by spectrophotometry (Infinite M200, Tecan, Austria) at a wavelength of 490 nm (background correction at 690 nm).

A negative control of LDH release was performed incubating cells with CCM only. The amount of LDH released in this case was considered 100%. A positive control of LDH release was provided by a lysis solution, provided in the kit. Released LDH (%) upon incubation with each sample was determined by comparison with the 100% of the negative control. All measurements were performed in triplicate.

### **3.8. Evaluation of macrophage ability to uptake LBG microparticles**

THP-1 cells were differentiated as described in section 3.6.2.1. THP-1 cells at concentration  $0.2 \times 10^6$  cells/mL were suspended in RPMI medium supplemented with 50 nM PMA and seeded in 5 mL/well in 6-well plates for cells in suspension (Greiner Bio-one, Germany). For NR8383 cells, those adhered to the flasks were removed with a scraper, suspended in Ham's F12, centrifuged and counted. They were seeded at a density of  $1.0 \times 10^6$  cells per well in 6-well plates for adhered cells (Orange Scientific, Belgium), with 2 mL of medium. This procedure was performed 24 hours before the test to ensure that 50 to 75% of the original population adheres to the well surface.

The evaluation of microparticle uptake by macrophages was performed by flow cytometry, which required the exposure to fluorescently-labelled LBG and PVA microparticles (described in section 3.1.3). The assay was performed testing two doses of microparticles: 250 and 50  $\mu\text{g}/\text{cm}^2$ . The higher dose was only tested for LBG microparticles and THP-1 cells and implied weighing approximately 3.5 mg of dry powder. In turn, the lower dose corresponded to approximately 1 mg and was tested in differentiated THP-1 cells and NR8383 cells, for both LBG and PVA microparticles).

Fluorescently-labelled microparticles were aerosolized onto the macrophage layer using a Dry powder Insufflator™ (Model DP-4, Penn-Century™, USA), as described in section 3.7. 1.2. Optimisation of insufflation using this device was performed for both formulations. In each assay, a negative control was used consisting of cells not exposed to microparticles but maintaining the same assay conditions.

After weighing the samples and having the insufflator ready to operate, culture medium was removed and microparticles insufflated over the monolayer of macrophages. The incubation was allowed for 2 hours at 37 °C, without CCM. After that time, the phagocytic process was finished by the addition of a cold solution of PBS.3% FBS (5 mL, two applications). Cells were then scraped and centrifuged (1500 rpm, 2 minutes, room temperature, centrifuge MPW – 223e, MedInstruments, Poland) in 2 mL of PBS.3% FBS. Afterwards were again re-suspended twice in 5 mL of PBS.3% FBS and centrifuged (1500 rpm, 2 minutes, room temperature). The cells were finally re-suspended in 1 mL of PBS.3% FBS, transferred for cytometry tubes (BD Biosciences, Belgium) and maintained at 4 °C until the analysis.

The occurrence of phagocytosis was determined by flow cytometry (FacScalibur cell analyser, BD Biosciences, Belgium). In the system, FSC-H/SSC-H channels were used to measure size (FSC-H) and granularity of the cells (SSC-H) and side scatter light was used to identify cell viable population. Gate 1 was defined with results from the two channels for unexposed cells. Region R was defined from the value of fluorescence intensity which is independent on cellular

autofluorescence and also on fluorescent molecule in FL-1 channel (blue laser; excitation 488, emission 530/30). The amount of cells having fluorescence was considered to have phagocytosed microparticles. The assay for each cell line, doses, microparticle formulations and controls was replicated at least three times.

### 3.9. Evaluation of microparticle capacity to activate macrophages

The capacity of LBG microparticles or unformulated LBG to activate macrophages was tested by measuring, upon incubation with macrophage-differentiated THP-1 cells, the release of the activation markers tumour necrosis factor- $\alpha$  (TNF- $\alpha$ ) and interleukin-8 (IL-8).

THP-1 cells were seeded on 96-well plates ( $0.035 \times 10^6$  cells/well, 50 nM PMA, 0.1 mL) and differentiated as described in section 3.6.2.1. After that, cells were exposed to a solution of LBG and to a dispersion of LBG.INH.RFB 10:1:0.5 microparticles at dose  $303 \mu\text{g}/\text{cm}^2$  for 24 hours. The exposure to lipopolysaccharide (LPS,  $10 \mu\text{g}/\text{mL}$ )<sup>35</sup> was used as positive control and cells incubated with CCM, mannitol microparticles or unformulated mannitol were used as negative control. The unformulated LBG solution, LBG microparticles and controls were prepared with pre-warmed CCM without FBS immediately before application to the cells. After 24 hours of exposure, cell supernatants were collected and centrifuged (10 minutes,  $16.000 \times g$ ,  $4^\circ\text{C}$ , Centrifuge 5804R, Eppendorf, Germany). The levels of IL-8 and TNF- $\alpha$  present in supernatants of macrophages were determined by quantitative enzyme-linked immunosorbent assay (ELISA) using human IL-8 and TNF- $\alpha$  ELISA Kits (Invitrogen Corporation, Camarillo, USA), according to the manufacturer's instructions.

The supernatants were appropriately diluted for IL-8 (approximately 2 times for LBG solution and microparticles, and 10 times for LPS). The assay was performed on two occasions with two replicates for test substance in each assay. The concentration of individual cytokines for each test substance is expressed as percentage of spontaneous release by cells not exposed any substance but presenting a basal level of these cytokines.

### 3.10. Statistical analysis

The student t-test and the one-way analysis of variance (ANOVA) with the pairwise multiple comparison procedures (Holm-Sidak method) were performed to compare two or multiple groups. For the analysis of results of *in vitro* release assay, a two-way ANOVA with Bonferroni's method for multiple comparison test was used. All analysis were run using the GraphPad Prism (version 6.07) and differences were considered to be significant at a level of  $p < 0.05$ .

## **4. Results and Discussion**

The development of antitubercular formulations to be directly delivered to the lungs by inhalation is considered a promising approach, as described in the introduction. Antitubercular drugs are usually administered orally, in prolonged treatments associated with severe side-effects, which may lead to reduced patient compliance and may increase the emergence of drug-resistant strains. Antitubercular therapy thus needs a critical change.<sup>102</sup> The search for new antitubercular drugs is of key importance but is not the unique option, as the development of new drug delivery strategies may also play an important role. Delivery of antibiotics via the pulmonary route has been used for the treatment of pulmonary infections, especially in complications of cystic fibrosis, but this route is now becoming increasingly interesting for other infectious diseases, including tuberculosis. This approach offers multiple advantages over oral delivery, as it enables site-specific drug deposition at high concentrations and favorable lung-to-plasma ratio,<sup>12,33</sup> provides the possibility of reducing administration doses and frequency, and might shorten treatment periods. This would improve efficacy of the treatment, reduce drug related toxicity and certainly improve patient compliance.

This constituted the major motivation of this project. The main goal was the development of a new delivery strategy, through the use of inhalable microparticles as carriers of two first-line antitubercular drugs (isoniazid and rifabutin). Specifically for these drugs, which present severe hepatic and other systemic side effects, the administration by pulmonary route for local action would be advantageous.<sup>23,70</sup> It is important to indicate that these drugs were considered as models, and other antibiotics could potentially be tested and loaded for the treatment of this or other lung infections, such as for example pneumonia.

### **4.1. Preparation of locust bean gum microparticles by spray-drying**

Obtaining a LBG dispersion that permitted spray-drying required great optimisation of each step, mainly due to the high viscosity of the polysaccharide. The thickening capacity of LBG is reported to depend on factors such as the particle size, solubilisation methods, polymer concentration, shear rate and molecular weight distribution.<sup>61</sup> LBG at a solid concentration of 2% (w/v) forms suspensions with too high viscosity to enable spray drying. At 1% (w/v) the viscosity is reported to be 2100 - 3750 cps,<sup>83</sup> which is much greater than the ideal for an operation with the spray-drying equipment (300 cps).<sup>48</sup> The literature reports that the rheological properties of LBG dispersion can be modified with the change of pH, addition of salts, and/or heating.<sup>84</sup> In this work, both the reduction of pH and the use of temperature were tested. Regarding the use of hydrochloric acid, it was found that a volume of 5 mL HCl 0.1 M for a total volume of 50 mL was enough to endow the adequate viscosity.

LBG was grinded in a glass mortar for reduction of particle size, followed by the addition of HCl and water. The reduction of particle size increased the contact between the polymer chain and the acid molecules. LBG is partially soluble in cold water and needs to be heated to reach maximum solubility. This is why the protocol of its solubilisation included the use of temperatures up to 85 °C. This is in line with reports on the literature saying that galactomannans having high molecular weight and low galactose content are only soluble at high temperatures.<sup>85</sup>

Considering both the pH obtained after dissolving the produced LBG MPs in water (pH about 4.3), which was considered low regarding an *in vivo* application, and also the results obtained in cytotoxicity assays, an attempt was made to reduce the final concentration of HCl in microparticles. HCl at concentrations of 0.01 and 0.001 M was thus tested. Unfortunately, none of the concentrations was successful in providing the adequate viscosity for spray-drying and the initial conditions (0.1 M HCl) were decided to be used. Another attempt was made associating the addition of 0.01 M HCl (10 mL in a final volume of 50 mL) with the heating of LBG dispersion in water-bath at 55 °C during the spray-drying process. Although a certain reduction of viscosity was appreciated, this was not enough to obtain an acceptable yield of spray-drying. The more significant reduction of viscosity in presence of HCl 0.1 M is attributed to high concentrations of H<sup>+</sup> in solution, which cause a weak deprotonation of hydroxyl groups of water and galactomannan molecules, resulting in the reduction of the number of hydrogen bonding. With a lower number of hydrogen bonds being established between water and LBG, and between the proper LBG molecules, there is less expansion of the LBG chain and, therefore, fewer interactions of galactomannans occur, causing viscosity reduction.<sup>85</sup>

The addition of salts, such as NaCl, KCl and CaCl<sub>2</sub> at concentrations between 5 and 50 mM is also reported as strategy to reduce the viscosity of LBG dispersions, and could be used in future approaches.

## **4.2. Characterisation of microparticles**

LBG microparticles were successfully obtained in a one-step spray-drying process and several formulations were produced. In general, and as observed in Figure 4.1, MPs presented irregular shapes and a convoluted/wrinkled surface.

For the formulations LBG.RFB and LBG.INH.RFB the shown microphotographs are representative of each group, as of these being composed of various formulations containing different amounts of RFB.

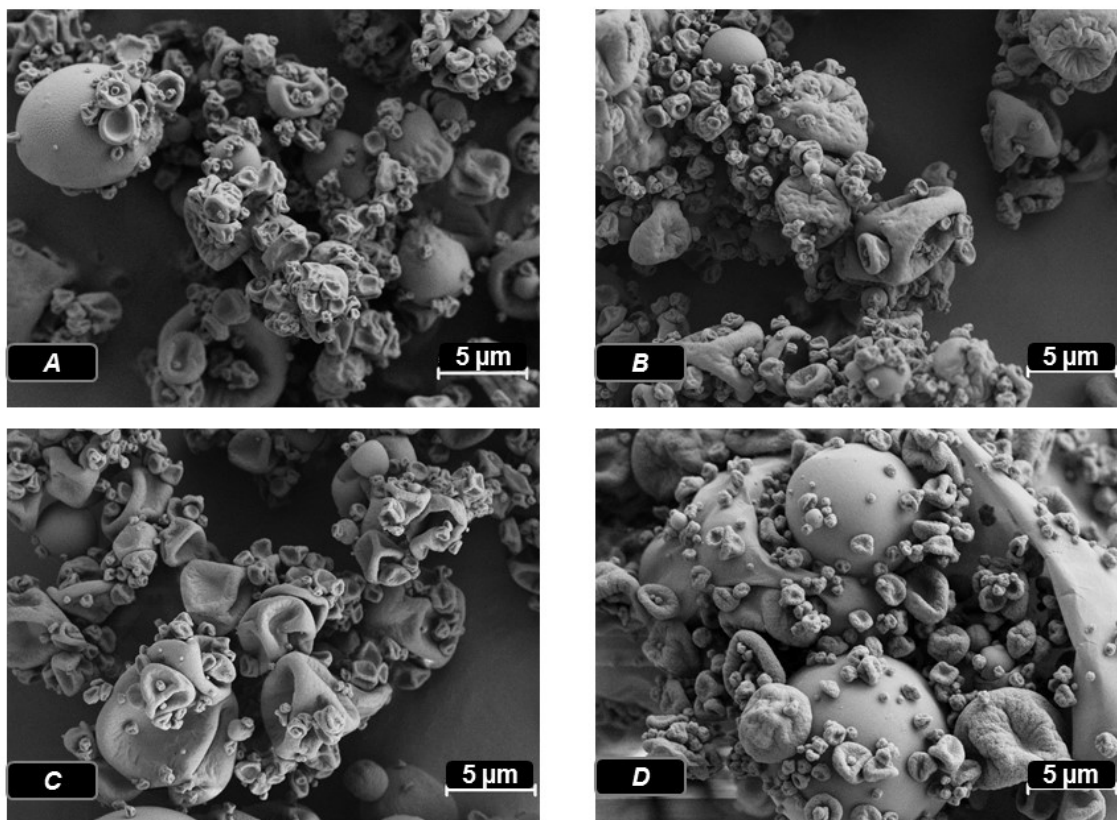


**Figure 4.1: Microphotographs of LBG-based microparticles viewed by scanning electron microscopy.** A) Unloaded LBG Microparticles; B) LBG.INH = 10:1 (w/w); C) LBG.RFB = 10:0.5 (w/w); D) LBG.INH.RFB = 10:1:0.5 (w/w).

These morphologies are similar to those reported for other polysaccharide microparticles produced by spray drying.<sup>86–88</sup> The affinity between a determined polymer and the solvent used in spray-drying are factors conditioning the morphological aspect of MPs. In fact, when the droplets of polymer dispersion start drying, a film of polymer is first formed on the surface that might interfere with diffusion of water from the inside out. This leads to an increase of the internal pressure that might reach a critical point where the particle deforms or even disintegrates.<sup>87</sup> The irregular morphologies could improve dispersibility and flow properties of dry powders, because surface irregularities reduce the contact between MPs and the possibility of establishing van der Waals forces that lead to agglomeration.<sup>47,87</sup>

The aim of this work, as previously established, was to develop microparticles of LBG with adequate aerodynamic properties for pulmonary administration with the particular requirement of reaching the alveolar zone. This is where alveolar macrophages, host of mycobacteria, reside. From a macroscopic observation, RFB-loaded microparticles had very acceptable flow properties, which were better than those observed for microparticles devoid of RFB. This suggests a favorable effect of RFB on microparticle flowing properties. However, more rigorous characterization of aerodynamic properties is required, relying on properties such as

Feret's diameter, density and aerodynamic diameter. Tables 4.1 and 4.2 present the results of this characterization.

**Table 4.1: Spray-drying production yields and microparticle Feret's and aerodynamic diameters (mean ± SD, n = 3)**

Drug:Polymer Ratio	Production Yield (%)	Diameter (µm)	
		Feret's	Aerodynamic, λ = 1.2
<b>Unloaded LBG</b>	70.1 ± 4.1	1.35 ± 0.73	1.45 ± 0.05
<b>LBG.INH</b>	<b>10:1</b>	66.0 ± 5.8	1.50 ± 0.80
	<b>10:0.2</b>	61.5 ± 0.7	1.26 ± 0.63
<b>LBG.RFB</b>	<b>10:0.5</b>	67.0 ± 2.8	1.10 ± 0.56
	<b>10:1</b>	70.1 ± 4.8	1.50 ± 0.86
<b>LBG.RFB.INH</b>	<b>10:1:0.5</b>	58.7 ± 5.9	1.11 ± 0.58
	<b>10:1:1</b>	71.7 ± 3.2	1.60 ± 0.17

INH: Isoniazid; LBG: Locust Bean Gum; RFB: Rifabutin

**Table 4.2: Microparticle real, bulk and tap densities and Carr's index (mean ± SD, n = 3)**

Drug:Polymer ratio	Density (g/cm <sup>3</sup> )			Carr's Index (%)	
	Real	Bulk	Tap		
<b>Unloaded LBG</b>	1.39 ± 0.01	0.24 ± 0.06	0.37 ± 0.08	34.32 ± 0.93	
<b>LBG.INH</b>	<b>10:1</b>	1.41 ± 0.02	0.24 ± 0.01	0.36 ± 0.00	34.52 ± 2.06
	<b>10:0.2</b>	1.41 ± 0.03	0.20 ± 0.01	0.32 ± 0.05	36.80 ± 2.74
<b>LBG.RFB</b>	<b>10:0.5</b>	1.33 ± 0.03	0.15 ± 0.04	0.25 ± 0.07	40.10 ± 0.65
	<b>10:1</b>	1.39 ± 0.02	0.14 ± 0.02	0.25 ± 0.02	42.89 ± 4.11
<b>LBG.RFB.INH</b>	<b>10:1:0.5</b>	1.43 ± 0.01	0.11 ± 0.00	0.19 ± 0.01	43.72 ± 1.50
	<b>10:1:1</b>	1.45 ± 0.01	0.13 ± 0.03	0.24 ± 0.05	45.35 ± 1.44

INH: Isoniazid; LBG: Locust Bean Gum; RFB: Rifabutin

Spray-drying yields varied between 59% and 72%, which are considered satisfactory and are similar to others found in literature for spray-dried polysaccharides.<sup>86,87</sup>

The particle size of a powder formulation proposed for inhalation is, together with the particle density, a prominent factor in the success of formulation, because it strongly influences the sedimentation and dispersion proprieties of the powder.<sup>89</sup> As mentioned before, the aerodynamic diameter of particles aimed at reaching the alveolar zone after inhalation should be of approximately 0.5 – 2 µm,<sup>27</sup> while a size of 1 - 2 µm is known to favour the phagocytosis by alveolar macrophages.<sup>63</sup> Among the various MP formulations that were developed, no

relevant differences were found on the Feret's diameter, which varied from 1.10  $\mu\text{m}$  to 1.60  $\mu\text{m}$ . Real, bulk and tap densities are also very similar amongst the seven formulations, with real density registering values of 1.3 or 1.4  $\text{g}/\text{cm}^3$ , very common values for spray-dried samples.<sup>87,90,91</sup> Bulk densities varied between 0.1 and 0.25  $\text{g}/\text{cm}^3$  and tap densities registered a slight increase in comparison with the former, which is expected because of the method used for the determinations. These results are identical to obtained for the microparticles obtained through SPD.<sup>92-94</sup> The real density values, along with Feret's diameters, resulted in aerodynamic diameters between 1.27 – 1.90  $\mu\text{m}$ . The morphology of these MPs is similar to that of the pollen-shaped particles described by Hassan *et al.*<sup>30</sup> Those were referred to closely resemble a spherical shape, but the irregular surface would cause a slightly higher shape factor as compared with spherical particles. This has a consequence in the calculation of  $D_{\text{aer}}$ , which considered the dynamic shape factor of 1.2, the same reported for the referred pollen-shaped particles.<sup>30</sup> The determined aerodynamic diameters are theoretically suitable for deep lung deposition upon inhalation,<sup>27</sup> although experimental determination of  $D_{\text{aer}}$  would be important to support this claim.<sup>75</sup>

The Carr's index is one of the parameters used to infer on the flowability of a powder and it is considered that values below 25% are indicative of good flowing properties.<sup>30</sup> In this work, the calculated values varied within 34% and 45%, and microparticles associating both drugs were those showing the worst values, in spite of the good flowing properties estimated macroscopically. In a further development of the work, the aerosolisations properties of the formulations from a dry powder inhaler will be tested and if a efficient aerodynamic behaviour is verified, a solution might comprise the incorporation of adjuvant excipients such as leucine, an amino acid with demonstrated ability to improve aerosolization properties.<sup>94</sup>

### **4.3. Association efficiency**

In developing an effective drug formulation, it is important to succeed on drug association. However, the process of association is affected by process variables, as the drug-polymer ratio, solvent, use of crosslinking agents, etc. Spray-drying is a technique usually providing high association efficiencies.<sup>49,87</sup> In the microparticles produced in this thesis, the percentage of drug associated is higher than 80%, as indicated in table 4.3.

**Table 4.3: Drug association efficiency and loading capacity** (mean  $\pm$  SD, n = 3)

Drug:Polymer Ratio		Association Efficiency (%)		Loading Capacity (%)	
LBG.INH	10:1	88.8 $\pm$ 1.5		8.8 $\pm$ 0.1	
	10:0.2	92.4 $\pm$ 6.0		1.8 $\pm$ 0.1	
LBG.RFB	10:0.5	86.3 $\pm$ 3.0		4.1 $\pm$ 0.1	
	10:1	102.81 $\pm$ 3.8		10.2 $\pm$ 0.4	
		INH	RFB	INH	RFB
LBG.RFB.INH	10:1:0.5	82.8 $\pm$ 4.7	91.5 $\pm$ 4.1	7.3 $\pm$ 0.4	4.0 $\pm$ 0.2
	10:1:1	87.9 $\pm$ 8.0	92.70 $\pm$ 7.7	7.9 $\pm$ 0.7	8.4 $\pm$ 0.4

INH: Isoniazid; LBG: Locust Bean Gum; RFB: Rifabutin

The association efficiency is a ratio between the real quantities of drug and the theoretical quantity of drug what was encapsulated. In turn, loading capacity concerns the real quantity of drug in a mass of microparticles. Despite the differences in the solubilities of isoniazid and rifabutin (125 mg/mL versus 0.19 mg/mL),<sup>23,24</sup> the two drugs could be incorporated within the LBG matrix with approximately equal efficiency. Isoniazid, owing to its hydrophilic nature, is easily incorporated in aqueous solutions, allowing obtaining high association (80 – 90%). These results are similar to those reported for other spray-dried formulations containing this drug.<sup>95–97</sup>

RFB is a lipophilic drug and its association required some optimizations. An adjuvant effect was tested using Tween 80® and HCl at different concentrations (0.001, 0.01 and 0.1 M). At the end, HCl 0.01 and 0.1 M were those yielding better association. In acid medium the hydrophobic molecule (Figure 1.5 B) is deprotonated, allowing an increase of its solubility in water and adequate incorporation in LBG dispersion. The concomitant trituration of LBG and RFB powders, further allowed increasing the loading of RFB. The incorporation of RFB in microparticles was tested at different ratios. The association efficiencies varied within 85-100% which is considered a good result. In formulations containing RFB only, it was when RFB was present at the ratio of 10:1 that the higher value of association was registered (around 100%,  $p < 0.05$ ). When both drugs were incorporated, the association of RFB was still high, but decreased to approximately 90%. The results are similar to those obtained by Muttil *et al.*, who developed INH- and RFB-loaded poly(lactic acid) microparticles obtained by spray drying.<sup>98</sup> Regarding the loading capacity, it varied between 2 and 10%, approximately respecting the theoretical loadings in most cases owing to the high association efficiencies.

In this thesis, the co-encapsulation of INH and RFB in inhalable LBG MPs was envisaged, complying with the requirements of WHO for a tuberculosis therapy comprising an association

of drugs. MPs formulations containing each of the drugs individually were also produced to enrich the state of the art, as LBG MPs were never reported before.<sup>10,38,99,100</sup> However, the *target formulation* is considered that combining both drugs. The choice of RFB instead of RIF, the latter being the most used drug in tuberculosis therapy along with INH, was due to the fact that RIF and INH form adducts when together in solution, which would be a limitation in microparticle formation.<sup>100</sup>

#### 4.4. *In vitro* drug release

*In vitro* drug release studies were performed at 37 °C, to mimic physiological temperature, in two media. The alveolar lung lining fluid has a pH of approximately 7,<sup>101</sup> and its composition consists of an aqueous solution<sup>102</sup> having a considerable content of surfactant proteins and phospholipids.<sup>103</sup> The dissolution media selected for evaluation of isoniazid release was PBS pH 7.4, that has been described as suitable for this application, resembling the local pH.<sup>73,104</sup> However, rifabutin is a hydrophobic molecule and, therefore, it was necessary to include a surfactant into the dissolution media (Tween 80) to enable drug dissolution and quantification.<sup>104</sup> Thus, the used medium every time RFB was present in the evaluated formulation, was PBS pH 7.4 added of 1% (v/v) Tween 80. As Tween is a tensioactive, this medium further resembles the lung lining fluid in a proper way, as this is composed as phospholipids, as mentioned above.

After phagocytosis, the microparticles are expected to be included in a phagosome that will then fuse with lysosome, forming the phagolysosome.<sup>98</sup> Inside this structure, microparticles will be digested and release the drug. The phagolysosome contains proteolytic enzymes, oxygen radicals, chelator precipitators and has a pH varying between 4.5 and 5.5.<sup>105</sup> In order to resemble this medium, a release medium of pH 5 (citric acid/sodium hydroxide solution) was also selected to perform release studies, as reported in other works.<sup>98</sup> It is important to highlight that, if microparticles are co-localized with bacteria in maturation-arrested phagosomes, the pH of these structures is 7.4<sup>98</sup> and, therefore, the other medium might resemble this condition regarding the pH.

It is also relevant to refer that the volume of alveolar lung lining fluid or phagolysosome represents only a residual amount of liquid. Taking this into account, the method used in this thesis to perform the determination of release profile, which is the generally reported and which follows the European Pharmacopea methods,<sup>73</sup> might not provide results resembling exactly what occurs *in vivo*. Although conscious of these issues, a volume of dissolution media had to be selected so that the drug dissolution conditions and quantification procedures were

not compromised.<sup>73</sup> Even if not absolute accurate, it is believed that the obtained results give an indication on the expected behaviours.

The *in vitro* release profiles of INH from LBG.INH MPs in two media described above are plotted in figure 4.2. A rapid release was observed in both media, with 70% - 80% of the drug being released approximately at 20 minutes. The release is apparently a little slower in pH 5, at least for the initial times. In this regard, 31% INH was detected at 10 minutes when the assay occurred in pH 5, while 61% were quantified at pH 7.4 for the same period, and statistically significant differences were found between two media ( $p < 0.05$ ). For this formulation, the maximum release was registered at about 240 minutes. In general, this profile of INH release is identical to that obtained by Zhou *et al.* when testing PLA microparticles in PBS pH 7.4 and pH 5.<sup>97</sup>

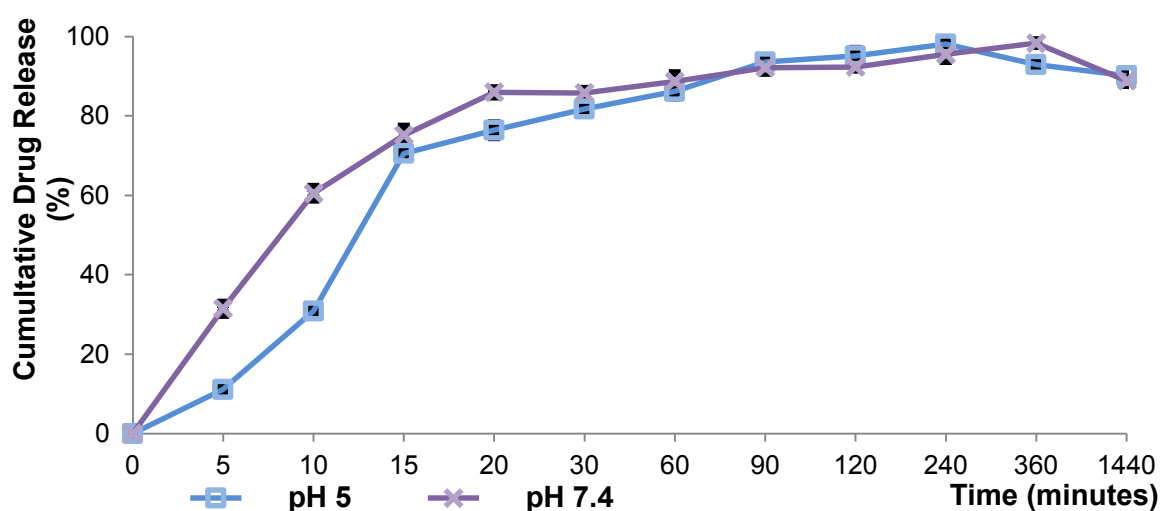


**Figure 4.2:** *In vitro* release of isoniazid (INH) from LBG.INH (10:1, w/w) microparticles, in pH 5 (blue line) and pH 7.4 (purple line) during 1440 minutes (24 hours). (Mean  $\pm$  SD, n = 3).

The rapid release that is observed is possibly due to three factors. First, the high specific surface area of these wrinkled MPs, which provides great contact with the release media. Second, the low particle density suggests that the internal structure might not be compact, which may facilitate the diffusion of INH through the LBG matrix.<sup>87</sup> A third reason might rely on the apparent absence or very low crystallinity pattern of INH, thus potentiating a rapid dissolution in release media.<sup>98</sup>

The *in vitro* release profiles of INH and RFB from LBG.INH.RFB 10:1:0.5 MPs in PBS.Tween 80® are depicted in figure 4.3. Curiously, it was observed that the profile was slower for both the drugs. RFB reaches 100% of release after 180 minutes and INH at 120 minutes. This shorter time taken by INH to completely release, as compared with RFB, might be justified by

its strong hydrophilic character. No statistically significant differences were found between the release profiles of both drugs, except at time point of 120 minutes. The sustained release that is observed has certainly a contribution from the gelling ability of LBG. When the assay starts and microparticles initiate the contact with the aqueous medium, the polymer matrix gradually begins to hydrate from periphery to center, forming a gelatinous swollen mass, which progressively allowed the release of drugs into the medium.<sup>106</sup>

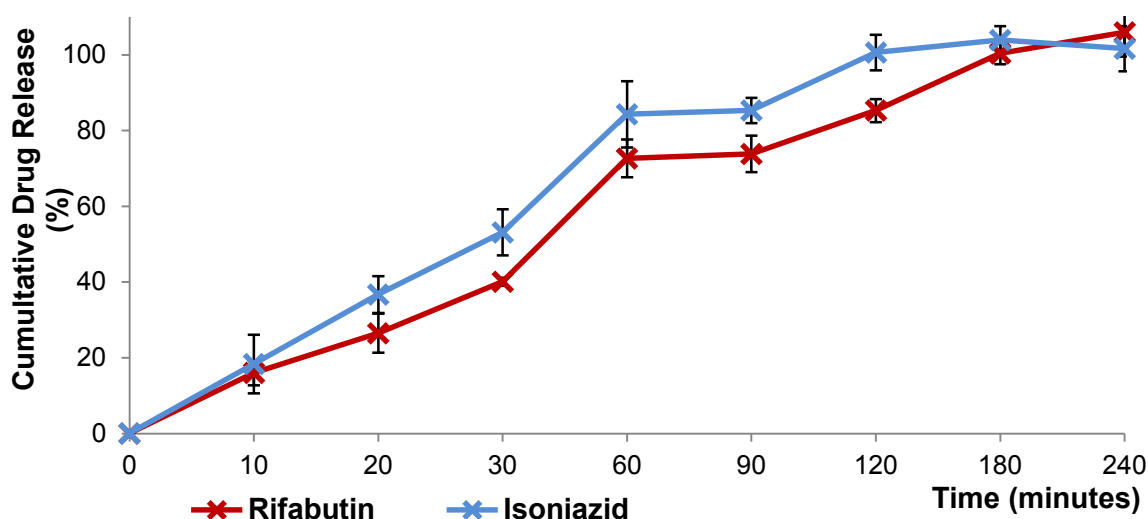


**Figure 4.3:** *In vitro* isoniazid (blue) and rifabutin (red) release from LBG.INH.RFB (10:1:0.5) microparticles in pH 7.4. (Mean  $\pm$  SD, n = 3).

When comparing figures 4.4 and 4.5, it is seen that the release profile of INH in pH 7.4 differs between the formulations LBG.INH (10:1) and LBG.INH.RFB (10:1:0.5). In this regard, the co-encapsulation with RFB yielded a much slower release, as already said, with only 53% being released at 30 minutes, while in the formulation as single drug the same period registered a release of 86% ( $p < 0.05$ ). One possible explanation for this effect is that RFB, when present in the microparticles, acts as surfactant<sup>98</sup> and somehow retains INH within the matrix for a longer time. Nishino *et al.* have verified that surfactant incorporation into polylactide matrix results in reduction of initial burst release of the encapsulated drug (irinotecan).<sup>107</sup>

#### 4.5. Crystallinity pattern of MP

X-ray diffractograms of the drugs before and after spray drying are presented in figure 4.4 for INH and figure 4.5 for RFB. INH was prepared as aqueous solution and RFB as acid solution.

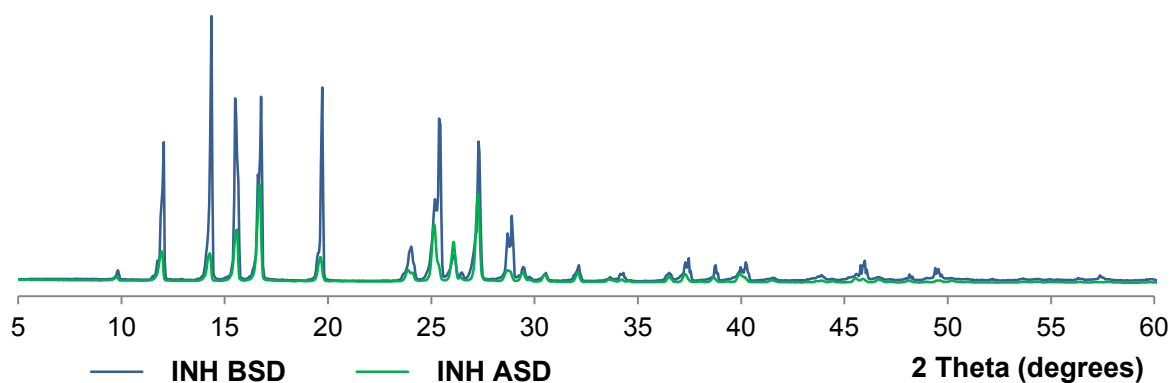


Figure 4.4: XRD spectra of Isoniazid before (BSD) and after spray drying (ASD).

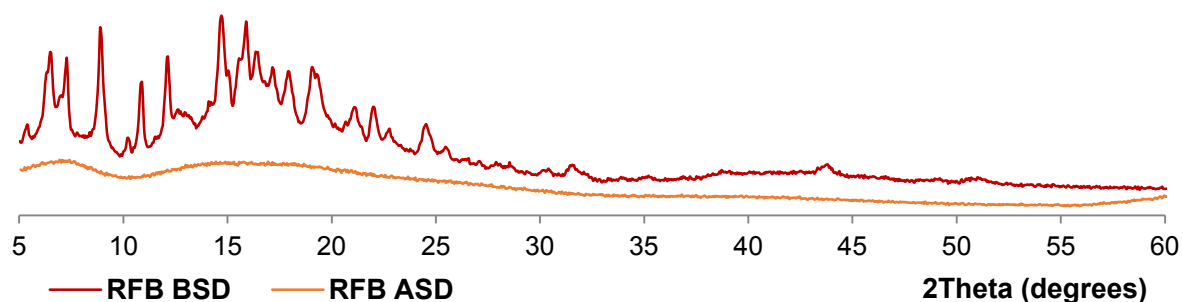


Figure 4.5: XRD spectra of Rifabutin before (BSD) and after spray drying (ASD).

INH displayed a profile corresponding to a crystalline drug and the obtained diffraction pattern is similar to that described in the literature. INH has sharp and intense peaks at  $2\theta$  of  $14^\circ$ ,  $16^\circ$  and  $20^\circ$  (among others), which are characteristic of its crystalline nature.<sup>108</sup> After the process of spray drying, a decrease in the intensity of some of the peaks was observed. This indicates that spray-drying itself changes the crystallinity of INH, probably as a consequence of drug recrystallization.<sup>109,110</sup>

Concerning RFB, it presented a XRD pattern corresponding to a crystalline drug, identical to the obtained in other analysis.<sup>111</sup> This profile presents characteristic peaks appeared in the XRD pattern of pure RFB at a diffraction  $2\theta$  angle of  $10.75^\circ$ ,  $12.63^\circ$ ,  $15.50^\circ$ ,  $17.9^\circ$ ,  $18.9^\circ$  and  $22.8^\circ$  (among others).<sup>111</sup> After spray-drying, no diffraction peaks were observed suggesting an amorphous state or the presence of very small crystals not identified by XRD.

X-ray diffractograms of LBG polymer, unloaded LBG MPs and drug-loaded LBG MPs are presented in figure 4.6. For the formulations containing RFB, the diffractograms of LBG.RFB

10:1 and LBG.INH.RFB 10:1.1 are presented, which are considered representative of the other ratios.

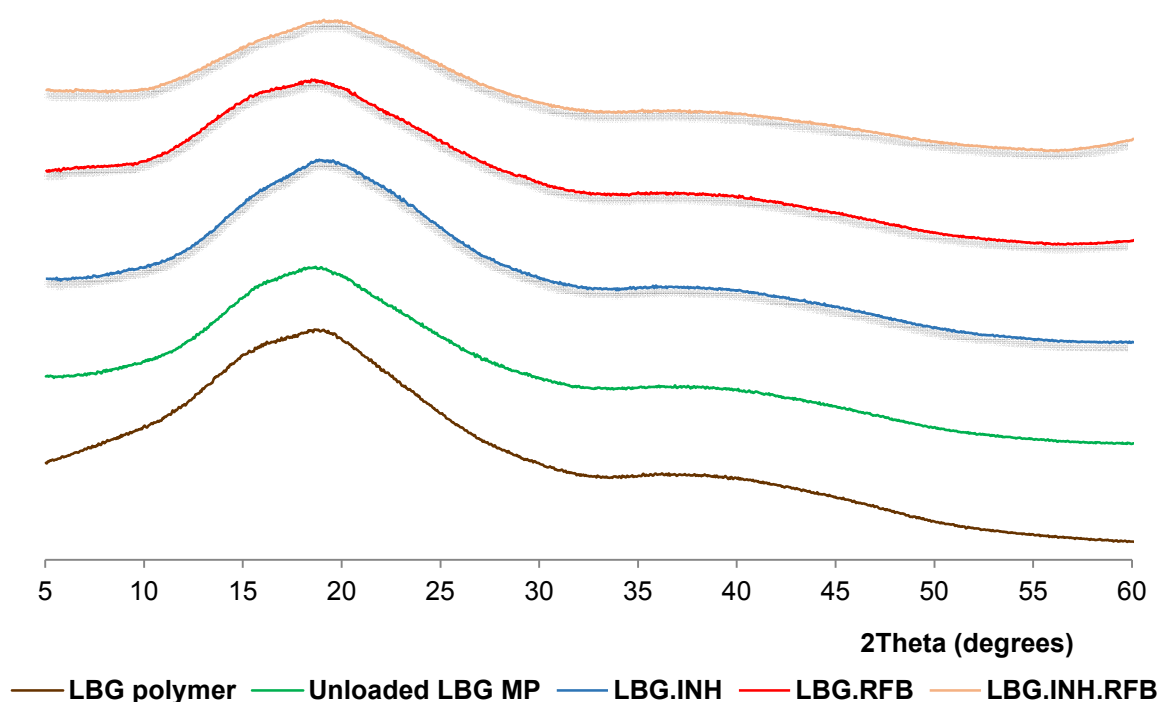


**Figure 4.6: XRD spectra of locust bean gum (LBG) raw material and spray dried formulations:** LBG raw material (brown line), unloaded LBG MPs (green line), LBG.INH 10:1 MPs (blue line), LBG.RFB 10:1 MPs (red line), LBG. INH.RFB 10:1:1 MPs (orange line). INH: Isoniazid; LBG: Locust bean gum; RFB: Rifabutin.

Locust bean gum does not show diffraction peaks, in agreement with its non-crystalline nature. Diffractograms obtained after and before spray drying are similar comparing to each other, and are also similar to those described in literature.<sup>112</sup> RFB shows peaks with lower intensity than INH, as shown in figures 4.4 and 4.5. Therefore, some diffraction peaks at least from INH were expected to be observed in microparticle formulations. In those containing INH (LBG.INH and LBG.INH.RFB), no diffraction peaks were identified. The diffractograms are identical among themselves and also similar to that of the polymer. This observation is common to other spray-dried microparticles,<sup>42,95,109,113</sup> where INH peaks disappeared in INH-loaded microspheres, only peaks from the matrix material being observed. This absence of INH peaks might be due to the fact that very small crystals appeared after INH recrystallization, which are under the detection limit of the equipment.<sup>108</sup> It can also be justified by the rapid process of drying occurring in spray-drying, which affects crystal rearrangement, leading to the formation of an amorphous structure.<sup>49</sup> High inlet temperatures used in the process have also been referred in the literature to possibly affect the final structure.<sup>114</sup> In this regard, the production of INH-

loaded microparticles was performed at 120 °C, but no differences on crystallinity were found (data not shown), indicating an absence of effect of inlet temperature in this case. Interestingly, the physical mixture of LBG and INH in the same polymer/drug ratio present in the formulation, has shown the INH peaks in the diffractogram (data not show), which reinforces that the proper spray-drying process is leading to a loss of crystallinity.

#### 4.6. Cell characterisation

The drug delivery approach proposed in this thesis was designed for inhaled TB therapy. As described, the microparticles present, at least from a theoretical point of view, an adequate  $D_{aer}$  to reach the alveolar zone, where they are expected to undergo phagocytosis by alveolar macrophages. For this reason, it was necessary and fundamental to perform analysis on the interaction of particles with the cells present in the alveolar zone. This zone is composed by alveolar epithelium cells, surfactant and alveolar macrophages, as described in figure 4.7.

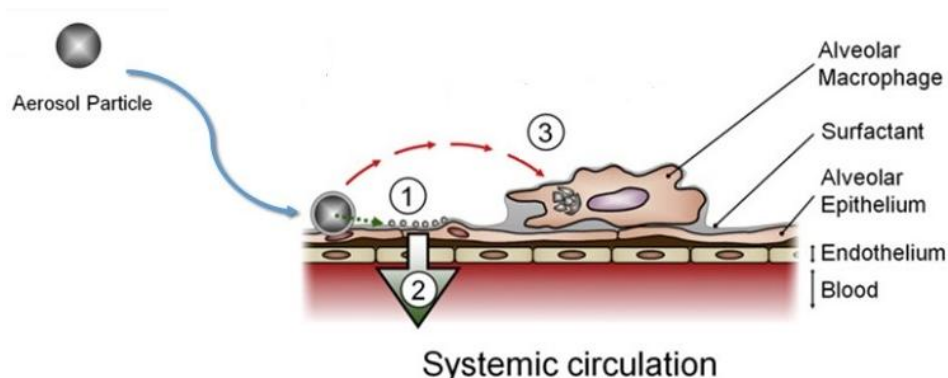


**Figure 4.7: Interaction between aerosol particle and alveolar epithelium:** When microparticles reach the alveolar zone, and deposit over the epithelium, their dissolution and consequent release of drug (1) might occur. The drug might penetrate the epithelium and reach the systemic circulation for systemic action (2), or act locally (1), or the microparticle can be phagocytosed by macrophages (3). Adapted from Carvalho *et al.*<sup>115</sup>

Cell culture models have been applied to investigate the interactions occurring between cells and drug delivery systems, including the study of processes such as phagocytosis, cell signaling pathways and cellular activation, apart from permitting an evaluation of toxicological events. Cell culture assays have been indicated in many cases as adequate to replace *in vivo* studies at initial stages of research. Therefore, it is essential that the established *in vitro* setups are accurately defined in order to mimic *in vivo* conditions the better possible. The cell culture studies included in this thesis were performed in three different cell lines, which selection is reasoned below.

A549 cells are a widely accepted model of the alveolar epithelium and derive from lung adenocarcinoma. Morphologically, these cells present several multilamellar cytoplasmic inclusion bodies, similar to those found in human lung alveolar type II cells.

As the drug carriers designed in this thesis are aimed at targeting the alveolar macrophages, it was important to also have cell lines representing macrophages. Human alveolar macrophages are represented by differentiated THP-1 cells, which are human leukemic monocytes. The differentiation performed with PMA, according to a protocol disclosed in the methods section, results in differentiated THP-1 cells that are reported to have alveolar macrophage characteristics.<sup>115,116</sup> A cell line of rat alveolar macrophages, NR8383, was also used to enable the establishment of comparisons between human and rat responses.

As referred above and in methods section, THP-1 cells in the monocyte state can be differentiated into a macrophage-like phenotype using either macrophage colony-stimulating factor, phorbol-12-myristate-13-acetate, or  $1\alpha, 25$ -dihydroxyvitamin D<sub>3</sub>.<sup>35</sup> In culture, THP-1 monocytes have a round shape and are in suspension in CCM. When contact with PMA is provided, several morphological, physiological and genetic alterations occur that lead to a differentiation into macrophage-like cells.<sup>80</sup> Figure 4.8 shows the morphologies of THP-1 and macrophage-differentiated THP-1 cells, which are representative of what was observed in our cell culture and experiments.

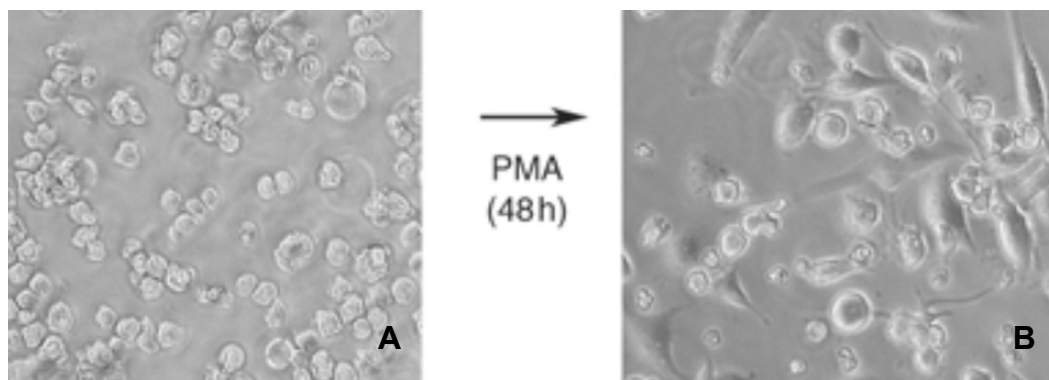


**Figure 4.8: Macrophage differentiation from THP-1 cells:** (A) Round shape THP-1 cells were exposed to 100 nM phorbol-12-myristate 13-acetate (PMA), and after 48 hours (B) macrophages were obtained, showing flattened and adherent cell morphology. Adapted from Raffetseder *et al.*<sup>117</sup>

Firstly, the concentration of PMA and time of exposure were optimized in THP-1 cells cultured in 6-well plates at a density of  $1.0 \times 10^6$  cells per well in 5 mL of RPMI. The conditions tested were: 5, 10, 50, 100 and 200 nM PMA four 3 days. In our conditions, it was verified that 50 nM with 48 hours of exposition was adequate for differentiation of THP-1 cells into macrophages, by observation that the macrophages exhibited an adhering phenotype onto the wells surface, as described in figure 4.8, and according to the literature.<sup>35,80</sup>

Apart from the observation of the adhering phenotype, several other methods have been described as more accurate for the characterization of fully differentiation of macrophage-like THP-1 cells. These include the expression of differentiation-dependent cell surface markers such as CD-14, CD36, TLR-2, and CR3 (CD11b/CD18).<sup>80</sup> The analysis of the cells (before and after differentiation) by flow cytometry, confirmed that differentiated cells present a distinct size (figure 4.9, panels A and B). This observation is concordant with that related by Grabowski.<sup>35</sup> Furthermore, an immunocytochemical characterisation might help on the confirmation of the correct phenotype. In this regards, an increase in the expression of CD11b is reported to be visible only on macrophage-differentiated THP-1 cells.<sup>80</sup> In our work we have confirmed the presence of this CD11b antibody in the population of THP-1 differentiated cells, as seen in panel C of figure 4.9. The percentage of undifferentiated THP-1 cells evidencing signal of the same antibody was considered residual, an effect that has been described by other authors.<sup>35</sup>

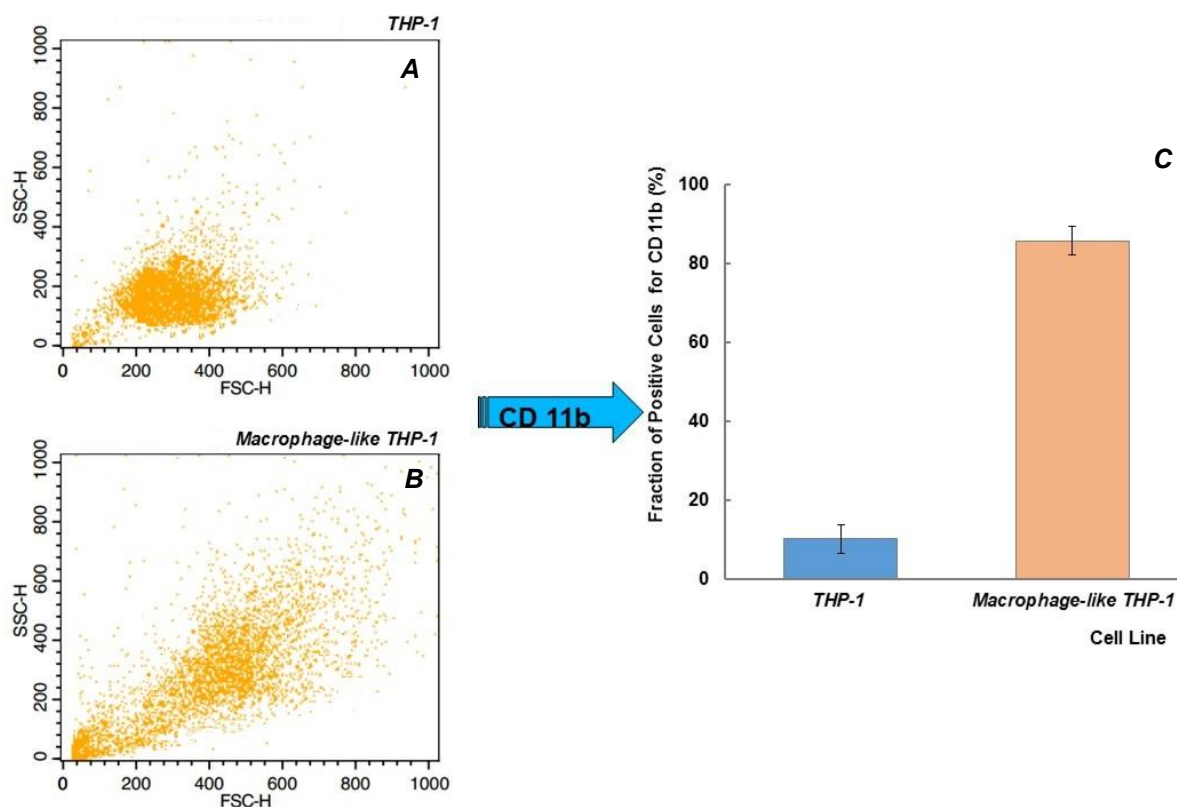


**Figure 4.9: Immunocytochemical characterization of THP-1 cells and macrophage-differentiated THP-1 cells.** Evaluation and comparison between size (axis FSCH) and structure/complexity (axis SSCH) of THP-1 (A) and macrophage-like THP-1 cells (B). One group of THP-1 cells was incubated for 48 hours with 50 nM of PMA, allowed their differentiation into macrophages-like THP-1. Marker anti-CD 11b allows distinguishing the population of undifferentiated THP-1 from THP-1 differentiated cells (C). This marker labels the CR3 receptor, present only in membrane of THP-1 differentiated cells. Results expressed as mean  $\pm$  SEM.

## 4.7. Cytotoxic evaluation

The evaluation of the biocompatibility profile of formulations designed for drug delivery is an up-to-date subject, referred as mandatory for any formulation being proposed.<sup>118</sup> This evaluation was performed in two cell lines, representing the alveolar epithelium (A549 cell line) and alveolar macrophages (THP-1 cells). For the analysis of pharmaceutical formulations, different *in vitro* tests have been employed that allow evaluating the integrity and function of different structures of cells after exposure to drug formulations. In this regard, this thesis encompassed the evaluation of metabolic activity (MTT assay) and membrane integrity (LDH release assay).

### 4.7.1. Samples presented in solution/suspension

The cytotoxicity evaluation (MTT) was analysed at two time points (3 and 24 hours) for each cell line and for each sample presented in solution/suspension. These assay times correspond to short and long term exposure of cells to the formulations,<sup>119</sup> and are usually applied in this type of analysis of pulmonary drug delivery systems.<sup>119,120</sup> For analysis and interpretation of results, it was considered that a sample evidences cytotoxic potential when cell viability values resulting from exposure to the material decrease to values below 70% (in all figures is indicated with dashed line), as indicated by the ISO 10993-5.<sup>121</sup>

For each cell line, the MTT assay protocol was adapted as a function of results obtained in optimization experiments. For THP-1, for instance, it was necessary to use SDS to dissolve formazan crystals, instead of DMSO.<sup>122,123</sup>

The cytotoxic evaluation of RFB as free drug required a previous solubilisation in DMSO at concentration 20 mg/mL (w/v), due to its hydrophobic character. After this, it was possible to perform the dilution of this solution in CCM to obtain the desired concentrations to be tested. Given the need to use DMSO, a cytotoxic evaluation of the solvent itself was also performed in both cell lines, between concentrations of 0.0313% and 2% (v/v). It was demonstrated an absence of cytotoxicity of DMSO at the tested concentrations (data not show). Specifically, for DMSO concentration of 0.5% (v/v), used in tested RFB solutions, registered cell viabilities corresponded to  $100 \pm 4\%$  in A549 cells and  $94 \pm 3\%$  in THP-1 cells.

In A549 cells, the cytotoxic evaluation of drugs after exposure for 3 and 24 hours is presented in figure 4.10. The same evaluation was performed for macrophage-like THP-1 cells, which is depicted in figure 4.11. For both cell lines, pure RFB demonstrated to induce a reduction of cell viability in higher concentrations after 24 hours of exposure ( $p < 0.05$ ). A concentration-

and time-dependent effect was observed for this drug. On the contrary, INH did not show any detrimental effect on cell viability.

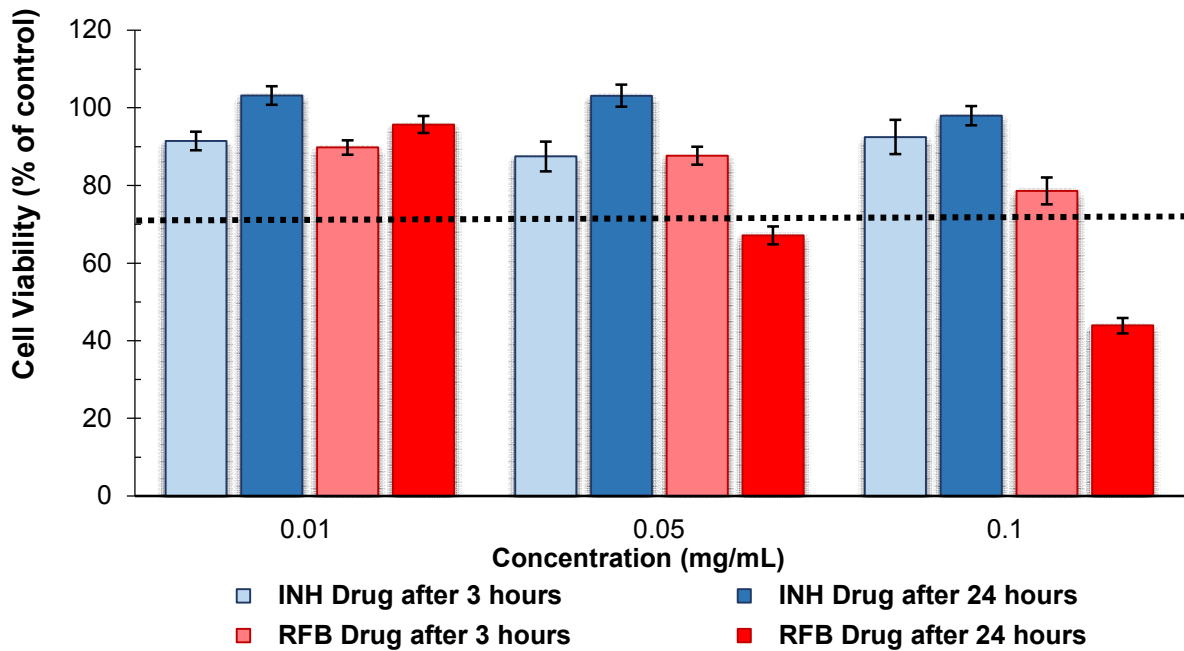


Figure 4.10: A549 cell viability after 3 and 24 hours of exposure to Drugs. INH: Isoniazid; RFB: Rifabutin; Results expressed as mean  $\pm$  SEM. Dotted line represents 70% cell viability.

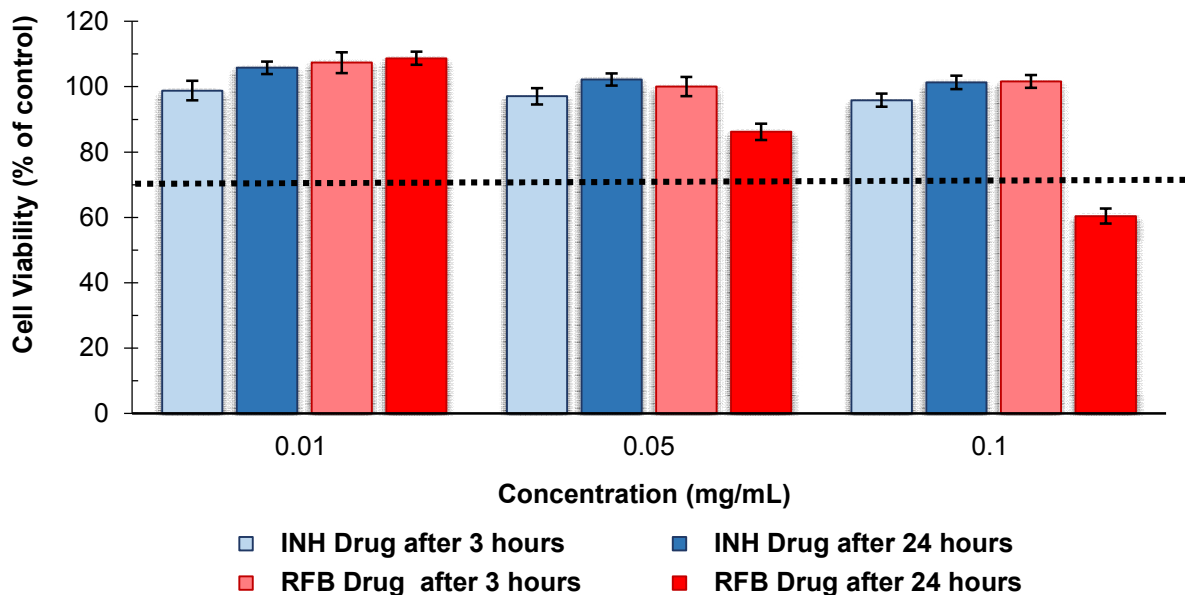
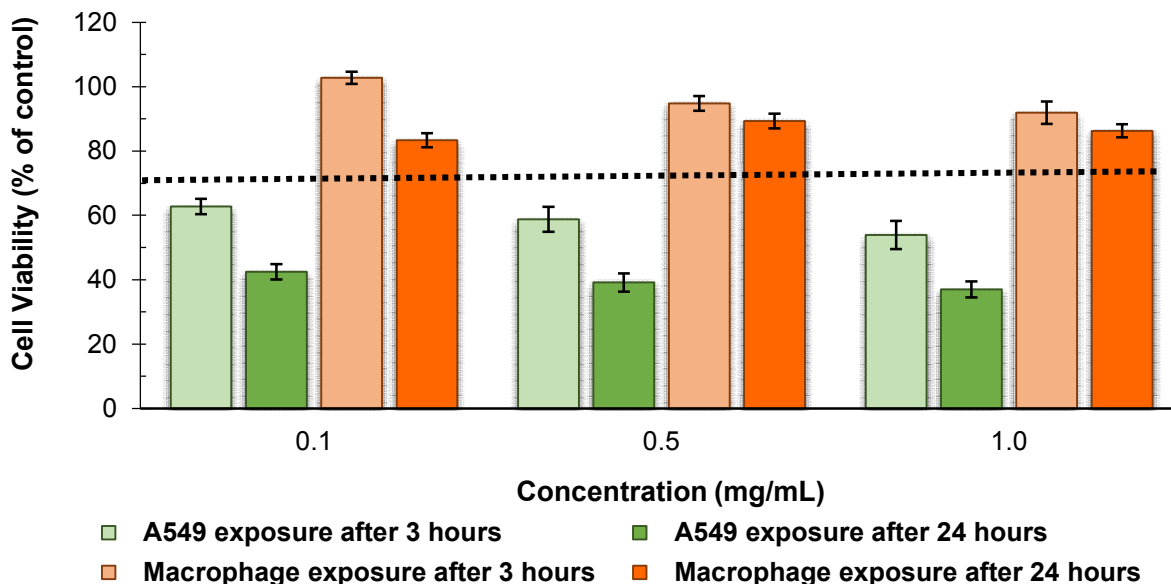


Figure 4.11: Macrophage-differentiated THP-1 cell viability after 3 and 24 hours of exposure to Drugs. INH: Isoniazid; RFB: Rifabutin; LBG: Locust bean gum. Results expressed as mean  $\pm$  SEM. Dotted line represents 70% cell viability.

The analysis of effect on cell viability of a solution prepared with the raw material (LBG) after 3 and 24 hours of exposition is presented in figure 4.12 for both cell lines. A549 cells demonstrate a clear reduction of cell viability at both times of exposure. Macrophage-like cells, in turn, seem to be more resistant to the effect of LBG, as cell viabilities remained above 80% in all tested conditions.



**Figure 4.12: Cell viability of A549 and differentiated THP-1 cells after 3 and 24 hours of exposure to Raw material (LBG).** INH: Isoniazid; RFB: Rifabutin; LBG: Locust bean gum. Results expressed as mean  $\pm$  SEM. Dotted line represents 70% cell viability.

The raw materials used in carrier matrix and the carriers should be evaluated separately,<sup>118</sup> as it is assumed that the carrier structure might affect the final toxicological behaviour.<sup>120</sup> It is curious to observe that, already at 3 hours, the LBG as polymer has a stronger effect on cell viability of A549 cell line comparing with unloaded LBG microparticles (figure 4.13,  $p < 0.05$ ). For LBG polymer, cell viability was below 70% (about 50-60%) for all tested concentrations. This effect remained for up to 24 hours, and was inclusively accentuated at this time, the polymer eliciting cell viabilities around 40% independently of the concentration. However, it is important to highlight that spray-drying the polymer reverted the effect, and unloaded LBG microparticles exhibited a very mild effect, with cell viabilities remaining above 75% in all cases, even after 24 hours incubation (Figure 4.13 and 4.14). This effect of LBG as raw material might be due to the fact that it presents a bulkier structure and higher size, causing a major effect of viscosity on liquid contacting with the cells, which can difficult the gaseous exchanges between cells, medium and air, leading to cell death. After spray drying, there is a reduction of size, and the suspension corresponding to the microparticle sample is macroscopically more fluid than that of LBG polymer. The literature already describes that

macrophage-like THP-1 cells are more sensitive to an insult than A549 cells.<sup>119</sup> As happened for LBG polymer, macrophage-differentiated THP-1 cells did not demonstrate any reduction of cell viability upon exposure to unloaded LBG microparticles.

The cytotoxic evaluation of drug-loaded formulations prepared with LBG is presented in the following figures. In general, the obtained results revealed that macrophages respond to these microparticles in a similar manner of A549 cells. Figures 4.13 and 4.14 show the results obtained upon exposure of A549 cells to unloaded and drug-loaded microparticles for 3 and 24 hours, respectively.

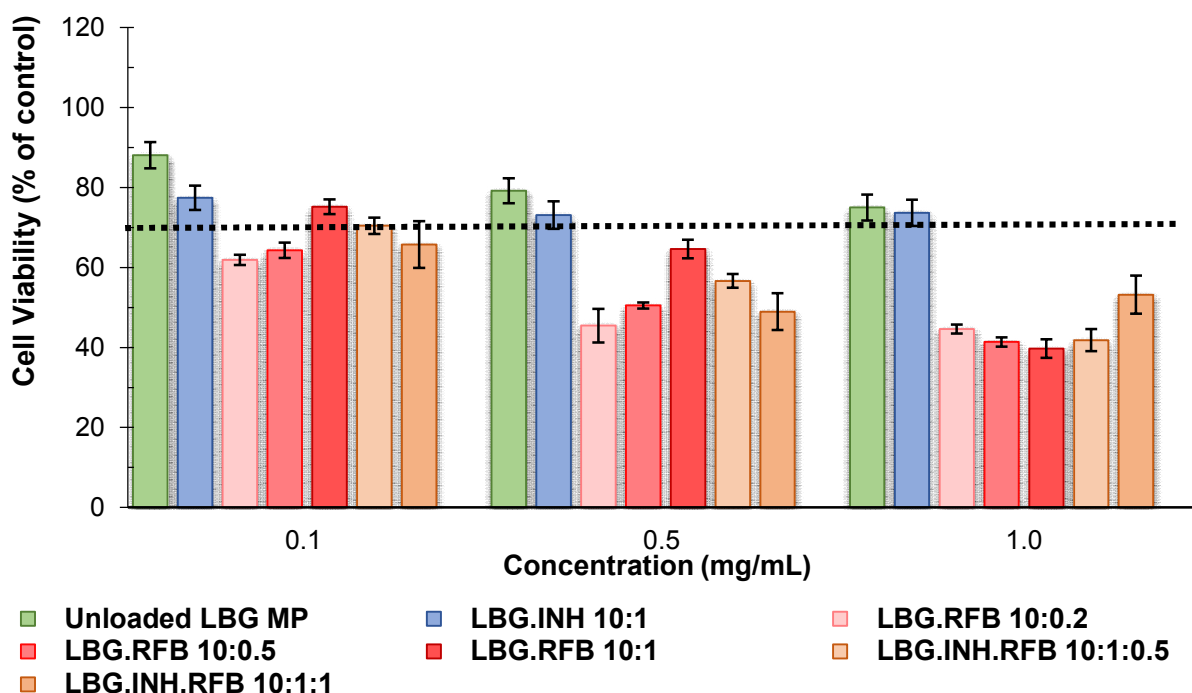


**Figure 4.13: A549 cell viability after 3 hours of exposure to formulations.** INH: Isoniazid; LBG: Locust bean gum. RFB: Rifabutin; Results expressed as mean  $\pm$  SEM. Dotted line represents 70% cell viability.

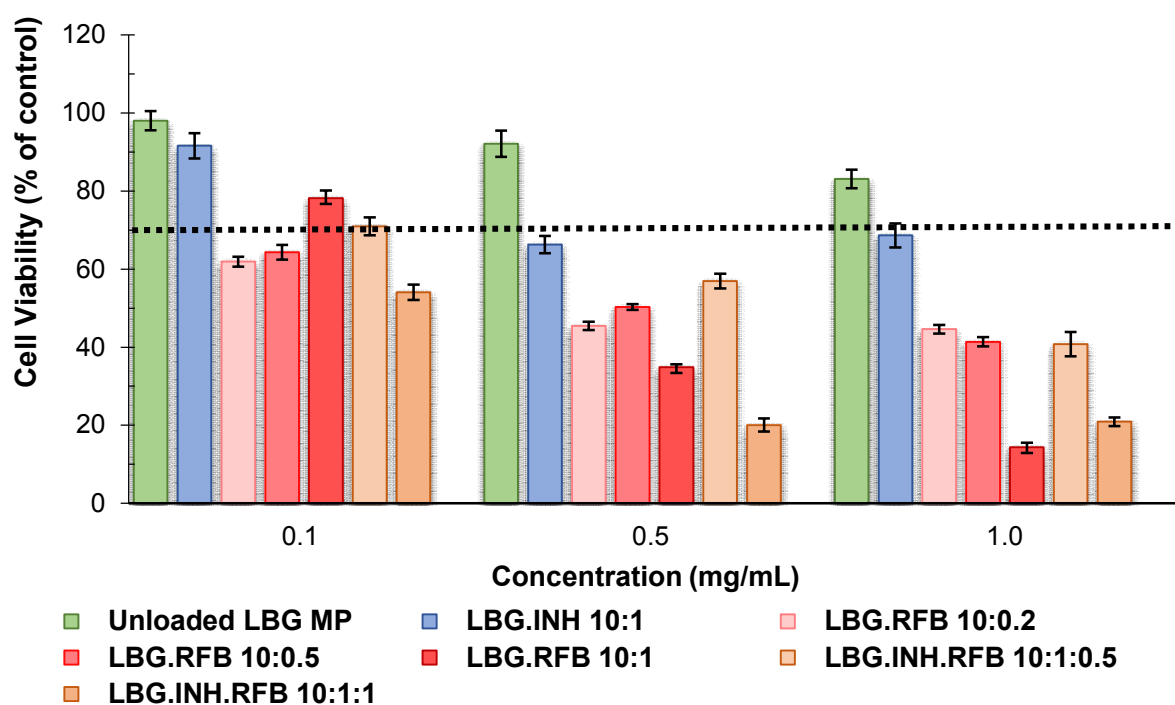


**Figure 4.14: A549 cell viability after 24 hours of exposure to Formulations.** Formulations with different ratio polymer: drug. INH: Isoniazid; LBG: Locust bean gum. RFB: Rifabutin; Results expressed as mean  $\pm$  SEM. Dotted line represents 70% cell viability.

For INH drug, its incorporation in microparticles did not result in a significant decrease of cell viability comparing with unloaded LBG MPs, all values being above 75% at 3 hours. The prolongation of the exposure to 24 hours revealed only a very slight decrease on cell viability to approximately 65% in this case (Figure 4.14). Therefore, no overt cytotoxic effect was considered to occur for INH-loaded microparticles. On the contrary, even after a short time of exposure (3 hours), RFB-loaded formulations generally evidenced a slight reduction of A549 cell viability to values below 70%, particularly for concentrations of 0.5 and 1.0 mg/mL (Figure 4.13). The effect was accentuated after 24 hours exposure, as seen in figure 4.14. RFB-loaded formulations demonstrated a concentration- and time-dependent effect and, actually, for the higher concentration and the longer exposure time, viabilities lower than 20% were obtained. Microparticles associating both drugs had a milder effect than those containing RFB only, but still a significant cytotoxic behavior was detected. Additionally, formulations having different amounts of RFB, demonstrated clear concentration-dependent effect. In these microparticles, not so low cell viabilities were found, but the formulation LBG.INH.RFB = 10:1:0.5 (w/w) still registered around 40% cell viability for the concentration of 1 mg/mL and less than 60% at 0.5 mg/mL.

The cytotoxic evaluation was also performed in macrophage-differentiated cells, results being presented in figures 4.15 (3 hours) and 4.16 (24 hours). Again, INH-loaded microparticles evidenced no toxic effect, as only after 24 hours exposure a very slight decrease on cell

viability was detected, which is devoid of significance as the values remained close to 80%–90% in all cases. Some authors have reported that INH drug presents an  $IC_{50}$  of 1000 mg/mL in alveolar macrophages (isolated from albino rats).<sup>124</sup> That study was performed in primary cells, thus different from those used in this study, but they mimic *in vivo* conditions in a closer way and in fact indicate that a high amount of INH is necessary to induce cytotoxicity.<sup>115</sup> RFB-containing microparticles elicited a reduction of cell viability, which was also stronger for microparticles associating RFB only (cell viabilities as low as 10% after 24 hours), as observed previously in A549 cells. The effect was again concentration- and time-dependent.

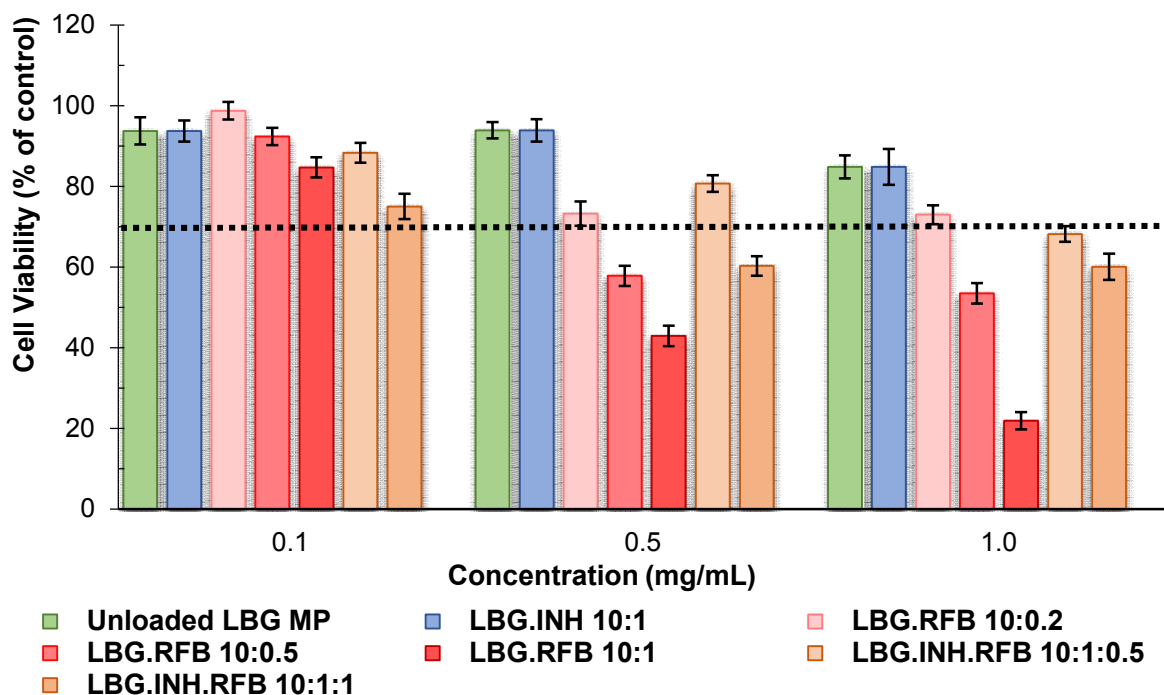


**Figure 4.15: Macrophage-like THP-1 cell viability after 3 hours of exposure to Formulations.** Formulations with different ratio polymer: drug. INH: Isoniazid; LBG: Locust bean gum. RFB: Rifabutin; Results expressed as mean  $\pm$  SEM. Dotted line represents 70% cell viability.

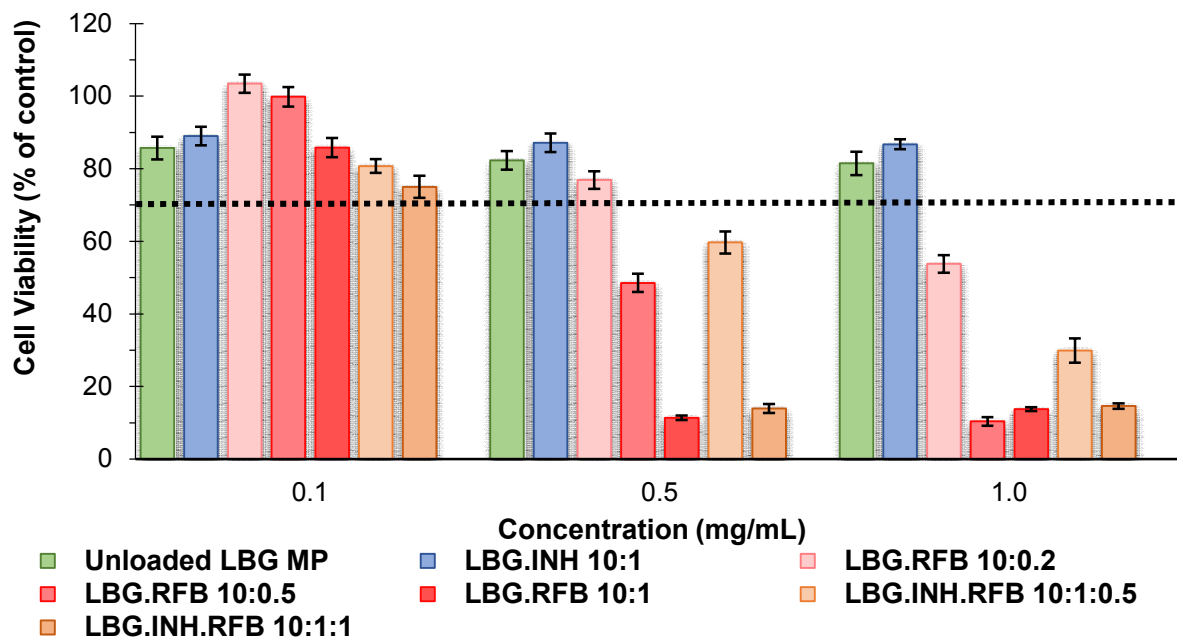


**Figure 4.16: Macrophage-like THP-1 cell viability after 24 hours of exposure to Formulations.** Formulations with different ratio polymer: drug. INH: Isoniazid; LBG: Locust bean gum. RFB: Rifabutin; Results expressed as mean  $\pm$  SEM. Dotted line represents 70% cell viability.

The general observation thus corresponds to an increased toxic effect, which reflects in lower viabilities, when RFB is included in the microparticles. The literature does not report studies on RFB impact in cell viability with the cell lines used in this study, but the high toxicity *in vivo* is well reported.<sup>125</sup> The cytotoxic behavior might be due in part to the lipophilic character of RFB. It presents a high membrane lipid tropism, resulting in high penetration into infected cells, which can impose increased toxicity.<sup>126</sup>

Focusing only the results from unloaded LBG MPs and LBG.RFB formulations (10:0.2, 10:0.5 and 10:1) at 24 hours, there is a statistically significant difference ( $p < 0.05$ ) for both cells lines. It was observed that, while the ratio 10:1 had a strong negative effect on cell viability, a ratio of 10:0.5 had a milder impact on cell viability. No significant difference was observed between formulations 10:0.5 and 10:0.2. As a whole, it is suggested that, apart from an RFB-related effect, there is possibly a contribution of the HCl content, which needs to be included in the formulation for solubilisation. LBG is believed to not contribute to the toxicological effect, given the absence of toxicity of LBG MPs, used as control. Microparticles with association of drugs display lower toxicity levels, generating higher values of cell viability, although still below 70% in most cases.

For interpretation of these results, a determination of the effect of RFB dissolved in either HCl or DMSO on cell viability was performed in both cell lines. It was determined that 1 mg microparticles have 0.0183 mg HCl and the amounts corresponding to MPs concentration of 0.1 and 0.5 mg/mL were also calculated. RFB was dissolved at 20 mg/mL in HCl 0.1M or

DMSO and subsequently diluted with CCM to obtain solutions of RFB at 0.01, 0.05 and 0.1 mg/mL and with, respectively, HCl concentrations of 0.0018, 0.0091 and 0.0183 mg/mL. The obtained cell viability of A549 cells for RFB at 0.1 mg/mL (the higher concentration tested) was  $43.9 \pm 2.1\%$  when drug was dissolved in DMSO and  $54.7 \pm 3.1$  when solvent was HCl. The latter thus induced higher viabilities, comparatively, although cell viability is considered low. However, in macrophage-differentiated cells there was an increase of toxicity of RFB dissolved in HCl, cell viability in DMSO being  $60.4 \pm 2.3\%$  and in HCl being  $38.8 \pm 3.7\%$ . For both cells lines was found a statistically significant differences ( $p < 0.05$ ) between RFB dissolved in DMSO and HCl. The literature does not describe the behaviour of RFB-loaded microparticles *in vitro*. However, RFB-loaded lipid nanoparticles were also demonstrated to reduce significantly A549 cell viability (50%) for concentrations of nanoparticles containing RFB (1 and 10 mg/mL) similar to those observed in these results.<sup>31</sup>

In similar project in our laboratory, it was possible to use HCl 0.01M for the solubilisation of RFB, in a glucomannan:RFB ratio of 10:0.5 and glucomannan:INH:RFB ratio of 10:1:0.5, and no reduction on cell viability beyond 70% was observed for A549 cells (data not show).

Although the mechanism might not be well established, the toxic effect is undoubtedly related with RFB. In this context, some authors have referred that at acidic pH values, RFB establishes more electrostatic interactions with lipid membranes, possibly leading to membrane disruption.<sup>127</sup>

Notwithstanding the determinations that were made, there is the expectation that the toxicity does not translate to *in vivo*, because the tested doses are supposedly much higher than real amounts expected to be in contact with cells after administration. The highest dose of MPs tested was  $303.03 \mu\text{g}/\text{cm}^2$ . The area of epithelial surface of alveolar zone is about  $5000 \text{ cm}^2$ ,<sup>128</sup> and if considered that distribution of MPs is uniform, for example a nominal proportion (e.g. a third) of an inhaled dose (consider 10 mg) deposits in a defined region (alveolar),<sup>90</sup> the dose estimated across this area is  $0.66 \mu\text{g}/\text{cm}^2$ . This dose is about 460 x lower than the  $303.03 \mu\text{g}/\text{cm}^2$  used in our study. Taking this into account, the effects would be much closer to those of the lower dose of 0.1 mg/mL to those of the higher dose. Considering the higher number of human alveolar macrophages (23 billion) distributed on surface area of human alveoli compared to that of the cell culture,<sup>129,130</sup> the hypothesized MPs dosage could be argued as potentially non-cytotoxic.<sup>130</sup> Unfortunately, we could not meet the conditions permitting weighing such a lower amount of dry powder that could resemble in a better way the *in vivo* conditions.

Another reason suggesting that the administration of these microparticles *in vivo* will not induce high cytotoxicity, is the capacity of microparticles to form complexes with polar heads of

groups of the phospholipids present in pulmonary surfactant lipids, allowing reaching high concentrations without causing damage on alveolar epithelium.<sup>127</sup> The higher partition of the drug at the studied pH 5.0 comparatively with neutral pH values is in agreement with the higher affinity of the drug to the infected cells, allowing to present a higher selectivity and higher concentrations on the pharmacological target.<sup>73,75</sup>

#### 4.7.2. Samples presented in aerosol

It is usual that cytotoxic studies of inhalable formulations perform an evaluation under liquid conditions, that is, as a suspension. However, these conditions not really resemble *in vivo* conditions. One of the most relevant aspects is that, after inhalation and, particularly if the alveolar region is reached, microparticles will not be submerged in liquid, simply because there is no such an amount of liquid permitting so. The lung lining fluid depth (alveolar surfactant) is an order of magnitude smaller (0.01 – 0.2  $\mu\text{m}$ ) than the diameter of respirable microparticles (1 – 3  $\mu\text{m}$ ).<sup>102,103</sup> For this reason, a preliminary assay was setup to perform the cytotoxic analysis with microparticles under the form of an aerosol. The literature describes some studies of deposition of inhalable particles that use various impactors coupled with tissue culture methods in an attempt to mimic *in vivo* drug deposition. These studies have proven useful in complementing *in vivo* data.<sup>103</sup> However, most of the assays designed in such a way are applied in transport and uptake studies and no report has been found addressing cytotoxicity.

For the development of this assay, different aspects were taken into account. First, the method for aerolisation of microparticles over cell monolayers was optimised to use the Penn Century Dry Powder Insufflator. An optimization of the device operating was performed with three formulations, mannitol MPs, unloaded LBG MPs and LBG.INH.RFB 10:1:10 (Figure 4.17).

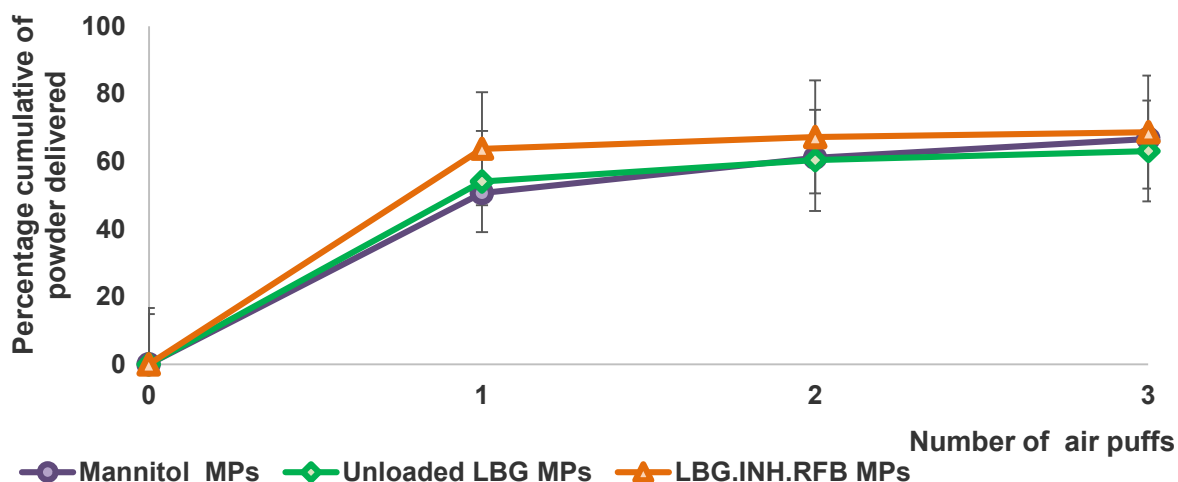


**Figure 4.17: Powder delivered from the dry powder insufflator.** Mass released after each insufflation with of 3 mL of air. Results are expressed as media percentage of initial mass of powder loaded in sample chamber and error bars correspond to standard deviation.

Dry powder insufflator is described in the literature to be used for dry powder characterization,<sup>132</sup> uptake,<sup>133</sup> and mucoadhesion<sup>87</sup> studies. For this study, an optimization was performed that included replicating the delivery of each formulation and calculating the mass of dry powder to weight before each assay.

In order to simulate the alveolar environment, and thus obtain results that predict *in vivo* responses, the assay testing samples as aerosols was performed using the cells in absence of CCM for a certain period, to simulate the real environment of the alveolar epithelium. The assay thus included an initial period of 2 hours where cells were in contact with the samples, which were aerosolised over the cell layers devoid of CCM. When CCM was aspirated, a very thin layer of liquid remained to maintain the hydration of cells. After that period, a determined amount of medium was added for the rest of the assay to not compromise the cell viability due to dryness. Some preliminary assays were performed that demonstrated no significant effect of the absence of CCM on cell viability for the period of 2 hours. Ideally, the cells should be exposed to an amount of volume that resembled the alveolar surfactant, but this volume was not possible to reproduce in *in vitro* conditions, as it is too short an amount. Alveolar surfactant content can be estimated as approximately 36 mL,<sup>102</sup> covering the alveolar zone that has an area of 5000 cm<sup>2</sup>.<sup>102,134</sup> In this manner, the volume of alveolar surfactant can be estimated is 7.2 µL/cm<sup>2</sup>. In 12-well plates, or 6-well plates, the volume to add would be respectively, 27.72 µL and 69.12 µL. These volumes are measurable, but not enough to cover the entire area of the cell layer.<sup>102</sup> Instead, volumes of 250, 500 and 750 µL were tested and it was found that 500 µL was the volume not compromising cell viability.

Cytotoxicity assays performed upon sample aerosolisation tested two different doses, 303 and 50 µg/cm<sup>2</sup>. The formulations selected to be tested were unloaded LBG MPs and the formulation with both drugs, LBG.INH.RFB 10:1:0.5. Figure 4.18 depicts the macrophage viability after 24 hours exposure of two different doses tested of unloaded LBG MPs and LBG.INH.RFB 10:1:0.5.

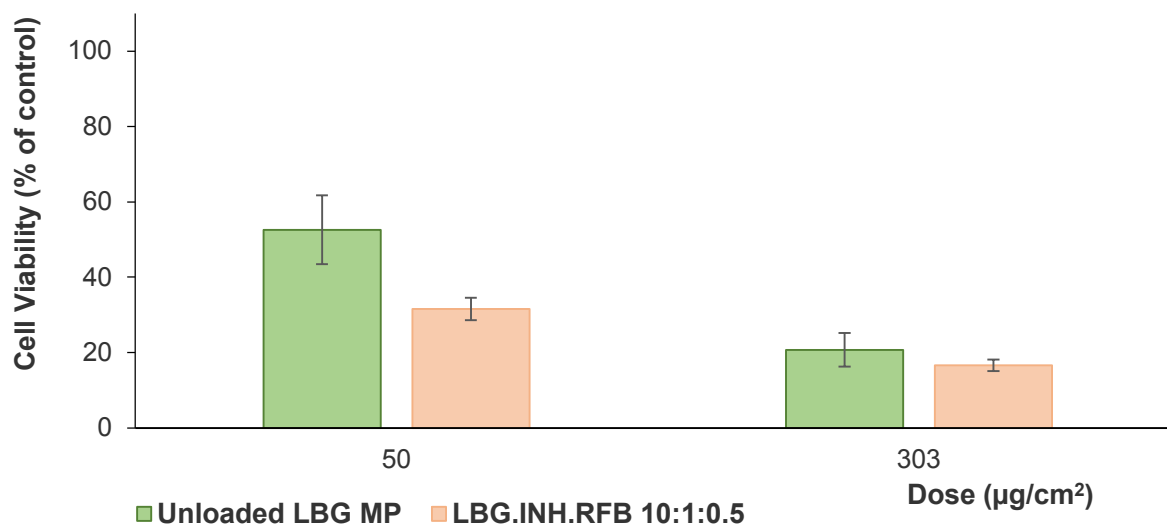


**Figure 4.18: Macrophage-like THP-1 cell viability after 24 hours of exposure to unloaded LBG MPs and LBG.INH.RFB 10:1:0.5 formulations at two doses.** Results expressed as mean  $\pm$  SEM.

The highest dose induces a greater reduction in cell viability for both formulations ( $p < 0.05$ ). When the dose was reduced to 50  $\mu\text{g}/\text{cm}^2$ , higher cell viabilities were observed. In this case, drug-loaded microparticles were observed to induce a much lower viability (around 35%,  $p < 0.05$ ) than unloaded microparticles (50%). Unloaded LBG MP, when exposed as aerosol, elicit a higher reduction of cell viability comparatively with the exposure as suspension, when the same dose is administered (303  $\mu\text{g}/\text{cm}^2$ ). As also referred before, it can be argued that the swelling capacity of LBG induces the formation of a viscous polymeric mass that difficult gaseous exchanges between air/CCM/cells. The same might happen in LBG.INH.RFB 10:1:0.5 microparticles, aggravated by the dissolution of RFB in CCM and its direct exposure to the cells.

It is possible that the lower tested dose is still various orders of magnitude above the real contact dose *in vivo*, as exposed in a previous section. Therefore, future design of these studies should reduce the dose in order to better mimic the *in vivo* conditions. As reducing the amount of weighed dry powder is not possible, the best solution would be using a larger surface for cell deposition. This is quite a new strategy to evaluate the cytotoxicity of inhalable dry powders and is recognised to require further optimisation.

#### 4.7.3. Determination of rifabutin IC<sub>50</sub>

It was verified that major toxic effect is observed for microparticles containing RFB. In section 4.7.1 is discussed the RFB toxicity and therefore it was decided to calculate an IC<sub>50</sub>. The IC<sub>50</sub> value is defined as the concentration of drug required to induce 50% of cell death. IC<sub>50</sub> was

determined for both cell lines. In A549 cells it was determined to be 100.70  $\mu\text{g/mL}$  ( $R^2$  is 0.999), while for macrophage-like THP-1 cells it was 87.08  $\mu\text{g/mL}$  ( $R^2$  is 0.996), indicating the higher sensitivity of THP-1 cells, as already suggested in the MTT assays. In formulations LBG.RFB whit ratio 10:0.2 and 10:0.5, the maximum drug concentration tested is respectively 20 and 50  $\mu\text{g/mL}$ . Better results could thus have been expected taking into account the  $\text{IC}_{50}$ , but as referred, the presence of HCl in microparticles is probably leading to a synergic effect that resulted in a further reduction of cell viability.

#### **4.7.4. LDH Release**

The release of LDH indicates the disruption of cell membrane, thus permitting the leaking of this cytoplasmic enzyme. The loss of intracellular LDH and its release to the culture medium is, therefore, an indicator of irreversible cell death due to cell membrane damage.<sup>135</sup> The assay thus evaluates cell membrane integrity and complements the results obtained by the MTT assay.

For both cell lines, the results obtained with the analysis of LDH release are concordant and complement the MTT results above described, reinforcing the observations regarding the cytotoxicity of RFB. Comparatively with the LDH released by untreated cells in both cell lines, INH does not increase significantly the value of LDH, while for RFB is verified an increase to 150 - 170%, which is particularly noticeable at the concentration of 0.1 mg/mL. Contrary to the observation from the MTT assay, in the present assay A549 cells (Figure 4.19 A) appeared to be more sensitive to the effect of the drug than macrophage-differentiated THP-1 cells (Figure 4.19 B), which present only a significant change at the higher concentration.

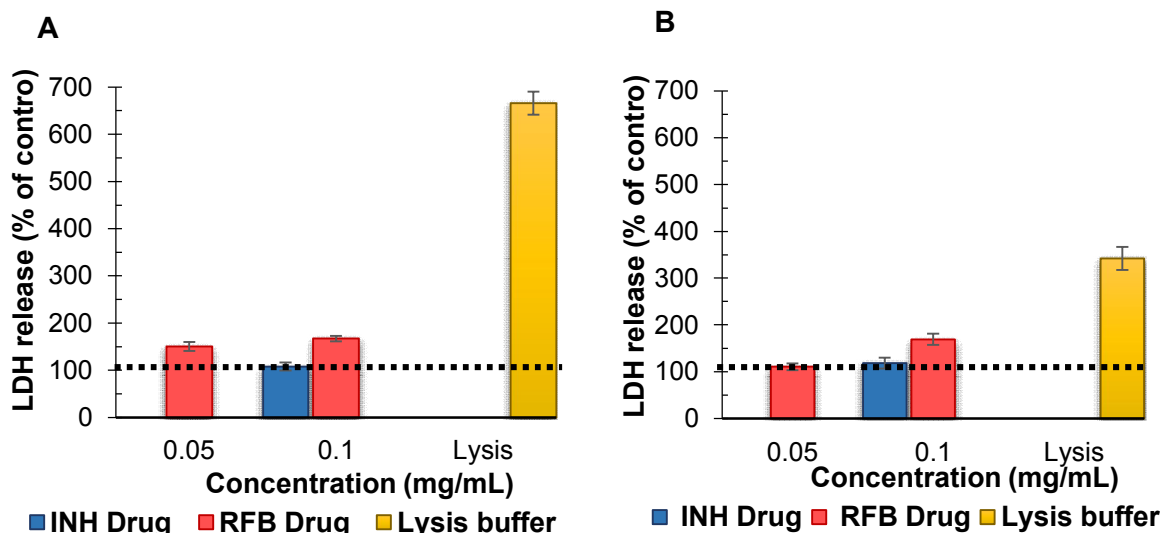


**Figure 4.19: LDH released from A549 cells (A) and macrophage-like THP-1 cells (B) after 24 hours exposure to the drugs.** Amount of LDH released from cells incubated with cell culture medium is assumed as 100% (dotted line). INH: Isoniazid; LBG: Locust bean gum. RFB: Rifabutin; Results expressed as mean  $\pm$  SEM.

LDH release after exposure of A549 (Figure 4.20) and macrophage-like THP-1 cells (Figure 4.21) to raw material (LBG) and several formulations is depicted below.

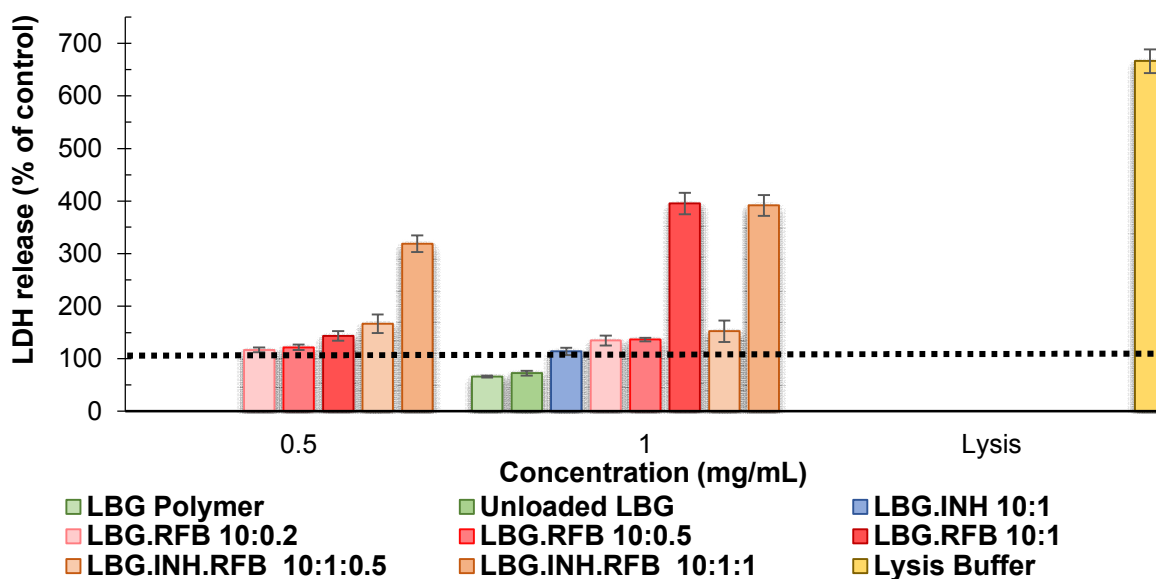


**Figure 4.20: LDH released from A549 cells after 24 hours exposure to LBG polymer, microparticles and lysis buffer.** Amount of LDH released from cells incubated with cell culture medium is assumed as 100% (dotted line). INH: Isoniazid; LBG: Locust bean gum. RFB: Rifabutin; Results expressed as mean  $\pm$  SEM.

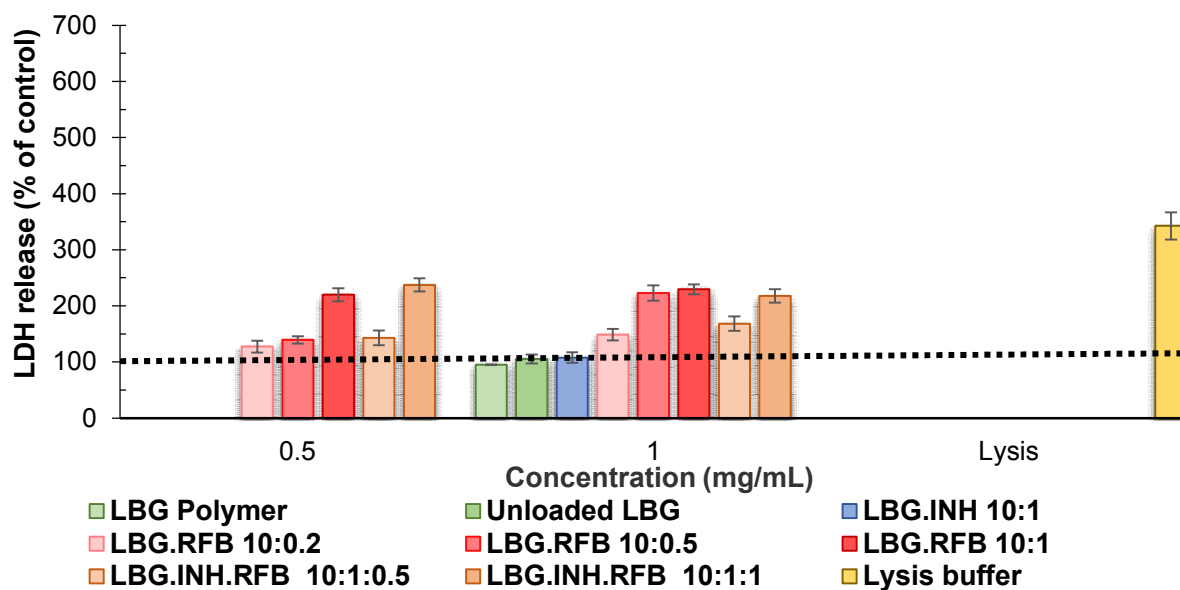


**Figure 4.21: LDH released from macrophage-like THP-1 cells after 24 hours exposure to LBG polymer, microparticles and lysis buffer.** Amount of LDH released from cells incubated with cell culture medium is assumed as 100% (dotted line). INH: Isoniazid; LBG: Locust bean gum. RFB: Rifabutin; Results expressed as mean  $\pm$  SEM.

As observed in the figures above, the exposure of both cell lines to the original LBG polymer, unloaded LBG microparticles and INH-loaded microparticles did not induce any physiologically relevant alteration in the amount of released LDH. However, RFB-loaded microparticles, either when drug was associated alone or in combination with INH, elicited a significant increase in LDH release, indicating cytotoxicity. For A549 cells, the formulations LBG.RFB 10:0.5 and 10:0.2 induced a very slight increase in LDH release at both concentrations (around 110-120%). However, the formulation LBG.RFB 10:1 elicited a stronger increase in LDH release ( $p < 0.05$ ) which reached almost 400% at the concentration of 1 mg/mL, indicating a clear concentration-dependent effect. A similar effect was observed for the microparticles associating both drugs and containing the same amount of RFB (LBG.INH.RFB = 10:1:1), while that of LBG.INH.RFB = 10:1:0.5 exhibited a much milder effect (LDH release around 150% at 1 mg/mL,  $p < 0.05$ ).

THP-1 cells were not as sensitive to the contact with the microparticles, but cytotoxic effects were also observed. As seen in Figure 4.21, the formulations LBG.RFB 10:0.5 (at concentration 0.5) and 10:0.2 (at concentration 0.05 and 1.0) make a very slight increase in LDH release (around 125 – 150%), while the higher concentrations of LBG.RFB 10:0.5 induce a strong release of LDH (around 225%). This result is similar to that caused by the exposition to LBG.RFB 10:1 in the two tested concentrations (around 220 – 230%). In formulations associating both drugs, the results of LDH release are similar to those obtained for formulations containing only RFB when the same RFB amount is associated.

Although in both cell lines the values reached by RFB-loaded microparticles were much lower than those of the lysis buffer, it is clear that RFB has a cytotoxic effect that is dependent on its concentration. This is visible when evaluating the same concentration of microparticles having different amounts of RFB and when evaluating the same formulation at different concentrations. None of the works reporting the application of LBG microparticles provides data on LDH release from cells upon exposure to the carriers. The same occurs for drugs, which have no available reports on these cell lines, thus impairing more comprehensive comparisons.

#### **4.8. Evaluation of macrophage ability to uptake LBG microparticles**

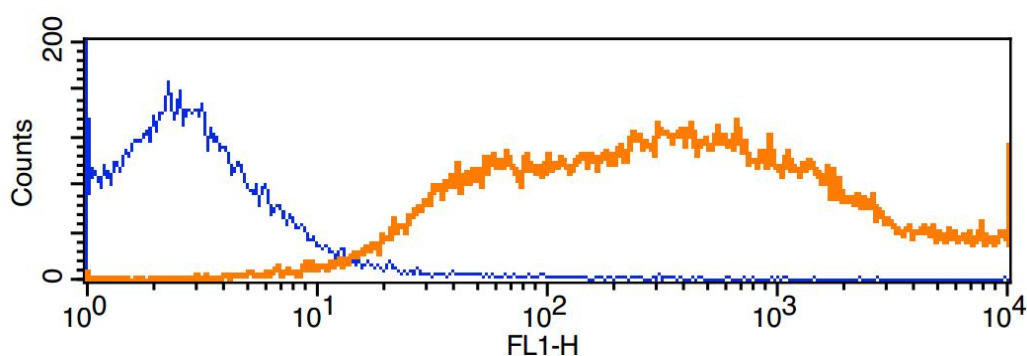
The pulmonary delivery of antitubercular drugs, upon loading in a carrier system capable of undergoing recognition by alveolar macrophages with consequent phagocytosis,<sup>63</sup> is proposed in this thesis as an improvement to the current oral therapy. The affinity and selectivity of alveolar macrophage surface receptors offers a unique opportunity for selective targeting of antitubercular drugs.<sup>67</sup> In this perspective, the ability of macrophages to uptake LBG microparticles was evaluated in two cell lines representing macrophages (macrophage-differentiated THP-1 cells and NR8383 cells).

To perform this assay, fluorescently labelled LBG and PVA microparticles were produced, to permit the analysis by flow cytometry. The Feret's diameters of these microparticles were similar to that of unloaded LBG MPs.

An amount of microparticles corresponding to either 250 or 50  $\mu\text{g}/\text{cm}^2$  was tested, in line with the amounts tested in cytotoxicity assays when samples were presented as an aerosol. The microparticles were exposed to the cells in the form of aerosol and the contact was allowed for 2 hours. Phagocytosis is a fast process, usually 50–75% of the particles are phagocytosed in 2–3 hours, 90% or more by 10 hours, and nearly 100% by 24 hours after particle deposition.<sup>136</sup> The time for occurrence of phagocytosis for allowing a differential uptake is 2-3 hours. The selected time of 2 hours, which is deemed adequate for the occurrence of phagocytosis, was also used by other authors.<sup>137</sup> In order to simulate the alveolar environment, the assay was performed in the absence of CCM, only a very thin layer of liquid remained to maintain the hydration of cells.

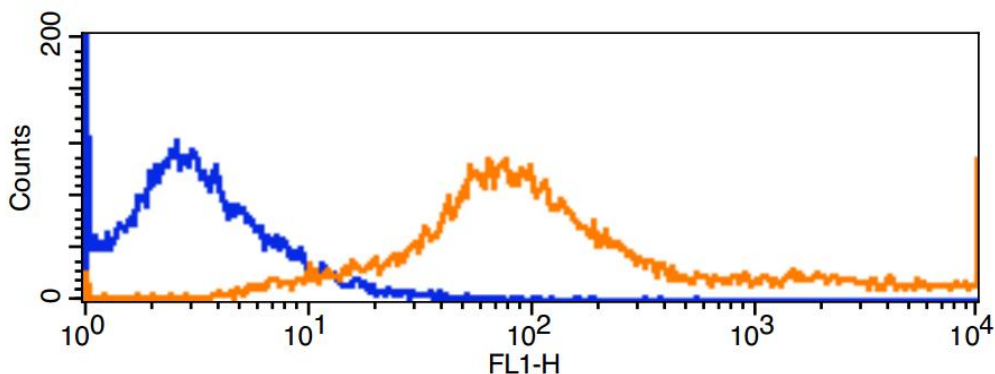
At the higher dose, the percentage of macrophage-differentiated THP-1 cells that phagocytosed fluorescently-labelled LBG microparticles was  $99.63 \pm 0.18\%$ . A very similar value ( $99.50 \pm 0.43\%$ ) was determined upon reduction of the dose to 50  $\mu\text{g}/\text{cm}^2$ . This evidences an absence of effect of the concentration and suggests a high affinity of

macrophages for LBG microparticles. Other microparticles also developed by the research team, for instance composed of fucoidan or carrageenan, evidenced a lower ability for macrophage targeting (data not shown). Also relevant is the fact that the dose of  $50 \mu\text{g}/\text{cm}^2$  indicated for other polymers a dose-dependent process,<sup>63</sup> which did not occur for LBG. Figure 4.22 depicts the histogram obtained from the cytometry analysis of two populations of macrophage-like THP-1 cells, the blue line evidencing the results for cells not exposed to fluorescently-labelled LBG MPs, while the orange line corresponds to the results elicited by fluorescent microparticles. In the latter, an intense fluorescent signal is observed indicating the uptake of microparticles by macrophages.



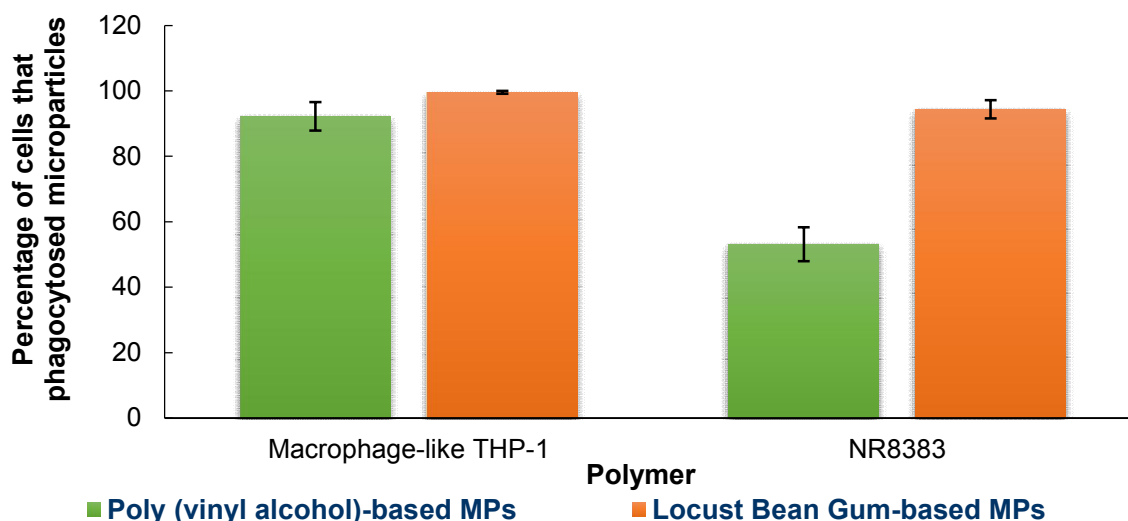
**Figure 4.22:** Fluorescent signal of macrophage-differentiated THP-1 cells upon 2 hours exposure to  $50 \mu\text{g}/\text{cm}^2$  of unlabelled LBG microparticles (blue line) and fluorescently-labelled LBG microparticles (orange line). Cells not exposed show auto-fluorescence, while cells exposed to fluorescent MPs increase the fluorescence signal, and the population moves to the right, in the axis of FL1-H, which reflects the intensity of fluorescence.

Figure 4.23 represents the histogram also obtained by flow cytometry analysis of two populations of NR8383 cells. The construction is identical to the one mentioned above and the obtained results are also similar to those elicited by differentiated THP-1 cells. Although phagocytosis is occurring, a strong increase of intensity as that observed in human macrophages was not registered.



**Figure 4.23:** Fluorescent signal of NR8383 cells upon 2 hours exposure to 50  $\mu\text{g}/\text{cm}^2$  of unlabelled LBG microparticles (blue line) and fluorescently-labelled LBG microparticles (orange line). Cells not exposed show auto-fluorescence, while cells exposed to fluorescent MPs increase the fluorescence signal, and the population moves to the right, in the axis of FL1-H, which reflects the intensity of fluorescence.

Alveolar macrophages are predominant cells in the uptake of inhaled particulates from the alveolar region.<sup>63</sup> In the two lines representative of macrophages, human and rat derived, it was compared the uptake of fluorescently-labelled PVA and LBG microparticles at the dose of 50  $\mu\text{g}/\text{cm}^2$  (figure 4.24).



**Figure 4.24:** Uptake of fluorescently-labelled PVA and LBG MPs by macrophage-differentiated THP-1 cells and NR8383 cells upon exposure to 50  $\mu\text{g}/\text{cm}^2$  for a period of two hours. Results expressed as mean  $\pm$  SEM.

It is observed that both cell lines showed high percentage of phagocytosis of LBG microparticles. PVA microparticles were also strongly phagocytosed by THP-1 cells, no significant statistical difference being observed when comparing with LBG microparticles. In turn, a statistical significant difference was obtained for NR8383 cells, almost 94% macrophages phagocytosing LBG microparticles while only 53% phagocytosed PVA

microparticles ( $p < 0.05$ ). This observation is indicative of non-preference of NR8383 by this polymer.

LBG has in its chemical structure mannose and galactose, these units being reported to be recognised by macrophage receptors, promoting phagocytosis.<sup>17</sup> Mannose receptor CD 206, can be involved in this specific recognition.<sup>66</sup> PVA is an alcohol, composed of repeating units of  $(-[\text{CH}_2-\text{CH}(\text{OH})]-)$ .<sup>72</sup> As it does not present specific groups recognized by macrophage receptors, it was selected as control in this assay.

The detection and phagocytosis of inhaled microparticles by alveolar macrophages mainly occurs through a series of recognition receptors, called scavenger receptors. This family of receptors includes the mannose receptor (CD 206),<sup>17</sup> and is responsible for the process of recognition of foreign particles and subsequent propagation of phagocytosis.<sup>63</sup> The mannose receptor, specifically, is reported as capable of recognising mannose, *N*-acetylglucosamine units and sulphated sugars.<sup>17</sup> When THP-1 cells were exposed to 50 nM of PMA, a differentiation occurred from which resulted macrophages in the state of activation M0.<sup>61,138</sup> In this state of activation, it has been reported that macrophages do not express receptors of this family,<sup>17,139</sup> but only express receptors of the family of Toll-like receptors (TLRs) and immunoglobulin superfamily (Fc receptors).<sup>129</sup> TLRs present a central role in the innate immune response; although not mediating the phagocytosis, these receptors are responsible for recognizing foreign particles and intracellular pathogens, leading to the engulfment of these by macrophages.<sup>140,141</sup> Considering these assumptions, it is possible that when microparticles based on PVA or LBG were presented to macrophages, no specific recognition mediated by the receptor CD206 occurs, which a possible explanation for the similar results is obtained in THP-1 cells. In turn, NR8383 cell line is a mannose receptor positive, which means that the cells naturally express a functional mannose receptor in cell culture.<sup>142</sup> Therefore, when LBG- and PVA-based microparticles were exposed to alveolar rat macrophages, a preferential affinity for LBG was verified, thus resulting in higher uptake of these microparticles.

Nevertheless, in both cases it is likely that TLR receptors just recognised the microparticles as foreign particulates, promoting the uptake.<sup>129</sup> It is important to highlight that macrophages are endowed with a natural ability to uptake particulates<sup>63</sup> and, therefore, a certain degree of phagocytosis was expected in any case. In this regard, LBG and PVA microparticles have similar particle size (about 1.5  $\mu\text{m}$ ) and density (ca. 1.40  $\text{g}/\text{cm}^3$ ) and present a spherical shape, characteristics that are referred to enhance macrophage uptake in the context of passive targeting.<sup>63</sup> Additionally, the time that microparticles remained in contact with macrophages was perhaps too long to permit a differentiation of affinities and this is possibly a variable to address in future studies.

TLRs recognise a variety of microbial components, including lipoproteins, peptidoglycan and lipoarabinomannan. Given that the LBG structure presents mannose units and is similar in a certain way to microbial products, TLR can initiate a signal transduction pathway for phagocytosis and activation upon contacting with LBG.<sup>140</sup> This similarity can explain the high percentage of uptake of this polymer, comparatively with PVA.

Comparatively with other galactomannans also tested in our laboratory, which is the case of partially hydrolysed guar gum (composed by M/G ratio of 2:1), LBG was still showing higher uptake ability in the two cell lines (data not shown). This observation indicated the expected preference of macrophages by mannose units in detriment of galactose. As a future study, it would be very interesting to activate the macrophages to an M2 state (by incubation with interleukin-4, for instance) and provide the exposure of macrophages to LBG microparticles and controls under that state. Upon infection by *M. tuberculosis* macrophages assume that activation state and express CD206,<sup>67</sup> thus being the ideal situation to demonstrate the affinity of LBG microparticles.<sup>138,139</sup>

#### 4.9. Macrophage activation evaluation

As already stated, this thesis intends to use LBG-based microparticles for production of drug delivery system capable of delivering antibiotics to the macrophages in a targeted strategy, by inducing macrophage binding and internalisation. In the last section, the high affinity of macrophages for these microparticles was described. When macrophages phagocytose *M. tuberculosis*, a state of activation is induced, which results in the release of several activation markers that lead to a final increase of the bactericidal ability of macrophages.<sup>17,100</sup> It has been reported that the phagocytosis of particulates might induce the same activation state, which would be a great achievement for the strategy being proposed in this thesis. If an activation occurs, the increased release of activation markers (cytokines), such as tumour necrosis factor alpha (TNF- $\alpha$ ), interleukin-1 and interleukin-8 (IL-8), which are characteristic of the M1 state, are expected.<sup>17,19</sup>

In order to evaluate this activation a polysaccharide solution and a suspension of microparticles of the formulation LBG.INH.RFB 10:1:0.5 (dose of 303  $\mu\text{g}/\text{cm}^2$ ) were incubated with the macrophages for 24 hours. Released TNF- $\alpha$  and IL-8 after exposure were determined.

The amount of basal release of cytokines was determined, corresponding to cells exposed only to CCM, which was used as control. The cells were further exposed to mannitol, a solution of LBG, dispersion of the microparticles and LPS. Mannitol does not have in its structure residues of mannose or galactose, thus serving as another control. LPS is a bacterial

constituent with high capacity to activate macrophages into M1 state,<sup>138</sup> and a consistent up-regulation of the production of TNF- $\alpha$  and IL-8 has been described.<sup>143</sup>

After 24 hours of exposition to the matrix polysaccharide solution and microparticles, the cytokines figure 4.25) and figure 4.26 (IL-8). Matrix LBG solution and LBG-based microparticles demonstrated capacity to stimulate the release of both cytokines, to a level that was similar or superior to that elicited by LPS. As expected, mannitol solution did not present capacity to activate macrophages and in fact there is a reduction of the amount released in comparison with the basal release.

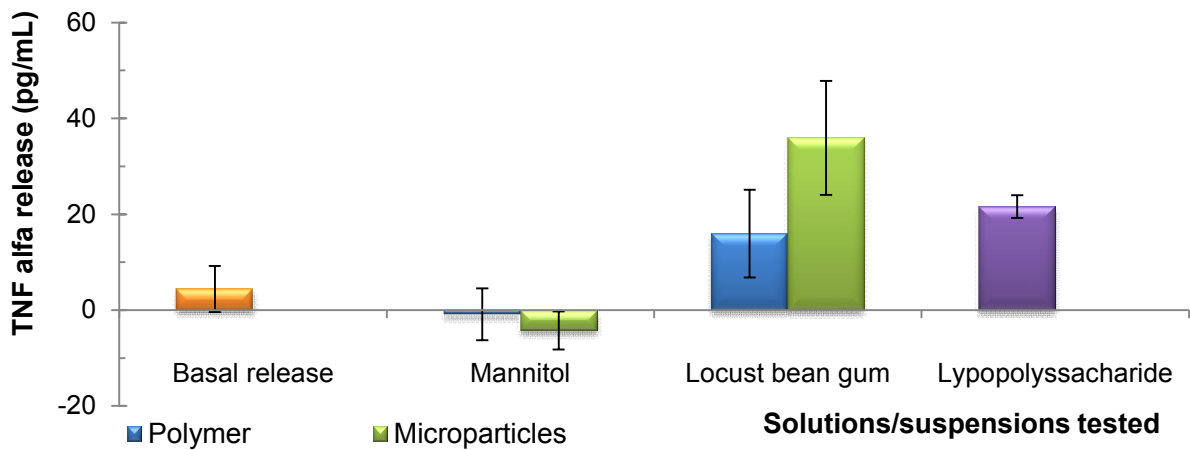


**Figure 4.25: TNF- $\alpha$  released from macrophage-like THP-1 cells after exposure to LBG the form of solution or dispersion of microparticles.** Exposure lasted 24 hours. Results are expressed as mean  $\pm$  SEM.

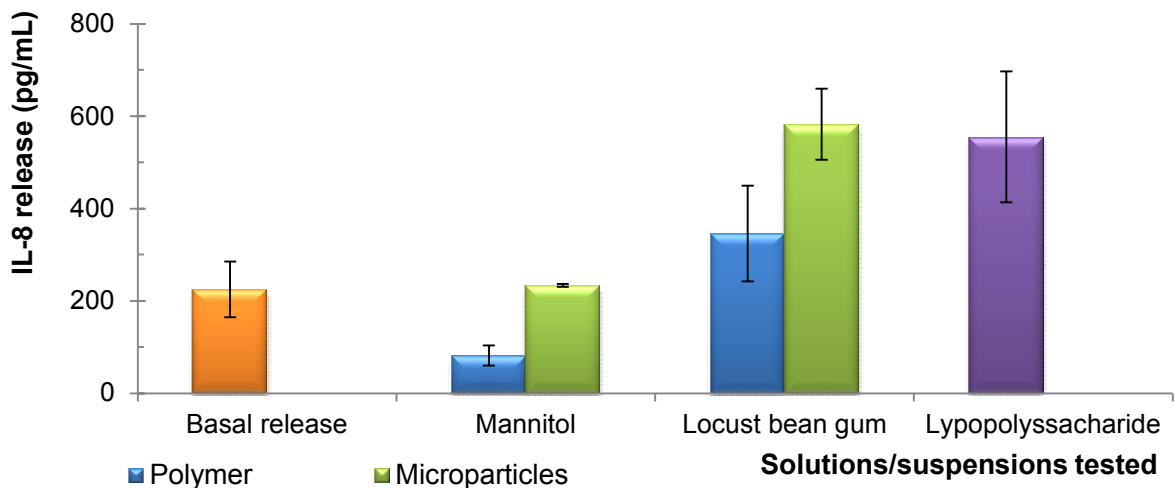


**Figure 4.26: IL-8 released from macrophage-like THP-1 after exposure to LBG the form of solution or dispersion of microparticles.** Exposure lasted 24 hours. Results are expressed as mean  $\pm$  SEM.

In both figures is observed that macrophage-differentiated THP-1 cells expressed a basal level of secretion of both cytokines. Differentiated THP-1 with PMA (5 ng/mL for 48 hours) expressed at basal level IL-8 ( $393 \pm 25$  pg/mL) and TNF- $\alpha$  (1952 pg/mL).<sup>144</sup> When exposed to LPS the secretion increases as expected ( $p < 0.05$ ), as LPS in a known activator. Other studies demonstrated that this molecule induces an increase of expression of TNF- $\alpha$ ,<sup>145</sup> thus justifying its use as positive control. When the cells were exposed to the LBG MPs, a significant increase of the expression of both cytokines ( $p < 0.05$ ) was observed, which did not occur for mannitol-based MPs. LBG solution significantly stimulates the production of IL-8 ( $p < 0.05$ ), but not TNF- $\alpha$  ( $p=0.065$ ). The obtained results indicate that LBG MPs present a similar capacity to induce expression of both cytokines, being able to activate macrophages.

The literature makes available only few studies about saccharide-induced activation of macrophage-derived THP-1 cells. Mannose coating of drug delivery systems has been proved to activate macrophages (bone marrow-derived macrophages), with significant increase of TNF- $\alpha$  and another pro-inflammatory cytokines.<sup>146</sup> Other works have been using mannose functionalisation for macrophage targeted drug delivery strategies.<sup>17</sup> Galactose and di-mannose were reported to functionalise the surface of polyanhydride nanoparticles and target alveolar macrophages (murine alveolar macrophages wild type and knock-down for mannose receptor), which showed an increase of production of pro-inflammatory cytokines, such as TNF- $\alpha$  and IL-1 $\beta$ .

Results obtained in the two last sections indicated that LBG-based microparticles present a high percentage of uptake by macrophages and demonstrate capacity to activate macrophages, mediated by the production of TNF- $\alpha$  and IL-8, indicating the potential of these microparticles for macrophage targeting and activation strategies.

## 5. Conclusion

Microparticle-based carriers hold a considerable potential for the delivery of antibiotic drugs in infectious respiratory diseases. The administration of drug carriers directly to the lung, by means of inhalation, might be an effective therapeutic approach. In this context, this thesis proposed the development of a dry powder formulation composed of locust bean gum (LBG) and produced by spray-drying. Considering the structural composition of LBG, the polymer was deemed adequate to design a delivery strategy targeted to the alveolar macrophages, as a strategy in tuberculosis therapy.

Locust bean gum microparticles were successfully produced by spray-drying although a content of HCl is needed to reduce the viscosity of the spraying dispersion. Despite the differences of solubility of Isoniazid and Rifabutin, the two model antibiotics selected, both were successfully incorporated in LBG microparticles, with association efficiencies above 82%. The aerodynamic properties of microparticles suggest their suitability for the objective of deep lung delivery in the ambit of tuberculosis therapy. These presented an aerodynamic diameter between 1.27 to 1.90  $\mu\text{m}$ , Feret's diameter of 1.26 - 1.50  $\mu\text{m}$  and a pollen-shaped shape. These characteristics were considered at least theoretically to render the ability to reach the alveolar zone where macrophages hosting mycobacteria are located.

The analysis by XRD showed an absence of crystalline profile of the microparticles as is characteristic of formulations obtained by spray-drying.

The release assays determined a rapid release of INH from microparticles LBG.INH, which was a little slower when both drugs were associated in the same formulation. In that case, RFB release was also more prolonged and similar to INH release, with 70-80% of drugs being released in 60 minutes. The cytotoxic behaviour of microparticles was characterized in two cell lines representative of the alveolar zone (A549 cells for alveolar epithelium and THP1 cells for macrophages). The general conclusion was that RFB imposes a certain degree of toxicity in both cell lines, especially for prolonged exposition (24 hours). INH in turn, does not exhibit any cytotoxic effect. It was also indicated that RFB toxicity is potentiated by the association of RFB to HCl. In this perspective, a lower amount of RFB is suggested to be encapsulated and possibly another excipient to reduce LBG viscosity. Another alternative could be the substitution of RFB by another drug such as pyrazinamide or a new-drug (for example, PA-824). Formulations presented as aerosol elicited higher level of toxicity but it is suggested that tested doses are still very high comparing with the *in vivo* conditions. A clear dose-dependent effect was anyway demonstrated.

It was demonstrated that macrophages have high affinity for LBG microparticles in two cell lines, human macrophage-like THP-1 cells and rat alveolar macrophages (NR8383). The

exposure to LBG microparticles was also shown to activate macrophages. These results as a whole demonstrate the potential of LBG to be used as matrix material in microparticles aimed at an application as inhalable antibiotic carriers in the ambit of lung tuberculosis therapy. These formulations presented the advantage of producing microparticles with mannose, without an extra-step, to attach ligands. The composition of these carrier can be properly designed to have a composition that favours both the interaction with these cells, mediated a specific recognition, and the consequent internalisation, which will ensure the localisation of drugs inside the infected niche. And a capacity of activation macrophage, benefits an improve in inflammatory response

This strategy would accumulate the drugs in the primary site of infection, possibly increasing the drug therapeutic effect and decreasing the side effects. As a whole, this would definitely lead to increased patient compliance and to the successful treatment of some concerning diseases associated with macrophage parasites.

## 6. References

1. Andrade, F. *et al.* Nanotechnology and pulmonary delivery to overcome resistance in infectious diseases. *Adv. Drug Deliv. Rev.* **65**, 1816–1827 (2013).
2. Hittinger, M. *et al.* Preclinical safety and efficacy models for pulmonary drug delivery of antimicrobials with focus on in vitro models. *Adv. Drug Deliv. Rev.* **xxx**, 1–13 (2014).
3. Flume, P. a. & VanDevanter, D. R. Clinical applications of pulmonary delivery of antibiotics. *Adv. Drug Deliv. Rev.* **85**, 1–6 (2014).
4. Van der Poll, T. & Opal, S. M. Pathogenesis, treatment, and prevention of pneumococcal pneumonia. *Lancet* **374**, 1543–1556 (2009).
5. Muttill, P., Wang, C. & Hickey, A. J. Inhaled drug delivery for tuberculosis therapy. *Pharm. Res.* **26**, 2401–2416 (2009).
6. Alexandru-flaviu, T. & Cornel, C. Macrophages Targeted Drug Delivery as a Key Therapy in Infectious Disease. *Biotechnol. Mol. Biol. NANOMEDICINE* **2**, 19–21 (2014).
7. Dube, D., Agrawal, G. P. & Vyas, S. P. Tuberculosis: From molecular pathogenesis to effective drug carrier design. *Drug Discov. Today* **17**, 760–773 (2012).
8. Traini, D. & Young, P. M. Delivery of antibiotics to the respiratory tract: an update. *Expert Opin. Drug Deliv.* **6**, 897–905 (2009).
9. Tiddens, H. A. W. M., Bos, A. C., Mouton, J. W., Devadason, S. & Janssens, H. M. Inhaled antibiotics: dry or wet? *Eur. Respir. J.* **44**, 1308–1318 (2014).
10. Pham, D. D., Fatal, E. & Tsapis, N. Pulmonary drug delivery systems for the treatment of tuberculosis. *Drug Deliv. Syst.* **23**, 474–480 (2015).
11. Costa, H. & Grenha, A. Natural carriers for application in tuberculosis treatment. *J. Microencapsul.* **30**, 1–12 (2012).
12. Hoppentocht, M., Hagedoorn, P., Frijlink, H. W. & De Boer, a. H. Developments and strategies for inhaled antibiotic drugs in tuberculosis therapy: A critical evaluation. *Eur. J. Pharm. Biopharm.* **86**, 23–30 (2014).
13. World Health Organization. Global tuberculosis report 2014 (WHO/HTM/TB/2014.08). *World Health Organization* 1 – 171 (2014). doi:WHO/HTM/TB/2014.08
14. Nunes-Alves, C. *et al.* In search of a new paradigm for protective immunity to TB. *Nat. Rev. Microbiol.* **12**, 289–299 (2014).
15. Ramakrishnan, L. Revisiting the role of the granuloma in tuberculosis. *Nat. Rev. Immunol.* **12**, 352–366 (2012).
16. Ehlers, S. & Schaible, U. E. The granuloma in tuberculosis: Dynamics of a host-pathogen collusion. *Front. Immunol.* **3**, 1–9 (2012).
17. Rodrigues, S. & Grenha, A. Activation of macrophages: Establishing a role for polysaccharides in drug delivery strategies envisaging antibacterial therapy. *Curr. Pharm. Des.* **21**, (2015).
18. Van der Meer-Janssen, Y. P. M., van Galen, J., Batenburg, J. J. & Helms, J. B. Lipids in host-pathogen interactions: Pathogens exploit the complexity of the host cell lipidome. *Prog. Lipid Res.* **49**, 1–26 (2010).
19. Liu, Y.-C., Zou, X.-B., Chai, Y.-F. & Yao, Y.-M. Macrophage polarization in inflammatory diseases. *Int. J. Biol. Sci.* **10**, 520–9 (2014).
20. Young, D., Hussell, T. & Dougan, G. Chronic bacterial infections: living with unwanted guests. *Nat Immunol* **3**, 1026–1032 (2002).
21. Lamichhane, G. Novel targets in M. tuberculosis: Search for new drugs. *Trends Mol. Med.* **17**, 25–33 (2011).
22. Timmins, G. S. & Deretic, V. Mechanisms of action of isoniazid. *Mol. Microbiol.* **62**, 1220–1227 (2006).

23. Chem, P. Isoniazid. *National Center for Biotechnology Information. PubChem Compound Database*; 1–61 (2015). at <<https://pubchem.ncbi.nlm.nih.gov/compound/3767>>
24. Compounds, S. RIFABUTIN | C46H62N4O11 - *PubChem Página 1 de 39 NIH*. (2015).
25. Gaspar, M. M. *et al.* Developments on drug delivery systems for the treatment of mycobacterial infections. *Curr. Top. Med. Chem.* **8**, 579–591 (2008).
26. Nuernberger, E. L., Spigelman, M. K. & Yew, W. W. Current development and future prospects in chemotherapy of tuberculosis. *Respirology* **15**, 764–778 (2010).
27. Loira-Pastoriza, C., Todoroff, J. & Vanbever, R. Delivery strategies for sustained drug release in the lungs. *Adv. Drug Deliv. Rev.* **75**, 81–91 (2014).
28. Daniher, D. I. & Zhu, J. Dry powder platform for pulmonary drug delivery. *Particuology* **6**, 225–238 (2008).
29. Kelly, C. & Cryan, D. S.-A. Development of Nano- and Microparticle Technologies for Targeted Gene Silencing through RNA Interference: Manipulation of the Immune Response in Inflammatory Lung Disease. *School of Pharmacy Doctor of*, (Dublin: Roya College of Surgeons in Irland, 2011).
30. Hassan, M. S. & Lau, R. W. M. Effect of particle shape on dry particle inhalation: study of flowability, aerosolization, and deposition properties. *AAPS PharmSciTech* **10**, 1252–1262 (2009).
31. Ribeiro, R. Development and Characterization of Nanocarrier Systems for the Delivery of Antitubercular Drugs. (Universidade do Porto, 2013).
32. Scherbart, A. M. Mechanisms and Consequences of Particle Uptake in Alveolar Macrophages. (Heinrich-Heine-Universität Dusseldorf, 2010).
33. Nahar, K. *et al.* In vitro, in vivo and ex vivo models for studying particle deposition and drug absorption of inhaled pharmaceuticals. *Eur. J. Pharm. Sci.* **49**, 805–818 (2013).
34. Pilcer, G. & Amighi, K. Formulation strategy and use of excipients in pulmonary drug delivery. *Int. J. Pharm.* **392**, 1–19 (2010).
35. Grabowski, N. Toxicologie pulmonaire de nanoparticules biodégradables: effets cytotoxiques et inflammatoires sur cellules épithéliales et macrophages. (UNIVERSITÉ PARIS-SUD 11, 2014).
36. Zhou, Q. T. *et al.* Inhaled formulations and pulmonary drug delivery systems for respiratory infections ☆. *Adv. Drug Deliv. Rev.* **xxx**, xxx (2014).
37. Quon, B. S., Goss, C. H. & Ramsey, B. W. Inhaled antibiotics for lower airway infections. *Ann. Am. Thorac. Soc.* **11**, 425–434 (2014).
38. Misra, A. *et al.* Inhaled drug therapy for treatment of tuberculosis. *Tuberculosis* **91**, 71–81 (2011).
39. Zumla, A., Nahid, P. & Cole, S. T. Advances in the development of new tuberculosis drugs and treatment regimens. *Nat. Rev. Drug Discov.* **12**, 388–404 (2013).
40. Zahoor, A., Sharma, S. & Khuller, G. K. Inhalable alginate nanoparticles as antitubercular drug carriers against experimental tuberculosis. *Int. J. Antimicrob. Agents* **26**, 298–303 (2005).
41. Chimote, G. & Banerjee, R. In vitro evaluation of inhalable isoniazid-loaded surfactant liposomes as an adjunct therapy in pulmonary tuberculosis. *J. Biomed. Mater. Res. Part B Appl. Biomater.* **94B**, 1–10 (2010).
42. Hoppentocht, M., Hagedoorn, P., Frijlink, H. W. & de Boer, a H. Technological and practical challenges of dry powder inhalers and formulations. *Adv. Drug Deliv. Rev.* **75**, 18–31 (2014).
43. Onoshita, T. *et al.* The behavior of PLGA microspheres containing rifampicin in alveolar macrophages. *Colloids Surfaces B Biointerfaces* **76**, 151–157 (2010).

44. Manca, M. L. *et al.* Isoniazid-gelatin conjugate microparticles containing rifampicin for the treatment of tuberculosis. *J. Pharm. Pharmacol.* **65**, 1302–11 (2013).
45. Chow, a. H. L., Tong, H. H. Y., Chattopadhyay, P. & Shekunov, B. Y. Particle engineering for pulmonary drug delivery. *Pharm. Res.* **24**, 411–437 (2007).
46. Safety, C. C. for C. P. *Guidelines for Safe Handling of Powders and Bulk Solids.* (John Wiley & Sons, 2010). at <<https://books.google.com/books?id=cp3zopuBur4C&pgis=1>>
47. Yang, M. Y., Chan, J. G. Y. & Chan, H. K. Pulmonary drug delivery by powder aerosols. *J. Control. Release* **193**, 228–240 (2014).
48. Buchi. *Laboratory Scale Spray Drying of Inhalable Drugs: A Review.* *Nano* (2010). at <[www.buchi.com](http://www.buchi.com)>
49. Krzysztof, S. & Krzysztof, C. Spray Drying Technique: II. Current Applications in Pharmaceutical Technology. *J. Pharm. Sci.* **99**, 587–597 (2010).
50. Grenha, A. & Dionísio, M. Locust bean gum: Exploring its potential for biopharmaceutical applications. *Journal of Pharmacy and Bioallied Sciences* **4**, 175 (2012).
51. Prajapati, V. D., Jani, G. K., Moradiya, N. G., Randeria, N. P. & Nagar, B. J. Locust bean gum: A versatile biopolymer. *Carbohydr. Polym.* **94**, 814–821 (2013).
52. Park, J. H., Ye, M. & Park, K. Biodegradable polymers for microencapsulation of drugs. *Molecules* **10**, 146–161 (2005).
53. Liu, J., Willför, S. & Xu, C. A review of bioactive plant polysaccharides: Biological activities, functionalization, and biomedical applications. *Bioact. Carbohydrates Diet. Fibre* **5**, 31–61 (2015).
54. Beneke, C. E., Viljoen, A. M. & Hamman, J. H. Polymeric plant-derived excipients in drug delivery. *Molecules* **14**, 2602–2620 (2009).
55. Devi, N. & Maji, T. K. Preparation and evaluation of gelatin/sodium carboxymethyl cellulose polyelectrolyte complex microparticles for controlled delivery of isoniazid. *AAPS PharmSciTech* **10**, 1412–1419 (2009).
56. Park, J. H. *et al.* Chitosan microspheres as an alveolar macrophage delivery system of ofloxacin via pulmonary inhalation. *Int. J. Pharm.* **441**, 562–569 (2013).
57. Lacerda, L., Parize, A. L., Fávère, V., Laranjeira, M. C. M. & Stulzer, H. K. Development and evaluation of pH-sensitive sodium alginate/chitosan microparticles containing the antituberculosis drug rifampicin. *Mater. Sci. Eng. C* **39**, 161–167 (2014).
58. Hwang, S. M., Kim, D. D., Chung, S. J. & Shim, C. K. Delivery of ofloxacin to the lung and alveolar macrophages via hyaluronan microspheres for the treatment of tuberculosis. *J. Control. Release* **129**, 100–106 (2008).
59. Kundawala, A. J. *et al.* Preparation of Biodegradable Microspheres By Spray Drying. *Int. J. Pharm.* **3**, 82–90 (2013).
60. Smith, B. M. *et al.* Composition and molecular weight distribution of carob germ protein fractions. *J. Agric. Food Chem.* **58**, 7794–7800 (2010).
61. Barak, S. & Mudgil, D. Locust bean gum: Processing, properties and food applications- A review. *Int. J. Biol. Macromol.* **66**, 74–80 (2014).
62. Dey, P., Sa, B. & Maiti, S. Carboxymethyl Ethers of Locust Bean Gum a Review. **3**, 2–5 (2011).
63. Patel, B., Gupta, N. & Ahsan, F. Particle engineering to enhance or lessen particle uptake by alveolar macrophages and to influence the therapeutic outcome. *Eur. J. Pharm. Biopharm.* **89**, 163–174 (2015).
64. Carrillo-Conde, B. *et al.* Mannose-functionalized ‘pathogen-like’ polyanhydride nanoparticles target C-type lectin receptors on dendritic cells. *Mol. Pharm.* **8**, 1877–1886 (2011).

65. Brandhonneur, N. *et al.* Specific and non-specific phagocytosis of ligand-grafted PLGA microspheres by macrophages. *Eur. J. Pharm. Sci.* **36**, 474–485 (2009).
66. Kang, P. B. *et al.* The human macrophage mannose receptor directs Mycobacterium tuberculosis lipoarabinomannan-mediated phagosome biogenesis. *J. Exp. Med.* **202**, 987–999 (2005).
67. Azad, A. K., Rajaram, M. V. S. & Schlesinge, L. S. Exploitation of the Macrophage Mannose Receptor (CD206) in Infectious Disease Diagnostics and Therapeutics. *J Cytol Mol Biol.* **1**, 1–10 (2014).
68. Ahsan, F., Rivas, I. P., Khan, M. a. & Torres Suárez, A. I. Targeting to macrophages: Role of physicochemical properties of particulate carriers - Liposomes and microspheres - On the phagocytosis by macrophages. *J. Control. Release* **79**, 29–40 (2002).
69. Sigma-Aldrich. Isoniazid. *Sigma-Aldrich* **54**, 50–52 (2015).
70. Chem, P. RIFABUTIN | C46H62N4O11 - PubChem. *National Center for Biotechnology Information. PubChem Compound Database*; (2015). at <<http://pubchem.ncbi.nlm.nih.gov/compound/rifabutin#section=2D-Structure>>
71. Sigma-Aldrich. Mannitol. *Sigma-Aldrich* **1** (2015). at <<http://www.sigmaaldrich.com/catalog/product/sial/m0200000?lang=pt&region=PT>>
72. Sigma-Aldrich. Polyvynilalcohol. *Sigma-Aldrich* **44**, 1 (2015).
73. Daman, Z., Gilani, K., Rouholamini Najafabadi, A., Eftekhari, H. & Barghi, M. Formulation of inhalable lipid-based salbutamol sulfate microparticles by spray drying technique. *DARU J. Pharm. Sci.* **22**, 50 (2014).
74. Palazzo, F. *et al.* Development of a spray-drying method for the formulation of respirable microparticles containing ofloxacin-palladium complex. *Int. J. Pharm.* **440**, 273–282 (2013).
75. Hamishehkar, H., Rahimpour, Y. & Javadzadeh, Y. in *Recent Advances in Novel Drug Carrier System, InTech Open Access Publisher* (ed. Javadzadeh) 39–66 (InTech, 2012). doi:10.5772/51209
76. Hardesty, J. & Attili, B. Spectrophotometry and the Beer-lambert Law: An Important Analytical technique in Chemistry. 1–6 (2010).
77. Lopes, C. M. Liberação modificada em sistemas matriciais sólidos contendo ibuprofeno. (Universidade do Porto, 2006).
78. Foster, K. a, Oster, C. G., Mayer, M. M., Avery, M. L. & Audus, K. L. Characterization of the A549 cell line as a type II pulmonary epithelial cell model for drug metabolism. *Exp. Cell Res.* **243**, 359–366 (1998).
79. Sigma-Aldrich. Phorbol 12-myristate 13-acetate. *Sigma-Aldrich* **1** (2015). at <<http://www.sigmaaldrich.com/catalog/product/sigma/p8139?lang=pt&region=PT>>
80. Chanput, W., Mes, J. J. & Wichers, H. J. THP-1 cell line: An in vitro cell model for immune modulation approach. *Int. Immunopharmacol.* **23**, 1–9 (2014).
81. ATCC. NR8383 [AgC11x3A, NR8383.1] (ATCC ® CRL-2192™). ATCC 8383 (2015). at <<http://www.lgcstandards-atcc.org/products/all/CRL>>
82. Penn-Century Inc. Dry Powder Insufflator™ – Model DP-4M. *Penn-Century, INC.* 3–4 (2015). at <<http://penncentury.com/products/dry-powder-devices/dry-powder-insufflator-dp-4m/model-dp-4m/>>
83. Sigma-Aldrich. Locust bean gum from Ceratonia siliqua seeds. *Sigma-Aldrich* **1** (2015). at <<http://www.sigmaaldrich.com/catalog>>
84. Haddarah, A. *et al.* The structural characteristics and rheological properties of Lebanese locust bean gum. *J. Food Eng.* **120**, 204–214 (2014).

85. Farahnaky, a, Darabzadeh, N., Majzoobi, M. & Mesbahi, G. Physicochemical Properties of Crude and Purified Locust Bean Gums Extracted from Iranian Carob Seeds. **16**, 125–136 (2014).
86. Al-Qadi, S., Grenha, A. & Remuñán-López, C. Microspheres loaded with polysaccharide nanoparticles for pulmonary delivery: Preparation, structure and surface analysis. *Carbohydr. Polym.* **86**, 25–34 (2011).
87. Osorio, D. T. Desarrollo de micro- y nanopartículas de polisacáridos para la administración pulmonar y nasal de macromoléculas terapéuticas. (Universidad de Santiago de Compostela, 2007).
88. Surendrakumar, K., Martyn, G. P., Hodggers, E. C. M., Jansen, M. & Blair, J. a. Sustained release of insulin from sodium hyaluronate based dry powder formulations after pulmonary delivery to beagle dogs. *J. Control. Release* **91**, 385–394 (2003).
89. Grenha, A., Seijo, B. & Remuñán-López, C. Microencapsulated chitosan nanoparticles for lung protein delivery. *Eur. J. Pharm. Sci.* **25**, 427–437 (2005).
90. Grenha, A. M. M. 'Microencapsulación de nanopartículas de quitosano para la administración pulmonar de macromoléculas terapéuticas'. (UNIVERSIDAD DE SANTIAGO DE COMPOSTELA, 2006).
91. Pereira, F., Martins, T. & Grenha, A. Guar Gum-based Microparticles as Carriers for Lung Delivery of Anti-tubercular Drugs. in *Respiratory Drug Delivery Europe 2015. Volume 2* (ed. Respiratory Drug Delivery Europe 2015) 5–8 (Davis Healthcare International, 2015).
92. Bosquillon, C., Lombry, C., Préat, V. & Vanbever, R. Influence of formulation excipients and physical characteristics of inhalation dry powders on their aerosolization performance. *J. Control. Release* **70**, 329–339 (2001).
93. Schoubben, A., Giovagnoli, S., Tiralti, M. C., Blasi, P. & Ricci, M. Capreomycin inhalable powders prepared with an innovative spray-drying technique. *Int. J. Pharm.* **469**, 132–139 (2014).
94. Pham, D. D., Fattal, E., Ghermani, N., Guiblin, N. & Tsapis, N. Formulation of pyrazinamide-loaded large porous particles for the pulmonary route: Avoiding crystal growth using excipients. *Int. J. Pharm.* **454**, 668–677 (2013).
95. Kundawala, A. J., Patel, V. a, Patel, H. V & Choudhary, D. Isoniazid loaded chitosan microspheres for pulmonary delivery: Preparation and characterization. *Der Pharm. Sin.* **2**, 88–97 (2011).
96. Yai, H. Preparation of isoniazid as dry powder formulations for inhalation by physical mixing and spray drying. *Malaysian Jpurnal Pharm. Sci.* **4**, 43–63 (2006).
97. Zhou, H. *et al.* Microparticle-based lung delivery of INH decreases INH metabolism and targets alveolar macrophages. *J. Control. Release* **107**, 288–299 (2005).
98. Muttill, P. *et al.* Inhalable microparticles containing large payload of anti-tuberculosis drugs. *Eur. J. Pharm. Sci.* **32**, 140–150 (2007).
99. Sharma, R. *et al.* Uptake of inhalable microparticles affects defence responses of macrophages infected with Mycobacterium tuberculosis H37Ra. *J. Antimicrob. Chemother.* **59**, 499–506 (2007).
100. Sharma, R., Yadav, A. B., Muttill, P., Kajal, H. & Misra, A. Inhalable microparticles modify cytokine secretion by lung macrophages of infected mice. *Tuberculosis* **91**, 107–110 (2011).
101. Almeida, A. & Grenha, A. in *Mucosal Delivery of Biopharmaceuticals* (eds. Neves, J. A. G. & Sarmiento, B.) 283–312 (Springer Science + Business Medi, 2014). doi:10.1007/978-1-4614-9524-6
102. Fronius, M., Clauss, W. G. & Althaus, M. Why do we have to move fluid to be able to breathe? *Front. Physiol.* **3**, 1–9 (2012).

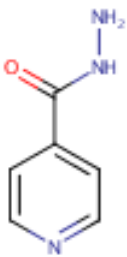
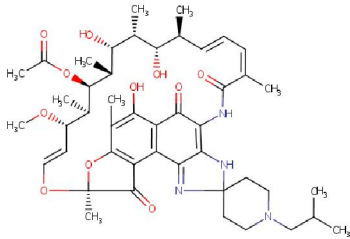
103. Haghi, M., Ong, H. X., Traini, D. & Young, P. Across the pulmonary epithelial barrier: Integration of physicochemical properties and human cell models to study pulmonary drug formulations. *Pharmacol. Ther.* **144**, 235–252 (2014).
104. Copley, M. & Son, Y. *Dissolution testing for inhaled drugs. Pharmaceutical technology Europe* (2010).
105. Kreyling, W. G. Intracellular particle dissolution in alveolar macrophages. *Environ. Health Perspect.* **97**, 121–126 (1992).
106. Chauhan, Dharmarajsinh, Patel, Axay, Shah, S. Influence of Selected Natural Polymers on In-vitro Release of Colon Targeted Mebeverine HCl Matrix Tablet. *Int. J. Drug Dev. Res.* **4**, 315–321 (2012).
107. Nishino, S., Kishida, A. & Yoshizawa, H. Morphology control of polylactide microspheres enclosing irinotecan hydrochloride with polylactide based polymer surfactant for reduction of initial burst. *Int. J. Pharm.* **330**, 32–36 (2007).
108. Angadi, S. C., Manjeshwar, L. S. & Aminabhavi, T. M. Interpenetrating polymer network blend microspheres of chitosan and hydroxyethyl cellulose for controlled release of isoniazid. *Int. J. Biol. Macromol.* **47**, 171–179 (2010).
109. Rojanarat, W. *et al.* Isoniazid proliposome powders for inhalation-preparation, characterization and cell culture studies. *Int. J. Mol. Sci.* **12**, 4414–4434 (2011).
110. Chan, J. G. Y. *et al.* A novel dry powder inhalable formulation incorporating three first-line anti-tubercular antibiotics. *Eur. J. Pharm. Biopharm.* **83**, 285–292 (2013).
111. Shanmuga Priya, A., Sivakamavalli, J., Vaseeharan, B. & Stalin, T. Improvement on dissolution rate of inclusion complex of Rifabutin drug with  $\beta$ -cyclodextrin. *Int. J. Biol. Macromol.* **62**, 472–480 (2013).
112. Giri, T. K., Pure, S. & Tripathi, D. K. Synthesis of graft copolymers of acrylamide for locust bean gum using microwave energy: swelling behavior, flocculation characteristics and acute toxicity study. *Polimeros* **25**, 168–174 (2015).
113. Mahajan, H. S. & Gundare, S. a. Preparation, characterization and pulmonary pharmacokinetics of xyloglucan microspheres as dry powder inhalation. *Carbohydr. Polym.* **102**, 529–536 (2014).
114. Ógáin, O. N., Li, J., Tajber, L., Corrigan, O. I. & Healy, A. M. Particle engineering of materials for oral inhalation by dry powder inhalers. I—Particles of sugar excipients (trehalose and raffinose) for protein delivery. *Int. J. Pharm.* **405**, 23–35 (2011).
115. Carvalho, C. de S., Daum, N. & Lehr, C. M. Carrier interactions with the biological barriers of the lung: Advanced in vitro models and challenges for pulmonary drug delivery. *Adv. Drug Deliv. Rev.* **75**, 129–140 (2014).
116. Daigneault, M., Preston, J. a, Marriott, H. M., Whyte, M. K. B. & Dockrell, D. H. The identification of markers of macrophage differentiation in PMA-stimulated THP-1 cells and monocyte-derived macrophages. *PLoS One* **5**, e8668 (2010).
117. Raffetseder, U. *et al.* Differential regulation of chemokine CCL5 expression in monocytes/macrophages and renal cells by Y-box protein-1. *Kidney Int.* **75**, 185–196 (2009).
118. Gaspar, R. & Duncan, R. Polymeric carriers: Preclinical safety and the regulatory implications for design and development of polymer therapeutics. *Adv. Drug Deliv. Rev.* **61**, 1220–1231 (2009).
119. Lanone, S. *et al.* Comparative toxicity of 24 manufactured nanoparticles in human alveolar epithelial and macrophage cell lines. *Part. Fibre Toxicol.* **6**, 14 (2009).
120. Rodrigues, S., Cardoso, L., da Costa, A. & Grenha, A. Biocompatibility and Stability of Polysaccharide Polyelectrolyte Complexes Aimed at Respiratory Delivery. *Materials (Basel)*. **8**, 5647–5670 (2015).
121. International Organization for Standardization. Biological Evaluation of Medical Devices Part 5: Tests for In Vitro Cytotoxicity. *Iso 10993–5*. **5**, 1 – 52 (2009).

122. Carmichael, J., Degraff, W. G., Gazdar, A. F., Minna, J. D. & Mitchell, J. B. Evaluation of a Tetrazolium-based of Chemosensitivity Testing<sup>1</sup> Semiautomated Colorimetric Assay: Assessment of Chemosensitivity Testing. *Cancer Res.* **47**, 936–942 (1987).
123. Rosada, R. S. *et al.* Protection against tuberculosis by a single intranasal administration of DNA-hsp65 vaccine complexed with cationic liposomes. *BMC Immunol.* **9**, 1 – 13 (2008).
124. Parikh, R., Dalwadi, S., Aboti, P. & Patel, L. Inhaled microparticles of antitubercular antibiotic for in vitro and in vivo alveolar macrophage targeting and activation of phagocytosis. *J. Antibiot. (Tokyo)*. **0**, 1–8 (2014).
125. Barluenga, J. *et al.* New rifabutin analogs: Synthesis and biological activity against *Mycobacterium tuberculosis*. *Bioorganic Med. Chem. Lett.* **16**, 5717–5722 (2006).
126. Pinheiro, M. *et al.* Differential interactions of rifabutin with human and bacterial membranes: Implication for its therapeutic and toxic effects. *J. Med. Chem.* **56**, 417–426 (2013).
127. Pinheiro, M. *et al.* The influence of Rifabutin on human and bacterial membrane models: Implications for its mechanism of action. *J. Phys. Chem. B* **117**, 6187–6193 (2013).
128. Widdicombe, J. H. Volume of airway surface liquid in health and disease. *Am. J. Respir. Crit. Care Med.* **165**, 1566 (2002).
129. Hirota, K. & Terada, H. in *Molecular Regulation of Endocytosis pinocytosis* (ed. Intech) 413–428 (Intech, 2012). doi:10.5772/45820
130. Maretti, E. *et al.* Inhaled Solid Lipid Microparticles to target alveolar macrophages for tuberculosis. *Int. J. Pharm.* **462**, 74–82 (2014).
131. Pinheiro, M., Silva, A. S. & Reis, S. Molecular interactions of rifabutin with membrane under acidic conditions. *Int. J. Pharm.* **479**, 63–69 (2015).
132. Duret, C. *et al.* In vitro and in vivo evaluation of a dry powder endotracheal insufflator device for use in dose-dependent preclinical studies in mice. *Eur. J. Pharm. Biopharm.* **81**, 627–634 (2012).
133. Diab, R., Brillault, J., Bardy, a., Gontijo, a. V. L. & Olivier, J. C. Formulation and in vitro characterization of inhalable polyvinyl alcohol-free rifampicin-loaded PLGA microspheres prepared with sucrose palmitate as stabilizer: Efficiency for ex vivo alveolar macrophage targeting. *Int. J. Pharm.* **436**, 833–839 (2012).
134. Scarpelli, E. M. Physiology of the alveolar surface network. *Comp. Biochem. Physiol. - A Mol. Integr. Physiol.* **135**, 39–104 (2003).
135. Fotakis, G. & Timbrell, J. a. In vitro cytotoxicity assays: Comparison of LDH, neutral red, MTT and protein assay in hepatoma cell lines following exposure to cadmium chloride. *Toxicol. Lett.* **160**, 171–177 (2006).
136. Geiser, M. Update on macrophage clearance of inhaled micro- and nanoparticles. *J. Aerosol Med. Pulm. Drug Deliv.* **23**, 207–217 (2010).
137. Martins, S. *et al.* Solid lipid nanoparticles as intracellular drug transporters: An investigation of the uptake mechanism and pathway. *Int. J. Pharm.* **430**, 216–227 (2012).
138. Chanput, W., Mes, J. J., Savelkoul, H. F. J. & Wichers, H. J. Characterization of polarized THP-1 macrophages and polarizing ability of LPS and food compounds. *Food Funct.* **4**, 266–276 (2013).
139. Littlefield, M. J. *et al.* Polarization of Human THP-1 Macrophages: Link between Adenosine Receptors, Inflammation and Lipid Accumulation. *Int. J. Immunol. Immunother.* **1**, 1–8 (2014).
140. Takeda, K. & Akira, S. Toll-like receptors in innate immunity. *Int. Immunol.* **17**, 1–14 (2005).

141. Smiderle, F. R. *et al.* Polysaccharides from *Agaricus bisporus* and *Agaricus brasiliensis* show similarities in their structures and their immunomodulatory effects on human monocytic THP-1 cells. *BMC Complement. Altern. Med.* **11**, 58 (2011).
142. Vigerust, D. J., Vick, S. & Shepherd, V. L. Characterization of functional mannose receptor in a continuous hybridoma cell line. *BMC Immunol.* **13**, 51 (2012).
143. Harrison, L. M., Hoogen, C. Van Den, Haafte, W. C. E. Van, Tesh, V. L. & Al, H. E. T. Chemokine Expression in the Monocytic Cell Line THP-1 in Response to Purified Shiga Toxin 1 and / or Lipopolysaccharides. *Society* **73**, 403–412 (2005).
144. Couleau, N. *et al.* Effects of Endocrine Disruptor Compounds, Alone or in Combination, on Human Macrophage-Like THP-1 Cell Response. *PLoS One* **10**, 1 – 16 (2015).
145. Yadav, A. B. *et al.* Microparticles induce variable levels of activation in macrophages infected with *Mycobacterium tuberculosis*. *Tuberculosis* **90**, 188–196 (2010).
146. Barros, D. F. dos S. Mannosylated Nanoparticles for Targeted Delivery of Amphotericin B Towards Visceral Leishmaniasis. (Universidade do Porto, 2012).
147. Kunin, C. M. Antimicrobial activity of rifabutin. *Clin. Infect. Dis.* **22 Suppl 1**, S3–S13; discussion S13–S14 (1996).

## **Annex**

**Table 1: Characterisation of Isoniazid and Rifabutin.** Adapted from reference 10, 23, 70,147.  
10,23,70,147

Characterisation	Isoniazid	Rifabutin
<b>Indication</b>	Antibacterial agent used primarily as a tuberculostatic. First-line agent.	A broad-spectrum antibiotic that is being used as prophylaxis against disseminated <i>Mycobacterium avium</i> complex infection in HIV-positive patients.
<b>Pharmacodynamics</b>	Isoniazid is a bactericidal agent active against some organisms of the genus <i>Mycobacterium</i> . It is a highly specific agent, ineffective against other microorganisms. Isoniazid is bactericidal to rapidly-dividing mycobacteria, but is bacteriostatic if the mycobacterium is slow-growing.	Rifabutin is an antibiotic that inhibits DNA-dependent RNA polymerase activity in susceptible cells. Specifically, it interacts with bacterial RNA polymerase but does not inhibit the mammalian enzyme. It is bactericidal and has a very broad spectrum of activity against most gram-positive and gram-negative organisms (including <i>Pseudomonas aeruginosa</i> ) and specifically <i>Mycobacterium tuberculosis</i> . Because of rapid emergence of resistant bacteria, use is restricted to treatment of mycobacterial infections and a few other indications.
<b>Mechanism of action</b>	A pro-drug activated by catalase peroxidase, the drug inhibit of synthesis of mycolic acids, through formation of a covalent complex with an acyl carrier protein and $\alpha$ -ketoacyl carrier protein synthetase.	Rifabutin acts via the inhibition of DNA-dependent RNA polymerase in gram-positive and some gram-negative bacteria, leading to a suppression of RNA synthesis and cell death.
<b>Minimum Inhibitory Concentration for <i>Mycobacterium tuberculosis</i> (<math>\mu\text{g/mL}</math>)</b>	0.01 – 0.2	0.125
<b>Chemical formula</b>	$\text{C}_6\text{H}_7\text{N}_3\text{O}$	$\text{C}_{46}\text{H}_{62}\text{N}_4\text{O}_{11}$
<b>Mass molecular (g/mol)</b>	137.14	847.01
<b>Structure</b>		
<b>Melting point (<math>^{\circ}\text{C}</math>)</b>	171.4 $^{\circ}\text{C}$	Not be determined
<b>Water Solubility</b>	1.4 E+ 005 mg/L (at 25 $^{\circ}\text{C}$ )	Minimally soluble (0.19 mg/mL)
<b>Partition-coefficient (logP)</b>	-0.70	4.1